UNIVERSITY OF CALIFORNIA
RIVERSIDE

Identification and Functional Characterizations of Novel Post-Translational Modifications of DNA Repair Proteins

A Dissertation submitted in partial satisfaction
of the requirements for the degree of

Doctor of Philosophy

in

Environmental Toxicology

by

Qian Cai

December 2014

Dissertation Committee:
Dr. Yinsheng Wang, Chairperson
Dr. Wenwan Zhong
Dr. Constance Nugent

The Dissertation of Qian Cai is approved:

_____

_____

_____

Committee Chairperson

University of California, Riverside

ACKNOWLEDGEMENTS

This dissertation can never be complete without the help and support from many people. I sincerely and gratefully thank all those who have made this dissertation possible and because of whom my graduate experience has been one that I will cherish forever.

First and foremost, I would like to give my deepest appreciation to my adviser, Professor Yinsheng Wang, for his guidance and memtorship, consistent support and patience during my PhD study at UCR. Giving me the opportunity, freedom and constructive suggestions to perform research I am interested in, Professor Wang has brought me to the world of mass spectrometry and led me grow as a solid biochemist. Not only had he taught me knowledge, but also the ability to think and solve problems independently. His passionate and diligent attitudes towards science have impressive impact on my life. Without his continuous encourage and valuble advices, I can never conquer the obstacles and stressful situations, not to mention the happen of completion my doctoral studies successfully.

I would like to acknowledge Professor Wenwan Zhong and Professor Constance Nugent, for reading my dissertation and offering me precious comments and their generous help over the past five years; Professor David Eastmond for introduced me into the world of toxicology and giving me the access to use the flow cytometry in his lab, Professor Sarjeet S.Gill, Professor Roger Atkinson and Professor Jeff Bachant for teaching me the knowledge in their classes; Professor Xuan Liu, for giving me the chance

to rotate in her lab for the first quarter of my PhD study and Professor Earnest Martinez for serving as my guidance committee and giving me help in my graduate studies.

I thank many staff members in Chemistry Department and Center of Plant Cell Biology and Core Instrumentation Facility at UCR including Dr. David Carter for his kind assistance and advice on confocal microscopy, Ms. Holly Eckelhoefer for her training and help with flow cytometry, Dr. Songqin Pan and Mr. Ronald New for their assistance on MALDI mass spectrometers, Dr. Christa Feasley in Thermo Scientific for the training on Orbitrap Fusion Tribrid, and Dr.Thomas Girke on the training of bioinformatics analysis.

Additionally, I am grateful to get lots of help and friendship from my group members. I would like to thank Dr. Bifeng Yuan, Dr. Changjun You, Dr. Xiaoli Dong, Dr. Hongxia Wang, Dr. Lei Xiong, Dr. Fan Zhang and Dr. Yongsheng Xiao for their generous help and patience when I started work in this group. Thanks also go to Dr. Nanqin Gan, Dr. Xiaoxia Dai, Lijuan Fu, and Zi Wang for their help in completing my research projects. And I would like to thank all other members in our lab for their support.

Last, but not least, I would like to thank my parents for their unconditional and endless love to me. They are always standing behind me, supporting and educating me during every stage of my life, no matter how far they are away from me. I especially thank my husband Peng Wang. I cherish every day in my PhD studies with his accompany, understanding, encourage and love.

COPYRIGHT ACKNOWLEDGEMENTS

The text and figures in Chapter 2, in part or in full, is a reprint of the material as it appears in ***Journal of Biological Chemistry 2014***, 289, p. 16046-16056 and the supporting information therein. The co-author (Dr. Yinsheng Wang) listed in this publication directed and supervised the research which forms the basis for this chapter. The co-authors Lijuan Fu listed in this publication helped with cell culture for DNA repair assay in this publication. The co-author Zi Wang listed in this publication helped with a binding assay electrophoretic mobility shift assay (EMSA) which is not shown in the manuscript. The co-author Dr. Nanqin Gan listed in the publication gave valuable advices for the immunofluorescence assay. The co-author Dr. Xiaoxia Dai listed in this publication offered meaningful discussion on the identification of the α-N-methylation.

ABSTRACT OF THE DISSERTATION

Identification and Functional Characterizations of Novel Post-Translational Modifications of DNA Repair Proteins

by

Qian Cai

Doctor of Philosophy, Graduate Program in Environmental Toxicology
University of California, Riverside, December 2014
Dr. Yinsheng Wang, Chairperson

Post-translational modification (PTM) constitutes a ubiquitous mechanism to expand proteins' structure, interactions, localization, and function. The research covered in this dissertation focuses on the identification and characterization of the functional roles of the novel PTMs of damaged DNA-binding protein 2 (DDB2) and MRG15, which are important in nucleotide excision repair (NER) and homologous recombination (HR), respectively.

In Chapters two and three, by employing LC-MS/MS, I discovered, for the first time, that DDB2 could be methylated on the α-amino group of N-terminal alanine (after cleavage of the initiating methionine) and phosphorylated at serine 26 in HEK293T human embryonic kidney epithelial cells. In addition, this α-N-methylation was found to be catalyzed by the N-terminal Xaa-Pro-Lys N-methyltransferase 1 (NTMT1). I also observed that the level of serine 26 phosphorylation was significantly reduced in cells

treated with flavopiridol, an inhibitor for cyclin-dependent kinases (Cdks), suggesting the involvement of Cdks in this phosphorylation.

The importance of this α-N-methylation and Ser26 phosphorylation of DDB2 is illustrated by the observation that methylation-defective mutant of DDB2 displayed a reduced efficiency, while DDB2 mutant deficient in Ser26 phosphorylation failed, to be recruited to ultraviolet (UV) light-induced cyclobutane pyrimidine dimer (CPD) foci. Moreover, while Ser26 phosphorylation was also demonstrated to crosstalk with DDB2 ubiquitination and critical for proteasomal degradation of DDB2, loss of α-N-methylation or Ser26 phosphorylation of DDB2 conferred reduced ATM activation, decreased efficiency in CPD repair, and elevated sensitivity of cells toward UV light exposure. Collectively, I concluded that α-N-methylation and the phosphorylation of Ser26 in DDB2 plays a significant role in NER. This study also expanded the biological functions of protein α-N-methylation to DNA repair.

In Chapter four, I further expanded the targets of NTMT1 in human cells to MRG15. Importantly, I demonstrated, for the first time, the involvement of α-N-methylation in protein-protein interaction. My results showed that the α-N-methylated N-terminus of MRG15 enables its interaction with TIP60 histone acetyltransferase through binding to the chromo domain of TIP60 and stimulates allosterically the enzymatic activity of the latter. In addition, I found that this α-N-methylation-chromo domain interaction is indispensable for the acetylation of lysine 16 in histone H4 (H4K16Ac), for DNA damage-induced ATM activation, for the repair of DNA double strand breaks via the homologous recombination pathway, and for protecting cells from the genotoxic

effects of ionizing radiation and interstrand cross-linking agents. Moreover, I defined MRG15 as a molecular determinant for a novel histone crosstalk between histone H3 lysine 36 trimethylation (H3K36me3) and H4K16Ac. Together, my study unveiled, for the first time, the α-N-methylation of MRG15 and discovered novel functions of protein α-N-methylation in the context of DNA damage response and repair. I also uncovered a novel trans-histone modification where H3K36me3 drives H4K16Ac in human cells, revealed the essential role of MRG15 in this process, and demonstrated the importance of this trans-histone modification in ATM activation and homologous recombination repair.

TABLE OF CONTENTS

LIST OF FIGURES

Chapter 1. General overview

1.1 Introduction

The introduction of novel technologies often leads to rapid advances in biology. For instance, Sanger sequencing paved a road for the completion of the sequencing of the human genome (1), and the development of next-generation sequencing technologies made it faster, easier and cheaper to sequence the whole genome (2). Likewise, the introduction of proteomics also revolutionalized biological research. The term "proteomics" was first introduced by Peter James (3), which is the study of all expressed proteins, in terms of its interactions, localization, modifications and ultimately function.

Modern techniques applied to proteomics include protein-detecting microarray and chromatin immunoprecipitation followed by sequencing (CHIP-seq) analysis (4,5), one-dimensional or two-dimensional polyacrylamide gel electrophoresis (1D/2D-PAGE) (7) and mass spectrometry (8).

Protein-detecting microarray is composed of a plethora of affinity reagents immobilized on a solid phase, which allows a great number of reactions occur in a very restricted space. However, this method is commonly used for targeted groups of proteins, thus requires existing knowledge about what proteins to study and is more biased as compared with other methods (5). In addition, the major impediment is generation of large quantities of affinity reagents.

For studying genome-wide protein-DNA interactions, CHIP-seq has evolved into a high-throughput method recently, yet the drawbacks are the high costs, restricted availability and bias towards the GC content of fragment selection (4).

PAGE is often used prior to mass spectrometric analysis to separate proteins to subgroups according to their molecular weight for 1D-PAGE and also according to their isoelectric focusing on immobilized pH gradient strip for 2D-PAGE (7). To determine identities of the proteins, the subgroups of protein bands could be cut out from the gels, enzymatically digested and detected by mass spectrometry. Despite the various applications for this techniques, it displayed limitations for detection of membrane proteins due to their low resolution of hydrophobic, acidic and alkaline proteins and poor loading capacities (11).

Owing to its rapid development, mass spectrometry (MS) has established itself as a powerful 'hypothesis-generating engine' for proteomics study (12). In general, the mass spectrometry-based proteomics have three applications. First, mass spectrometry is applied to quantitative proteomics for determining absolute and relative amounts of expressed proteins from samples with different physiological or pathophysiological conditions (e.g. 'disease' vs. 'normal', or 'drug-treated' or 'untreated') (13). Several strategies are widely used for protein quantification, includes stable isotope labeling by amino acids in cell culture (SILAC) (14), isotope-coded affinity tag (ICAT) (15), isobaric tag for relative and absolute quantitation (iTRAQ) (16), stable isotope dimethyl labeling (17) and absolute quantification of proteins (AQUA) (18). Second, mass spectrometry is well suited for mapping protein interactome (19). Other than expression level, protein interaction is a key parameter by which protein exerts its function. Bait, affinity purification and complex analysis are the three key components for elucidating protein interaction network. In theory, antibody that specifically interacts with the bait protein

can be used directly for enrichment. However, the antibody bank is not comprehensive and the quality is not adequate for some proteins. To overcome this problem, more frequently a tag allows for purification is attached to proteins. In 1998, Mann's group characterized the splicesome complex in mammalian cells, which is the first mass spectrometry-based study of protein complex (20). Investigations of numerous large complexes, for example, mitochondrial complex which is associated with apoptosis and glycolysis (21), were subsequently characterized. Along with this, technical developments like quantitative mass spectrometry-based approach combined with stable isotope labeling (22) were also developed to distinguish true binders from the non-specific binding contaminants. Third, mass spectrometry becomes widely employed for the study of post-translation modifications (PTMs) of proteins, which is the focus of this dissertation.

Although challenges still exist in two aspects: dynamic ranges of protein concentrations (five orders of magnitude difference between low and high abundance proteins), complexity of protein samples (i. alphabetic protein had 21 amino acids which comprise the basic structure, while DNA or RNA is composed of 4 bases; ii. biofluid samples are difficult to handle). Tremendous improvements in sample preparation, instrumentation, data processing and analysis for mass spectrometry-based proteomics over the past decades have brought great impact on medicine and biology.

1.2 Mass Spectrometry-based characterization of novel post-translational modifications

Proteins, after translation will undergo various decorations including PTMs to become mature. PTMs are often regulatory and reversible, which play significant roles in the localization, interaction and function of protein. Traditionally, dissection of PTMs relies on Edman degradation, amino acid analysis, isotopic labeling and immunochemistry (23). These methods are often time-consuming and painstaking, mass spectrometry-based method for the characterizations of protein PTMs overcomes these drawbacks and has become the main technology since its development. MS can provide the chemical nature, the exact site, and sometimes quantitative information about the modification in an efficient and cost-effective fashion. In this chapter, I will review the studies of PTMs by mass spectrometry from the following perspectives.

1.2.1 Instrumentation

Mass spectrometry is an analytical technique which comprises of an ion source, a mass analyzer which measures the mass-over-charge ratio (m/z) of the ionized analyte and a detector that records the ions at each m/z (24).

Two soft ionization techniques widely utilized to ionize proteins and peptides are electrospray ionization (ESI) (25) and matrix-assisted laser desorption/ionization (MALDI) (26). Due to the fact that ESI is capable of ionizing analyte out of a solution (27), it is suitable for the applications which are in combination with liquid-based separation tools (e.g., chromatography and electrophoresis). On the other hand, MALDI ionizes sample out of a dry and crystalline matrix via laser pulses. Therefore, ESI-MS is

preferred for the analysis of complicated samples. In ESI-MS, samples enter the ionization source through a fused silica capillary or needle, where a potential is applied which initiates the samples to spray and form highly charged fine droplets (12). In traditional electrospray ionization invented by Fenn et al. (28), samples were normally injected at a flow rate of 2-20 μl/min. Later, the development of nanospray ionization solved the problem faced by previous method when dealing with limited biological samples (29).

Mass analyzer is the heart of the mass spectrometer where ions are separated based on their m/z values. Four basic types of mass analyzers widely used in proteomics research are the ion trap, time-of-flight (TOF), quadruple and Fourier transform ion cyclotron resonance (FT-ICR). Each of these mass analyzers has its limitations and advantages in terms of sensitivity, resolution, mass accuracy, dynamic range and cost. Therefore, hybrid instruments, including the quadruple-time-of-flight (QTOF), are developed to accommodate the strengths of different types of mass analyzers. MS alone can provide valuable information in some circumstances, yet it is more informative to have tandem mass spectrometry (MS/MS) data. In tandem mass spectrometry, different stages of mass analysis can be performed in different mass analyzers (tandem-in-space) or in the same mass analyzer sequentially (tandem-in-time).

The main instrument used in this thesis is a Thermo Electron LTQ Orbitrap Velos which allows for acquiring MS/MS in both tandem-in-space and tandem-in-time modes. The unique advantage of this instrument lies in the capability of the Orbitrap mass

analyzer to offer high mass accuracy and high mass resolution, and ability of the linear ion trap to provide high scan speed and high sensitivity (30).

1.2.2 Dissociation methods

Several ion dissociation methods are frequently used in MS/MS analysis, which include collisionally induced dissociation (CID), higher energy collisional dissociation (HCD), electron capture dissociation (ECD) and electron transfer dissociation (ETD). CID is a common method which induces cleavage in peptides at the amide linkages and generates b and y ions as illustrated in Figure 1.1a. From these fragment ions, amino acid composition and sequence can be dissected (31,32). Nevertheless, for labile PTMs such as phosphorylation, glycosylation and sulfation, fragment ions arising from neutral loss of the modification moiety may dominate the spectrum, rendering it difficult to locate the site of modification (33). In this situation, MS^3 spectrum from further cleavage of the dominant neutral loss fragment sometimes helps to provide diagnostic fragment ions for determining the modification site (23). Alternatively, HCD, which was recently developed, is preferred for these circumstances for several reasons: (a) The high mass accuracy enables the determination of charge state; (b) immonium ions sometimes indicate the types of modifications (e.g. phosphotyrosine); (c) The mass range is dynamic (34). ECD (35), exclusively applied to FT-ICR, occurs for multiply protonated ions of peptides and proteins. In this method, cleavage of peptide backbones occurs mainly at the N-C_α bond and generates c and z ions (Figure 1.1a). Later, ETD was introduced by Hunt and co-workers (36). This dissociation method can be performed in linear ion trap, Orbitrap and QTOF instrument (37). ECD and ETD complement CID in several aspects.

First, labile PTMs remain intact; second, the fragmentation pattern is evenly distributed over the entire peptide backbone; third, in light of their capability to dissociate ions of high charge states, they are useful for large peptides and proteins (38,39). Collectively, these four different dissociation methods complement each other and combining some of these dissociation methods offers better characterizations of PTMs.

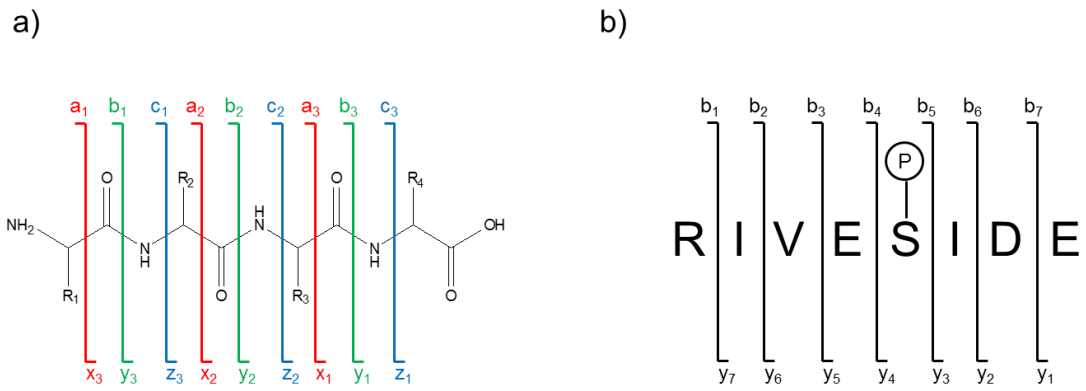

Figure 1. 1. Mass spectrometry-based identification of PTMs. a) Three peptide fragmentation patterns occur at the peptide bond. N-terminal b ions and C-terminal y ions are the major products observed in CID. b) The b and y ions can indicate the localization of a PTM on a peptide. The serine residue is phosphorylated in the artificial peptide "RIVER$_P$SIDE". The b_5-b_7 and y_4-y_7 ions with a mass shift (80-Da increment) indicating the site of phosphorylation.

1.2.3 Bottom-up, top-down and middle-down MS

Bottom-up is the traditional approach for PTM discovery which gained widespread applications. In this approach, peptides resulting from proteolytic digestion of whole proteins are separated by liquid chromatography and analyzed by MS and MS/MS. In light of its robustness and reproducibility, trypsin is always the first choice for protein digestion. Trypsin cleaves the amide bonds on the C-terminal sides of arginine and lysine and gives rise to peptides with basic amino acids at the C-termini. However, it is rare to obtain full sequence coverage with trypsin alone; in this case, multiple enzymes (e.g. Glu-c, Asp-N, and chymotrypsin) can be used in combination to provide better identification of PTMs that cannot be detected after trypsin digestion (40,41). The bottom-up approach is a mature approach, and full automation from high-resolution separations of peptide digestion mixtures to MS analysis is achieved by online HPLC-MS/MS system (42). More importantly, recent developments of bioinformatics tools, such as Peptide Sequence Tags (43), Sequest (44) and Mascot (45), render the facile interpretation of bottom-up proteomic data.

Another alternative approach is top-down MS, initially developed by McLafferty et al. (46,47). In top-down MS, intact proteins are directly ionized by ESI, fragmented by ECD or ETD, and analyzed in a mass analyzer with high resolution and high mass accuracy (e.g. FT-ICR, Orbitrap and Q-TOF). Therefore, it has advantages over conventional bottom-up approach in several applications including chromatin biology, protein-level variation and membrane proteins (48). Yet, top-down MS has not been widely employed since it is hampered by challenges in separation of large intact proteins

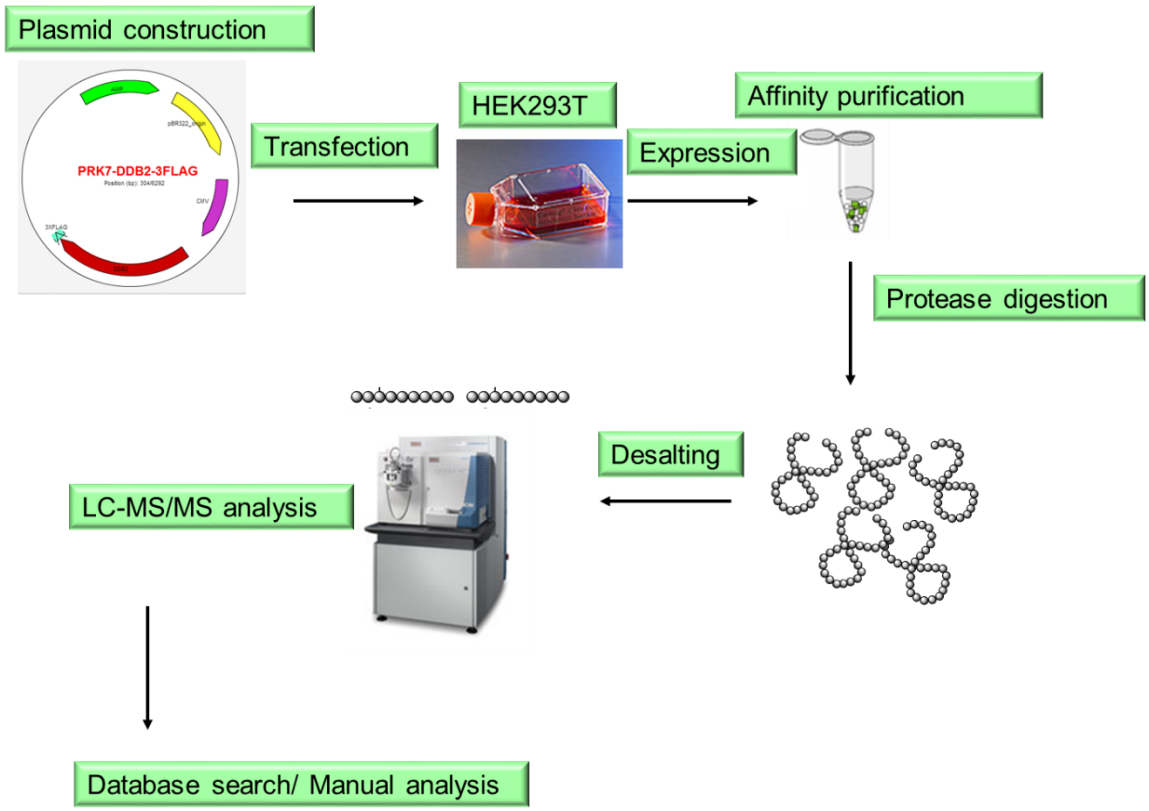

Scheme 1.1. A typical affinity-purification coupled with mass spectrometry-based PTM identification.

and limited computational tools (ProSight PTM is the only tool currently) for data analysis (49,50).

Middle-down approach is a combination of top-down and bottom-up, in which limited proteolysis (normally by Asp-N, Glu-C) is performed to produce peptides in a mass range of 3-20 kDa. This approach provides high efficiency by combining the advantages of top-down and bottom-up (51), yet, this limited digestion is unpredictable (52).

1.2.4 Affinity-purification coupled with mass spectrometry-based PTM identification

Detailed workflow of affinity-purification coupled with mass spectrometry-based PTM identification used in my thesis study is shown in Scheme 1.1. In this regard, to enrich the specific proteins of interest, we first construct plasmids allowing for the expression, in human embryonic kidney 293 (HEK-293) cells, of fusion proteins where a FLAG-tag was conjugated to the C-termini of these proteins. The FLAG-tagged proteins were isolated from the whole cell lysate by using affinity purification with anti-FLAG M2 beads. Using “bottom-up” approach, the purified proteins were digested on beads with appropriate proteases, and the resulting peptide mixtures were then subjected to LC-MS/MS analysis in data-dependent acquisition (DDA) or selected-ion monitoring (SIM) mode. Finally, the acquired mass spectrometric data were processed by searching tools such as Mascot and validated by manual analysis.

1.3 DNA damage and repair

DNA, a double helical molecule, encodes and stores the genetic information which ensures the proper function of all living organisms. However, every day cells incessantly encounter alterations of the chemical structure in DNA, resulting in DNA damage. Under normal physiological processes, errors can be introduced during DNA replication and DNA strand break can arise from abortive actions of topoisomerases I and II (53), and thousands of DNA lesions are generated per cell per day by DNA hydrolysis, deamination and non-enzymatic methylations (54). In addition, DNA lesions are generated by reactive oxygen species (ROS) emanating from normal aerobic metabolism and phagocytes at sites of inflammation (55,56). Aside from these, a plethora of DNA lesions arise from environmental agents including ultraviolet (UV) light from sunlight exposure, ionizing radiation and environmental toxins. To counteract the deleterious effects of endogenous and exogenous sources of genotoxic agents, cells respond to DNA damage by triggering the activation of several cellular pathways including DNA repair, cell cycle checkpoint, and apoptosis, thereby maintaining genome stability and delivering intact genetic material to the next generations.

The perplexing diversity of DNA lesions necessitates a diverse array of DNA-repair pathways. Some types of DNA lesions are coped with direct reversal pathway such as methylation of guanine bases is reversed by the protein methylguanine DNA methyltransferase (MGMT) (57) and pyrimidine dimers which are induced by UV light can be processed directly by photolyase that is catalyzed by blue light (350-450 nm) (58). To remove errors from newly synthesized DNA, mismatch repair (MMR) machinery

recognizes base-base mismatches and insertion/deletion loops and elicits incision in the newly synthesized DNA strand which are followed by polymerase synthesis and ligation (59). Base-excision repair (BER) and nucleotide excision repair (NER) constitute two major mechanisms for removing DNA lesions involving modifications of a single DNA strand. The former repairs chemical alterations of single nucleobases (60), whereas the latter targets helix-distorting base lesions (61). Double strand breaks (DSBs), where both strands are affected, are particularly lethal and are repaired by the homologous recombination (HR) and non-homologous end joining (NHEJ) pathways (62,63). While HR is restricted to S and G2 phase in the cell cycle because it requires the presence the sister-chromatid sequence as a template for error-free repair, NHEJ can operate through the entire cell cycle phases.

Here, I will focus on nucleotide excision repair and homologous recombination repair, in which the two proteins investigated in this thesis, i.e. damaged DNA-binding protein 2 (DDB2) and mortality factor on chromosome 4 (MORF4), are involved, respectively.

1.3.1 Nucleotide excision repair and DDB2

Nucleotide excision repair, a sophisticated DNA repair mechanism protects cells from catastrophic effects caused by a wide variety of helix-distorting DNA lesions, such as UV light-induced cyclobutane pyrimidine dimer (CPD) and pyrimidine(6-4)pyrimidone photoproducts (6-4PPs), as well as bulky DNA adducts induced by numerous environmental carcinogens. As displayed in Figure 1.2, although both CPD and 6-4PP result in distortion in DNA structure, 6-4PP induces a greater distortion to DNA

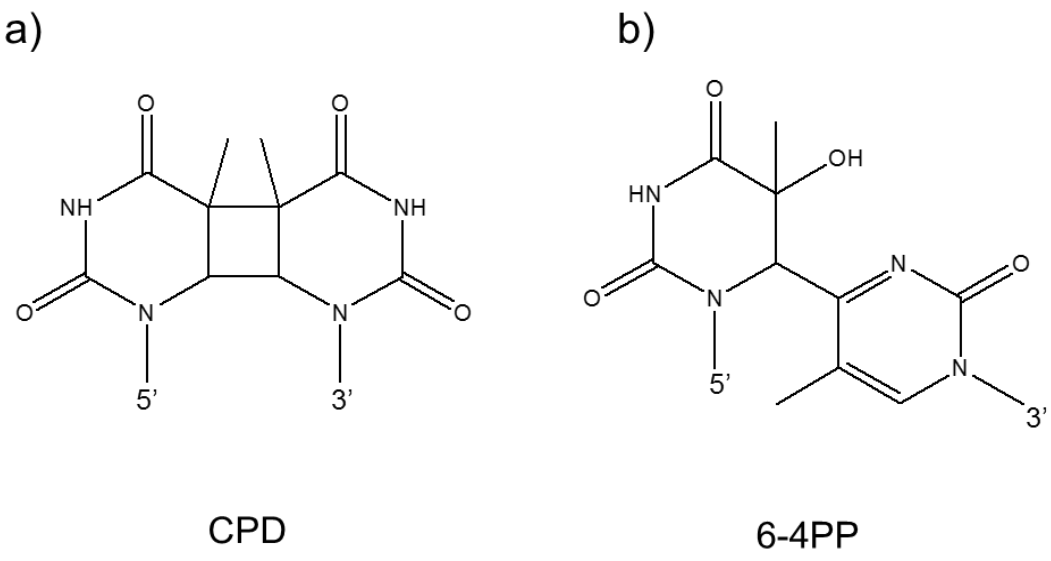

Figure 1. 2. Structure of UV-induced CPD and 6-4PP formed at neighboring thymines.

helical structure (64). In addition, CPD is the major form of DNA lesion formed from UV light exposure (64). Two distinct subpathways are involved in NER: global genome NER (GG-NER) and transcription-coupled NER (TC-NER), which removes lesions from the entire genome and from the template strand of actively transcribed genes, respectively (65,66).

Four continuous steps are involved in NER, lesion detection, local helical unwinding, an excision step of the damaged strand, and finally DNA synthesis and ligation. Figure 1.3 shows the details for these steps, GG-NER and TC-NER share many common factors except for the first DNA damage recognition step (67). Specifically in mammalian cells, while UV-DDB complex (which is composed of the DDB1/DDB2 heterodimer) and XPC-RAD23B are associated with GG-NER (68-70), whereas a stalled RNA polymerase together with CSA and CSB are involved in TC-NER (71-73). After detection of the helix-distorting DNA lesions, TFIIH unwinds a short region containing the UV-induced lesion (74). Meanwhile, XPA and RPA are recruited, which facilitate the translocation and damage verification by TFIIH. Endonuclease ERCC1/XPF (for 5' incision) and XPG (for 3' incision), although not recruited simultaneously, function together to remove approximately a 22-30 nt lesion-containing oligonucleotide (75). Finally, the resulting gap is filled in via DNA synthesis by DNA polymerases such as Polδ, Polε, Polκ together with replication factor PCNA, and ligation by DNA ligases I and III (67,71,76).

Three distinct genetic disorders are associated with defective NER, namely, xeroderma pigmentosum (XP), Cockayne syndrome (CS) and trichothiodistrophy (TTD).

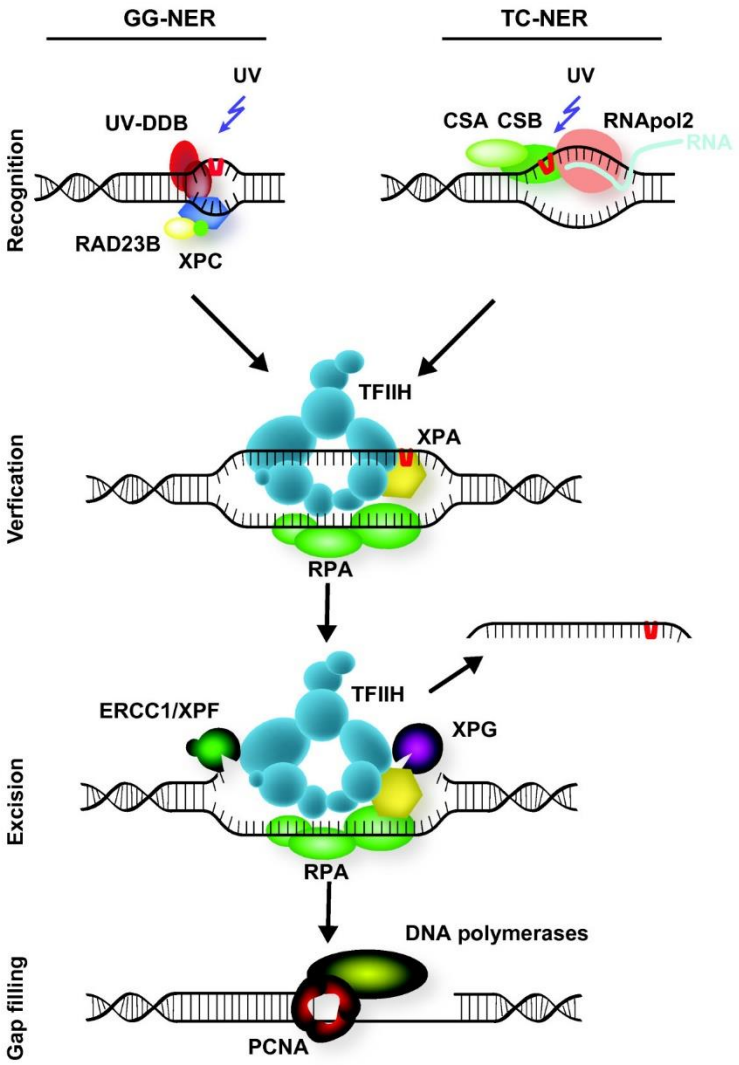

Figure 1. 3. Mammalian nucleotide excision repair pathway. (Adapted from Ref 67).

XP patients are hypersensitive to sunlight and predispose to skin cancers. Both TTD and CS patients are not susceptible to skin cancer development, but are associated with developmental and neurological abnormalities (77,78). XPE constitutes one of the eight complementation groups of XP (XPA-XPG and XPV) and the *XPE* gene encodes DDB2 (79). The presence of functional DDB2 is essential for efficient removal of CPD in GG-NER, as discussed previously (80-82).

DDB2, which is composed of an N-terminal helix-loop-helix segment and a 7-bladed WD40 β-propeller domain, exhibits high binding ability towards UV-damaged DNA (83). Previously, the importance of UV-DDB2 complex in NER is underestimated since *in-vitro* reconstitution assay shows sufficient repair capability even without the presence of UV-DDB2 (84-86). However, several lines of evidences suggest the critical role of UV-DDB2 in early detection of UV-damaged DNA in GG-NER *in vivo*. DDB2 binds to both CPDs and 6-4PPs independent of XPC (68,82); nevertheless, XPC in itself only localizes to 6-4PPs efficiently, but to a much lower extent to CPD (87,88).

DDB2 was found to be present in a complex with the DDB1-CUL4-ROC1 (CRL4) E3 ubiquitin ligase (89,90). In parallel, CSA, a TC-NER-specific protein which bears WD40 domains, also forms complex with CRL4 (91,92). In the complex, DDB2 functions as a dedicated substrate receptor (DCAF). In the absence of DNA damage, DDB2 associates with COP9 signalosome (CSN), which inhibits the E3 ligase activity. Upon DNA damage, CSN was released to allow for the E3 ligase activity that facilitates NER (90,92). The tight association of DNA with histones in chromatin precludes the access of DNA repair proteins in normal circumstances. One of the mechanisms

facilitating chromatin relaxation in DNA repair is through the PTMs of histone proteins. DDB2-associated CRL4 complex helps prepare the chromatin environment that is conducive the recruitment of repair proteins by monoubiquitination of histones H2A, H3 and H4 (93,94). Additionally, XPC and DDB2 are also polyubiquitinated by this E3 ligase complex (95-97). Polyubiquitination of XPC and DDB2 alters their binding affinity to UV-damaged DNA and is essential for the handover of XPC to DNA lesions (95). Although a mouse model suggested abrogation of DDB2 degradation triggers elevated CPD repair (98), the pervasive opinion is that XPC recruitment and proper NER depend on ubiquitination-mediated degradation of DDB2 (99-102).

DDB2 serves as a damage sensor to regulate cell fate upon low and high doses of UV damage (103,104). Under low-dose UV-irradiation, DDB2 promoted the degradation of $p53^{S18P}$ but not the levels of total p53. It is of note this degradation is not detected upon high-dose of UV (50 J/m^2). One of the p53 transcriptional target p21 abrogates DNA synthesis during NER through action on PCNA. Under all conditions DDB2 induced ubiquitination-mediated proteasomal degradation of p21. Therefore, as illustrated in Figure 1.4 (105), under low-dose UV-irradiation, DDB2 regulates the level of p21 both through ubiquitin-mediated proteasomal degradation and transcriptional regulation by p53 (103). However, under high-dose UV-irradiation, p53 level is maintained, which enables apoptosis (104). It is worth mentioning that DDB2 is transcriptionally regulated by p53 in humans, thus resulting in a UV-associated regulatory feedback loop (106,107).

In reminiscence of the observation of the UV damage-induced activation of the apical checkpoint kinase Mec1 (homolog of human ATR) and Rad53 (homolog of human

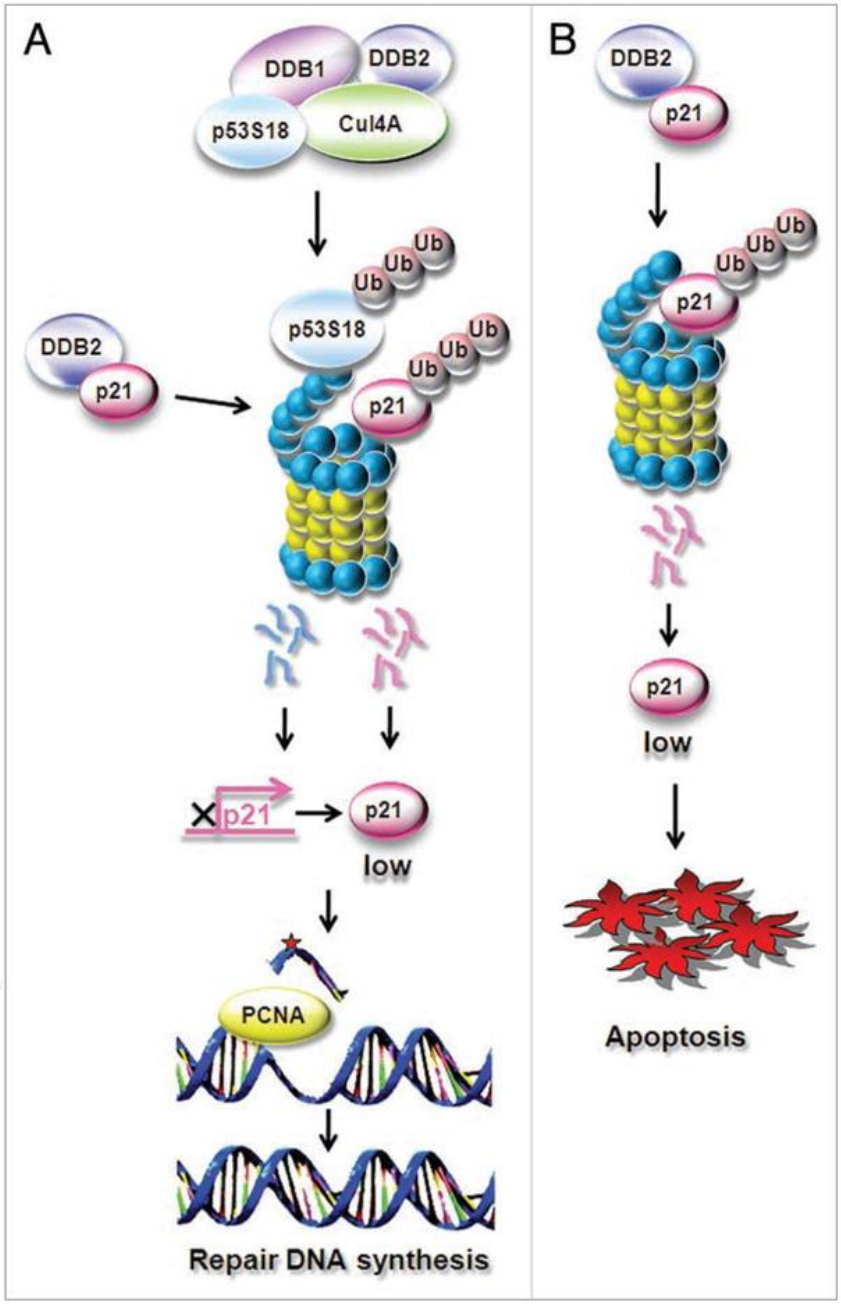

Figure 1. 4. The mechanisms that DDB2 decide cell fate upon low- and high-dose UV damage, A) DDB2 facilitates NER upon low-dose UV irradiation; B) DDB2 stimulates apoptosis under high-dose UV irradiation when DNA damage is irreversible (Adapted from Ref 105).

Chk2) in *Saccharomyces cerevisiaen* (108,109), recently human ATM and ATR were found to be recruited to UV-mediated DNA damage foci and activated, which is promoted by DDB2 and XPC through physical interaction (110).

Maintaining the proper function of DDB2 necessitates a delicate balance of regulation by a wide categories of PTMs, including α-N-methylation, phosphorylation, SUMOylation, ubiquitination and poly(ADP-ribosyl)ation (111-116). Moreover, many proteins, such as USP24, PCNA and p97, are responsible for the regulation of DDB2 stability (117-119). All these investigations shed light on the critical role of DDB2 in nucleotide excision repair, yet DDB2 also have roles in other cellular processes such as cell proliferation in breast cancer cell lines (120).

1.3.2 Homologous recombination repair and MRG15

Pleiotropic sources, such as replication-folk collapse and exposure to interstrand cross-linking agent and ionizing radiation (IR), can induce DSBs in DNA. IR can result from decay of radioactive compounds in nature or man-made radioisotopes. The common use of IR in cancer therapy renders it necessary to understand how cells respond to DSBs. Despite the employment of DSBs in controlling biological processes such as genetic recombination during meiosis (121), DSBs are the most devastating DNA lesions. One single DSB, if left unrepaired, may potentially lead to the loss of millions of base pairs of genetic information.

Present exclusively in late S- and G2-phase of the cell cycle, homologous recombination repair (HR), which operates in a template-dependent fashion, is one of the two major mechanisms for repairing DSBs (122). More than a dozen proteins are

involved in the HR, among which the MRE11-NBS1-RAD50 (MRN) complex is the earliest recruited to DSBs. The critical role of the MRN complex is highlighted by its ability to tether DNA ends and recruit ATM (123,124). ATM activation, which occurs within 5 min and reaches to the maximum level by 15 min (123), triggers a pleiotropic effect by phosphorylating hundreds of proteins (125). One of the critical target is H2AX, the protruded tail of which undergoes phosphorylation at serine-139 (126). Phosphorylated H2AX (γH2AX) spreads up to 2 million base pairs of chromatin which renders it a universal biomarker for DSBs. Importantly, γH2AX facilitates recruitment of MDC1 through its BRCT domain (127). The localization of MDC1 provides additional docking sites for DSB repair proteins MRN-ATM complex (128,129) and promotes recruitment of E3 ubiquitin ligases RNF8 and RNF168. The chromatin-wide ubiquitination by RNF8 and RNF168 further stimulates loading of BRCA1 and 53BP1 (130,131). In late S and G2 phase of cell cycle, BRCA1 counteracts 53BP1 to promote HR (132,133). Through physical interaction of BRCA2 via partner and localizer of BRCA2 protein (PALB2), BRCA1 is defined a critical determinant for the assembly of HR factors, including RAD51 which ensures filament formation (134-136).

MRG15, consisted of an N-terminal chromo domain and a C-terminal MORF4-related gene (MRG) domain, is first identified as a member of the highly conserved MRG family of proteins (137). MRG15 was found in several distinct protein complexes including the histone deacetylase (138) and histone acetyltransferase (HAT) complexes (139,140), which are critical in chromatin remodeling during transcriptional regulation and cell proliferation (141-145). The first clue that MRG15 is involved in DNA damage

repair in mammalian cells is that *MRG15*-null and heterozygous knockout mouse embryonic fibroblasts display DNA repair defects, as manifested by the delayed formation of γH2AX and 53BP1 foci (146). In addition, *Mrg15*$^{-/-}$ mice were found to be embryonically lethal with developmental delay in the few survivals (147). Further support for the role of MRG15 in DNA repair was evidenced by the fact that MRG15 interacts with PALB2 and plays a crucial role in repairing DNA DSBs and interstrand cross-link lesions through the HR pathway (148,149).

1.4 α-N-methylation

α-N-methylation, referred to methylation (mono-, di- or tri-methylation) on the α-amino group in the N-terminal amino acid of proteins, is a conserved PTM which has been known for several decades (150). Here, we review the studies of this type of PTM in the following aspects.

1.4.1 History of α-N-methylation: from bacteria to eukaryotes

The identification of α-N-methylation can be traced back to 1976 when the ribosomal proteins L16 (151) and L33 (152,153) in *Escherichia coli* were shown to carry this modification. Later, more proteins in bacteria were identified to be α-N-methylated, which include ribosomal protein L11 (154-157), S11 (158), the associated IF3 (159), pilin (160-164), and chemotaxi-flagellar apparatus (CheZ) (165). While the nature of α-N-methylation in these bacterial proteins have been reviewed in detail by Stock et al. (150), we will focus on α-N-methylated proteins in eukaryotes.

Histone H2B from different organisms are among the known α-N-methylated eukaryotic proteins. In this context, methylation of N-terminal proline has been observed in H2B from *Neurospora crassa* (40), *Drosophila melanogaster (166)* and from gonads of the *starfish Asterias rubens (167)*. Additionally, N-terminal alanine methylation was found for *Tetrahymena* histone H2B (168,169), and *Arabidopsis* histone H2B variants HTB9 and HTB11 (170). Other eukaryotic proteins known to be α-N-methylated include rabbit myosin light chain LC-1 (171) and LC-2 (172), cytochrome c-557 from *Crithidia oncopelti (173,174)*, and ribosomal proteins L12 (175-177) and S25 (178). Additionally, several human proteins including RCC1 (179), SET, and retinoblastoma (Rb) (180), centromere protein B (CENPB) (181), centromere protein A (CENPA) (182) and damaged DNA-binding protein 2 (DDB2) (183) were identified to be α-N-methylated, and these proteins were found to be substrates for the newly discovered human N-terminal methyltransferase 1 (NTMT1) (180).

1.4.2 Yeast and human α-N-methyltransferases and their substrate specificity

In 2010, the long-sought α-N-methyltransferase in yeast and human were discovered to be Ntm1 encoded by gene YBR261C/*TAE1* and its homolog NTMT1 encoded by gene *METTL11A*, respectively (180,184). Unlike N-terminal acetylation, which normally occurs in the cytoplasmic fraction, the α-N-methyltransferase is predominantly distributed in the nuclear fraction. Originally, Ntm1 in yeast and NTMT1 in human were thought to recognize a consensus N-terminal sequence motif of XPK ("X" represents S, P or A, with the initiator methionine removed) (180,184). Subsequent

studies to characterize substrates of human NTMT1 expanded this recognition motif (185). These investigations elevated the number of potential α-N-methylated proteins to be about 300, and thus unlike the previous view as a rare PTM, α-N-methylation could be a widespread PTM in cells. In addition, NTMT2 encoded by gene *METTL11B* in human is discovered to be an α-N-methyltransferase which primarily monomethylates the same categories of substrates as NTMT1 (186). As shown in Table 1.1, almost all identified α-N-methylated proteins from different organisms carry the same XPK motif, suggesting that the NTMT orthologs throughout the eukaryotic organisms carry the same enzymatic activity and are potential N-terminal methyltransferase. Blast result displayed in Figure 1.5 indeed show homologs of NTMT from *Schizosaccharomyces pombe*, *Drosophila melanogaster*, *Caenorhabditis elegans* and *Arabidopsis thaliana*, which all belong to class I methyltransferase family, shared conserved seven-stranded structure motif I, II and III (184). Indeed, NTMT homolog dNTMT in *Drosophila* was also demonstrated to catalyze α-N-methylation of H2B (187). Therefore, characterization of authentic N-terminal methyltransferase is in need for understanding better this conserved α-N-methylation.

1.4.3 Putting α-N-methyltransferase into a regulatory view

Various cellular stress such as high cell density, heat shock and arsenite treatment can stimulate the α-N-methylation in H2B from *Drosophila melanogaster* (166,187) and human CENPB (181). In addition, α-N-methylation in H2B from

Table 1.1. A list of known α-N-methylated eukaryotic proteins.

Proteins	N-terminal sequence	Reference
Histone H2B		
Neurospora crassa	PPKPADKK	44
Drosophila melanogaster	PPKTSGKA	166
Asterias rubens	PPKPSGKG	167
Tetrahymena thermophila	APKKAPAA	168,169
***Arabidopsis thaliana,* HTB11**	APKAEKKP	170
***Arabidopsis thaliana,* HTB9**	APRAEKKP	170
Other proteins		
***Saccharomyces cerevisiae* ribosomal protein S25**	PPKQQKSK	178
***Saccharomyces cerevisiae* ribosomal protein L12**	PPKQQKSK	175
***Saccharomyces pombe* ribosomal protein L12**	PPKFDPNE	176
***Arabidopsis thaliana* ribosomal protein L12**	PPKLDPSQ	177
Rabbit myosin light chain LC-1	APKKNVK	171
Rabbit myosin light chain LC-2	APKKAKR	172
***Crithidia oncopelti* cytochrome c-557**	PPKAREPL	173,174
Human RCC1	SPKRIAKR	179
Human SET translocation	APKRQSAI	180
Human retinoblastoma protein 1	PPKTPRKT	180
Human CENPB	GPKRRQLT	181
Human CENPA	GPRRRSRK	182
Human DDB2	APKKRPET	183

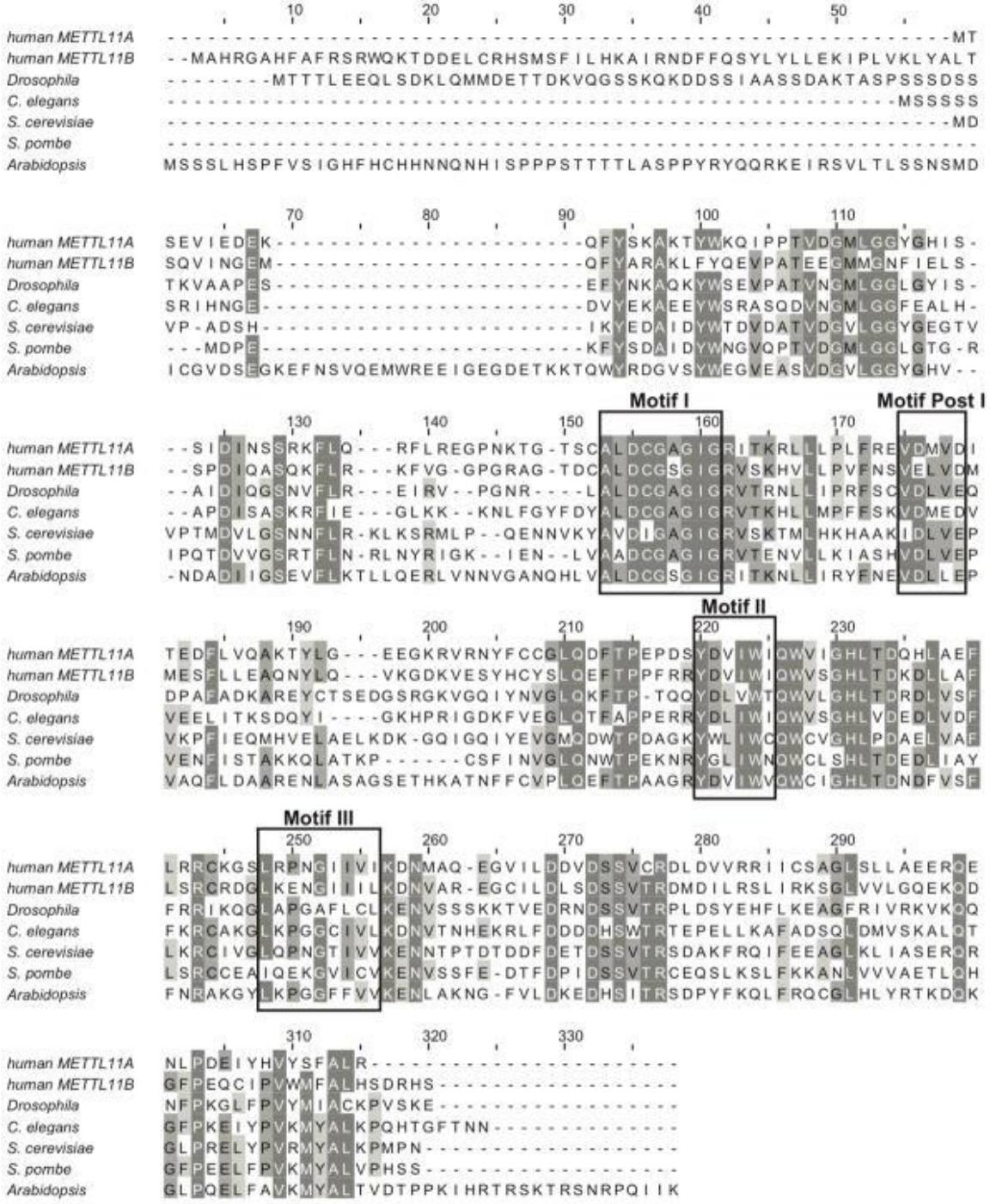

Figure 1. 5. Human NTMT1 and Yeast Ntm1 homologs in eukaryotes. (Adapted from Ref. 184).

Drosophila melanogaster and in human CENPA increases during development and cell cycle progression, respectively (182,187). Our unpublished data in Chapter 4 also revealed that α-N-methylation of human MRG15 is elevated under the treatment of radiomimetic drug neocarzinostatin (NCS) and interstrand cross-linking agent mitomycin C (MMC). These results suggest that α-N-methylation is dynamic and mechanisms must exist to control its level.

Two potential mechanisms for the regulation of α-N-methylation were proposed based on a study in *Drosophila melanogaster*, which revealed the interaction between dNTMT and histone arginine methyltransferase dART8 and the negative correlation between the expression level of dART8 and the level of α-N-methylation in H2B (187). One hypothesis attributed the observations to negative crosstalk between methylation at arginine 2 in histone H3 (H3R2me) and α-N-methylation in H2B. The other argues that the phenomena arise from the competition of these two enzymes for the same cofactor, namely, *S*-adenosyl-L-methionine (SAM). However, further studies are in need to characterize whether any binding partners of NTMT1 can regulate its enzyme activity in human cells.

While the above hypotheses may also apply to human cells, it is worth mentioning that NTMT1 exhibits high binding affinity towards its own product, i.e., fully α-N-methylated proteins (185). This binding is thought to occur through a cation-π interaction between a conserved triad of aromatic residues (Y19, W20 and H141) with the trimethylated amine group, as shown in Figure 1.6 (185). In this respect, a product feedback inhibition and competition between substrates are implicated to regulate

NTMT1. Additionally, other ways to restrict NTMT1 substrate include cellular localization (only nuclear protein can be α-N-methylated since NTMT1 is predominantly distributed in nuclear fraction) and tissue specificity (MLC9 from 293LT cell is N-terminally acetylated but from mouse spleen extract is N-terminally methylated) (185). Furthermore, it is of significance to examine whether NTMT1 carry important PTMs which control its function upon cellular stress.

Viewing the fact that demethylases such as LSD1 and LSD2 can regulate histone methylation by demethylation (188,189) and the great similarity between histone methylation and α-N-methylation, it is hypothesized that demethylase may also exist for α-N-methylation. Thus, demethylation is another potential mechanism through which α-N-methylation is regulated.

1.4.4 Functional implications of α-N-methylation

α-N-methylation was initially identified as an N-terminal blocking group which protects cells from digestion by aminopeptidases (155,174) and hinders the N-end rule pathway (190). Unlike N-terminal acetylation which removes the positive charge from N-terminus, α-N-trimethylation (or dimethylation of proline residue) introduces a permanent cation to the N-terminal amino group. This positive charge can be sustained even under hydrophobic environment where unmodified amino group is readily deprotonated (150). Therefore, α-N-methylation is well-suited to promote protein/DNA and protein/protein interactions.

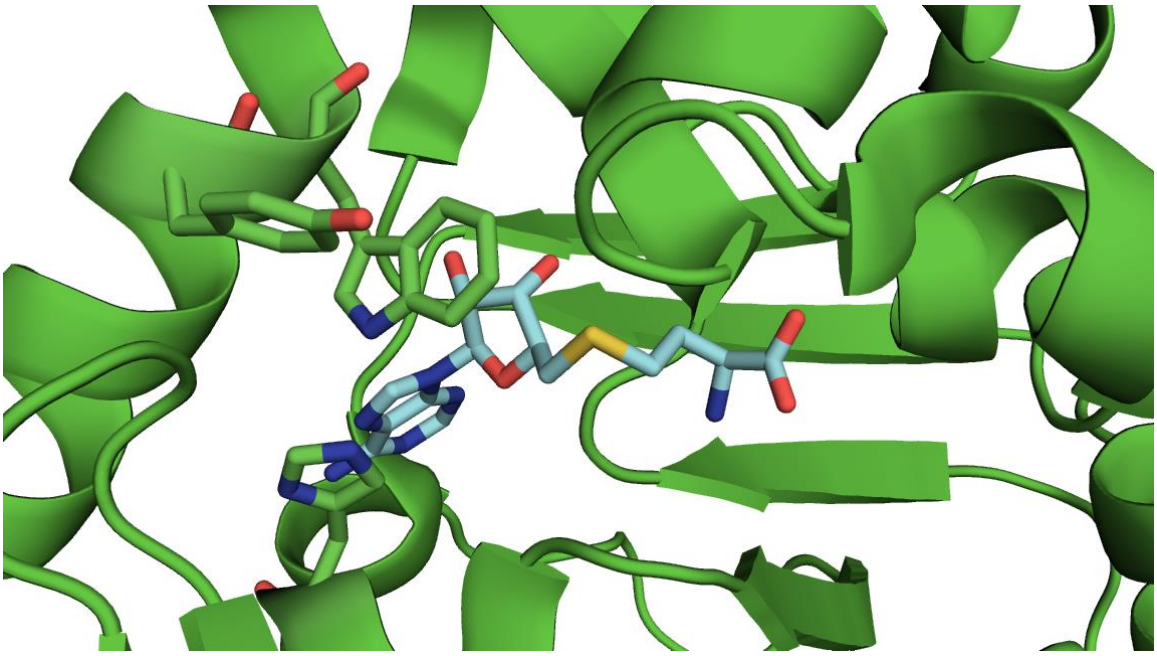

Figure 1. 6. Predicted binding module of NTMT1 for methylated peptide. (Adapted from Ref185).

Several lines of evidence support that α-N-methylation can promote the interaction of α-N-methylated protein to DNA, which carries negative charged phosphate groups, via electrostatic interaction. RCC1 mutants defective in N-terminal methylation bind much more weakly to chromatin during mitosis (179); in line with this observation, depletion of NTMT1 was found to exert similar effects (180). Likewise, loss of α-N-methylation of CENPB triggers a declined binding toward centromeric CENP-B box DNA (181), and α-N-methylation in DDB2 was found to promote its localization to DNA damage sites (183).

Since α-N-methylated proteins are often found to be present in multi-subunit complexes, it is proposed that α-N-methylation can promote protein-protein interaction (150,191). The "Royal Family" modules such as chromo, Tudor and PWWP domains possess an aromatic cage that can read specific histone methyl-lysine marks (192). We hypothesize that proteins containing this "Royal Family" module are promising readers for α-N-methylated proteins. Indeed, our unpublished data in chapter 4 revealed that the α-N-methylated N-terminal tail of MRG15 can be recognized by the chromo domain of TIP60, a histone acetyltransferase. Moreover, the interaction allosterically stimulates TIP60's enzyme activity.

The diversity of the proteins which can be α-N-methylated determined the dynamic range of its functional implications. In yeast, α-N-methylation in a proteasome protein Rpt1 was demonstrated to play a significant role in cell growth and stress tolerance (193). Strains which carry deletion for the *TAE1* gene that encodes yeast α-N-

methyltransferase Ntm1 display an altered ribosome profile with declined translation efficiency and fidelity (194). In human cells, reduced chromatin localization of α-N-methylation-defective mutant of RCC1 leads to a spindle pole defect and increased aneuploidy (179). Likewise, loss of α-N-methylation in DDB2 results in reduced repair efficiency toward CPDs, decreased ATM activation and less tolerance of the genotoxic effects of UV exposure (183). Moreover, α-N-methylation in MRG15 serves as a molecular hook to hold the chromo domain of TIP60 and promotes histone crosstalk between H3K36me3 and H4K16ac. In addition, defective α-N-methylation in MRG15 contributes to reduced HR and ATM activation (unpublished data in Chapter 4).

Consistent with the importance of α-N-methylation, abnormal NTMT1 expression has been recorded in numerous cancer cells. For instance, while up-regulation of NTMT1 was documented in colorectal cancers (195,196) and lymphomas (197), down-regulation of NTMT1 was observed in testicular seminomas (198) and the breast tumor stromal (199). Moreover, numerous phenotypes associated with defective DNA repair such as smaller size, female infertility, liver degeneration and premature death are displayed in NTMT1 knockout mice (191).

1.5 Phosphorylation

Unlike α-N-methylation, the functional importance of which has only begun to be investigated in the recent years, phosphorylation is a type of PTM of which the significance is well appreciated. In 1992, in light of "their discoveries concerning reversible protein phosphorylation as a biological regulatory mechanism", Edmond H.

Fischer and Edwin G Krebs were awarded with Nobel Prize in Physiology/Medicine. As a reversible modification, phosphorylation, which is carefully regulated by protein kinase and phosphatase, acts as a central mechanism to regulate almost every cellular process. Due to the strong correlation of misregulation of phosphorylation and cancer, kinases have been considered as good targets for drug development in cancer therapy (200).

Cyclin-dependent kinases (Cdks), which belong to serine/threonine kinases, being correctly switched on and off for their enzyme activity ensures the smooth transition between different phases of the cell cycle (201). Recently, the roles of Cdks were found to be beyond cell cycle regulation (202). For example, Cdk1-dependent phosphorylation of yeast nucleases Sae2 and Dna2 spur DNA-end resection and HR (203,204). Flavopiridol, a flavone synthetically derived from an alkaloid isolated from the leaves and stems from plants indigenous to India, is one of the effective inhibitors of Cdks (Cdk1, 2, 4, 6 and 7) (205,206).

Besides working individually, phosphorylation can crosstalk with other PTMs, one well-documented example of which is ubiquitination. In this respect, phosphorylation can regulate ubiquitination either through the substrates or the E3 ubiquitin ligase (207).

1.6 PTMs of core histones

In mammals the genetic information is compacted to a hierarchy structure-chromatin. Core unit of chromatin is nucleosome which is composed of 147 base pair DNA wrapping around a histone octamer consisting of two H2A-H2B dimers and a $(H3\text{-}H4)_2$ tetramer (208). The protruded N-terminal tails of histones render them good targets for PTMs. To regulate cellular function, some of the PTMs in histones directly modify

chromatin structure and others operate through binding modules for chromatin modifier proteins (209). Here I mainly discuss about two types of histone PTMs, i.e. acetylation of lysine 16 in histone H4 (H4K16ac) and trimethylation of histone H3 at lysine 36 (H3K36me3) which are highly relevant to the research in this dissertation.

1.6.1 H4K16ac

Previously, it was reported that high extent of acetylation hinders the higher order compaction of nucleosome arrays (210). Moreover, N-terminal tails of H4, specifically residues 14-19 were found to be critical for the formation of 30 nm chromatin fibers (211). In line with this, the acetylation of lysine 16 on H4 (H4K16ac) alone is found to be able to decompact the 30 nm fiber structure of chromatin (212). The relaxation of chromatin allows easy access of chromatin by non-histone proteins, which is important in many biological processes such as ATM activation (213). Not surprisingly, hypoacetylation of H4K16 is redeemed as a hallmark for human cancer (214).

1.6.2 H3K36me3

In human cells, H3K36 can be methylated by several histone methyltransferases (HMTs) which harbor the same catalytic SET domain to enable the mono-, di- or tri-methylation of substrate proteins (215). Among these HMTs, SETD2 is the sole enzyme responsible for the methylation of H3K36me2 to H3K36me3 (216). The role of H3K36me3 in regulation of gene expression is well established (215); however, the

critical role of H3K36me3 in DNA damage repair including MMR and HR was revealed only recently (217-220).

1.7 Scope of the dissertation

The research covered in this dissertation focuses on identification and functional characterizations of the novel PTMs of DDB2 and MRG15, which are important in NER and HR, respectively. These studies aim to improve our understanding of α-N-methylation in DNA repair pathway and delineate biological implications of a novel serine 26 phosphorylation in DDB2.

In Chapter two, by using LC-MS/MS, we found that, in human cells, the initiating methionine residue in DDB2 was removed and the N-terminal alanine could be methylated on its α-amino group, with trimethylation being the major form. I also demonstrated that the α-N-methylation of DDB2 is catalyzed by NTMT1. In addition, a methylation-defective mutant of DDB2 displayed diminished nuclear localization and was recruited at a reduced efficiency to UV-induced CPD foci. Moreover, loss of this methylation conferred compromised ATM activation, decreased efficiency in CPD repair, and elevated sensitivity of cells toward UV light exposure. Together, my study provided new knowledge about the post-translational regulation of DDB2 and expanded the biological functions of protein α-N-methylation to DNA repair.

In Chapter three, I reported that DDB2 could be phosphorylated at Serine 26 in HEK293T cells. The phosphorylation level was significantly reduced in cells treated with flavopiridol, an inhibitor for Cdks, suggesting the involvement of Cdks in this phosphorylation. I also found that a DDB2 mutant deficient in Ser26 phosphorylation

failed to be recruited to UV light-induced CPD foci. Furthermore, this phosphorylation was shown to be critical for proteasomal degradation of DDB2, ATM activation, CPD repair, and cellular resistance toward UV light. I conclude that the phosphorylation of Ser26 in DDB2 plays a significant role in NER.

In Chapter four, I further extended the target of NTMT1 in human cells to MRG15. I observed that the α-N-methylated N-terminus of MRG15 enables its interaction with TIP60 histone acetyltransferase through binding to the chromo domain of TIP60 and stimulates allosterically the enzymatic activity of the latter. Additionally, I found that this α-N-methylation-chromo domain interaction is indispensable for H4K16Ac, for DNA damage-induced ATM activation, for the repair of double strand breaks via the homologous recombination pathway, and for protecting cells from the genotoxic effects of ionizing radiation and interstrand cross-linking agents. Moreover, I observed that the function of α-N-methylation of MRG15 in H4K16Ac and DNA damage-induced ATM activation necessitate MRG15's binding to chromatin via the interaction between its chromo domain and H3K36me3. Collectively, my study unveiled, for the first time, the α-N-methylation of MRG15, and discovered novel functions of protein α-N-methylation in the context of DNA damage response and repair. I also uncovered a novel trans-histone modification where H3K36me3 drives H4K16Ac in human cells, revealed the essential role of MRG15 in this process, and demonstrated the importance of this trans-histone modification in ATM activation and homologous recombination repair.

Reference

1. (2004) Finishing the euchromatic sequence of the human genome. *Nature*, **431**, 931-945.

2. Metzker, M.L. (2010) Sequencing technologies - the next generation. *Nat Rev Genet*, **11**, 31-46.

3. James, P. (1997) Protein identification in the post-genome era: the rapid rise of proteomics. *Q Rev Biophys*, **30**, 279-331.

4. Park, P.J. (2009) ChIP-seq: advantages and challenges of a maturing technology. *Nat Rev Genet*, **10**, 669-680.

5. MacBeath, G. (2002) Protein microarrays and proteomics. *Nat Genet*, **32 Suppl**, 526-532.

6. Yee, A., Chang, X., Pineda-Lucena, A., Wu, B., Semesi, A., Le, B., Ramelot, T., Lee, G.M., Bhattacharyya, S., Gutierrez, P. *et al.* (2002) An NMR approach to structural proteomics. *Proc Natl Acad Sci U S A*, **99**, 1825-1830.

7. Vercauteren, F.G., Bergeron, J.J., Vandesande, F., Arckens, L. and Quirion, R. (2004) Proteomic approaches in brain research and neuropharmacology. *Eur J Pharmacol*, **500**, 385-398.

8. Tyers, M. and Mann, M. (2003) From genomics to proteomics. *Nature*, **422**, 193-197.

9. Rehm, T., Huber, R. and Holak, T.A. (2002) Application of NMR in structural proteomics: screening for proteins amenable to structural analysis. *Structure*, **10**, 1613-1618.

10. Christendat, D., Yee, A., Dharamsi, A., Kluger, Y., Savchenko, A., Cort, J.R., Booth, V., Mackereth, C.D., Saridakis, V., Ekiel, I. *et al.* (2000) Structural proteomics of an archaeon. *Nat Struct Biol*, **7**, 903-909.

11. Bunai, K. and Yamane, K. (2005) Effectiveness and limitation of two-dimensional gel electrophoresis in bacterial membrane protein proteomics and perspectives. *J Chromatogr B Analyt Technol Biomed Life Sci*, **815**, 227-236.

12. Cravatt, B.F., Simon, G.M. and Yates, J.R., 3rd. (2007) The biological impact of mass-spectrometry-based proteomics. *Nature*, **450**, 991-1000.

13. Bantscheff, M., Schirle, M., Sweetman, G., Rick, J. and Kuster, B. (2007) Quantitative mass spectrometry in proteomics: a critical review. *Anal Bioanal Chem*, **389**, 1017-1031.

14. Ong, S.E., Blagoev, B., Kratchmarova, I., Kristensen, D.B., Steen, H., Pandey, A. and Mann, M. (2002) Stable isotope labeling by amino acids in cell culture, SILAC, as a simple and accurate approach to expression proteomics. *Mol Cell Proteomics*, **1**, 376-386.

15. Gygi, S.P., Rist, B., Gerber, S.A., Turecek, F., Gelb, M.H. and Aebersold, R. (1999) Quantitative analysis of complex protein mixtures using isotope-coded affinity tags. *Nat Biotechnol*, **17**, 994-999.

16. Wiese, S., Reidegeld, K.A., Meyer, H.E. and Warscheid, B. (2007) Protein labeling by iTRAQ: a new tool for quantitative mass spectrometry in proteome research. *Proteomics*, **7**, 340-350.

17. Hsu, J.L., Huang, S.Y., Chow, N.H. and Chen, S.H. (2003) Stable-isotope dimethyl labeling for quantitative proteomics. *Anal Chem*, **75**, 6843-6852.

18. Gerber, S.A., Rush, J., Stemman, O., Kirschner, M.W. and Gygi, S.P. (2003) Absolute quantification of proteins and phosphoproteins from cell lysates by tandem MS. *Proc Natl Acad Sci U S A*, **100**, 6940-6945.

19. Trinkle-Mulcahy, L., Boulon, S., Lam, Y.W., Urcia, R., Boisvert, F.M., Vandermoere, F., Morrice, N.A., Swift, S., Rothbauer, U., Leonhardt, H. *et al.* (2008) Identifying specific protein interaction partners using quantitative mass spectrometry and bead proteomes. *J Cell Biol*, **183**, 223-239.

20. Neubauer, G., King, A., Rappsilber, J., Calvio, C., Watson, M., Ajuh, P., Sleeman, J., Lamond, A. and Mann, M. (1998) Mass spectrometry and EST-database searching allows characterization of the multi-protein spliceosome complex. *Nat Genet*, **20**, 46-50.

21. Danial, N.N., Gramm, C.F., Scorrano, L., Zhang, C.Y., Krauss, S., Ranger, A.M., Datta, S.R., Greenberg, M.E., Licklider, L.J., Lowell, B.B. *et al.* (2003) BAD and glucokinase reside in a mitochondrial complex that integrates glycolysis and apoptosis. *Nature*, **424**, 952-956.

22. Vermeulen, M., Hubner, N.C. and Mann, M. (2008) High confidence determination of specific protein-protein interactions using quantitative mass spectrometry. *Curr Opin Biotechnol*, **19**, 331-337.

23. Larsen, M.R., Trelle, M.B., Thingholm, T.E. and Jensen, O.N. (2006) Analysis of posttranslational modifications of proteins by tandem mass spectrometry. *Biotechniques*, **40**, 790-798.

24. Aebersold, R. and Mann, M. (2003) Mass spectrometry-based proteomics. *Nature*, **422**, 198-207.

25. Yamashita, M. and Fenn, J.B. (1984) Electrospray Ion-Source - Another Variation on the Free-Jet Theme. *J Phys Chem-Us*, **88**, 4451-4459.

26. Abate, R., Ballistreri, A., Montaudo, G., Garozzo, D., Impallomeni, G., Critchley, G. and Tanaka, K. (1993) Quantitative Applications of Matrix-Assisted Laser-Desorption Ionization with Time-of-Flight Mass-Spectrometry - Determination of Copolymer Composition in Bacterial Copolyesters. *Rapid Commun Mass Sp*, **7**, 1033-1036.

27. Fenn, J.B., Mann, M., Meng, C.K., Wong, S.F. and Whitehouse, C.M. (1989) Electrospray Ionization for Mass-Spectrometry of Large Biomolecules. *Science*, **246**, 64-71.

28. Whitehouse, C.M., Dreyer, R.N., Yamashita, M. and Fenn, J.B. (1985) Electrospray interface for liquid chromatographs and mass spectrometers. *Anal Chem*, **57**, 675-679.

29. Emmett, M.R. and Caprioli, R.M. (1994) Micro-electrospray mass spectrometry: Ultra-high-sensitivity analysis of peptides and proteins. *J Am Soc Mass Spectrom*, **5**, 605-613.

30. Olsen, J.V., Schwartz, J.C., Griep-Raming, J., Nielsen, M.L., Damoc, E., Denisov, E., Lange, O., Remes, P., Taylor, D., Splendore, M. *et al.* (2009) A dual pressure linear ion trap Orbitrap instrument with very high sequencing speed. *Mol Cell Proteomics*, **8**, 2759-2769.

31. Medzihradszky, K.F., Campbell, J.M., Baldwin, M.A., Falick, A.M., Juhasz, P., Vestal, M.L. and Burlingame, A.L. (2000) The characteristics of peptide collision-induced dissociation using a high-performance MALDI-TOF/TOF tandem mass spectrometer. *Anal Chem*, **72**, 552-558.

32. Tang, X.J., Thibault, P. and Boyd, R.K. (1993) Fragmentation reactions of multiply-protonated peptides and implications for sequencing by tandem mass spectrometry with low-energy collision-induced dissociation. *Anal Chem*, **65**, 2824-2834.

33. Mann, M. and Jensen, O.N. (2003) Proteomic analysis of post-translational modifications. *Nat Biotechnol*, **21**, 255-261.

34. Olsen, J.V., Macek, B., Lange, O., Makarov, A., Horning, S. and Mann, M. (2007) Higher-energy C-trap dissociation for peptide modification analysis. *Nat Methods*, **4**, 709-712.

35. Zubarev, R.A., Horn, D.M., Fridriksson, E.K., Kelleher, N.L., Kruger, N.A., Lewis, M.A., Carpenter, B.K. and McLafferty, F.W. (2000) Electron capture dissociation for structural characterization of multiply charged protein cations. *Anal Chem*, **72**, 563-573.

36. Syka, J.E., Coon, J.J., Schroeder, M.J., Shabanowitz, J. and Hunt, D.F. (2004) Peptide and protein sequence analysis by electron transfer dissociation mass spectrometry. *Proc Natl Acad Sci U S A*, **101**, 9528-9533.

37. Xia, Y., Chrisman, P.A., Erickson, D.E., Liu, J., Liang, X., Londry, F.A., Yang, M.J. and McLuckey, S.A. (2006) Implementation of ion/ion reactions in a quadrupole/time-of-flight tandem mass spectrometer. *Anal Chem*, **78**, 4146-4154.

38. Silva, A.M., Vitorino, R., Domingues, M.R., Spickett, C.M. and Domingues, P. (2013) Post-translational modifications and mass spectrometry detection. *Free Radic Biol Med*, **65**, 925-941.

39. Domon, B. and Aebersold, R. (2006) Mass spectrometry and protein analysis. *Science*, **312**, 212-217.

40. Xiong, L., Adhvaryu, K.K., Selker, E.U. and Wang, Y. (2010) Mapping of lysine methylation and acetylation in core histones of Neurospora crassa. *Biochemistry*, **49**, 5236-5243.

41. Xiong, L. and Wang, Y. (2011) Mapping Post-translational Modifications of Histones H2A, H2B and H4 in Schizosaccharomyces pombe. *Int J Mass Spectrom*, **301**, 159-165.

42. Farley, A.R. and Link, A.J. (2009) Identification and quantification of protein posttranslational modifications. *Methods Enzymol*, **463**, 725-763.

43. Mann, M. and Wilm, M. (1994) Error-tolerant identification of peptides in sequence databases by peptide sequence tags. *Anal Chem*, **66**, 4390-4399.

44. Eng, J.K., McCormack, A.L. and Yates, J.R. (1994) An approach to correlate tandem mass spectral data of peptides with amino acid sequences in a protein database. *J Am Soc Mass Spectrom*, **5**, 976-989.

45. Perkins, D.N., Pappin, D.J., Creasy, D.M. and Cottrell, J.S. (1999) Probability-based protein identification by searching sequence databases using mass spectrometry data. *Electrophoresis*, **20**, 3551-3567.

46. Fridriksson, E.K., Baird, B. and McLafferty, F.W. (1999) Electrospray mass spectra from protein electroeluted from sodium dodecylsulfate polyacrylamide gel electrophoresis gels. *J Am Soc Mass Spectrom*, **10**, 453-455.

47. Ge, Y., Lawhorn, B.G., ElNaggar, M., Strauss, E., Park, J.H., Begley, T.P. and McLafferty, F.W. (2002) Top down characterization of larger proteins (45 kDa) by electron capture dissociation mass spectrometry. *J Am Chem Soc*, **124**, 672-678.

48. Siuti, N. and Kelleher, N.L. (2007) Decoding protein modifications using top-down mass spectrometry. *Nat Methods*, **4**, 817-821.

49. Zhou, H., Ning, Z., Starr, A.E., Abu-Farha, M. and Figeys, D. (2012) Advancements in top-down proteomics. *Anal Chem*, **84**, 720-734.

50. LeDuc, R.D., Taylor, G.K., Kim, Y.B., Januszyk, T.E., Bynum, L.H., Sola, J.V., Garavelli, J.S. and Kelleher, N.L. (2004) ProSight PTM: an integrated environment for protein identification and characterization by top-down mass spectrometry. *Nucleic Acids Res*, **32**, W340-345.

51. Forbes, A.J., Mazur, M.T., Patel, H.M., Walsh, C.T. and Kelleher, N.L. (2001) Toward efficient analysis of >70 kDa proteins with 100% sequence coverage. *Proteomics*, **1**, 927-933.

52. Ge, Y., Rybakova, I.N., Xu, Q. and Moss, R.L. (2009) Top-down high-resolution mass spectrometry of cardiac myosin binding protein C revealed that truncation alters protein phosphorylation state. *Proc Natl Acad Sci U S A*, **106**, 12658-12663.

53. Jackson, S.P. and Bartek, J. (2009) The DNA-damage response in human biology and disease. *Nature*, **461**, 1071-1078.

54. Lindahl, T. (1993) Instability and decay of the primary structure of DNA. *Nature*, **362**, 709-715.

55. Wang, Y. (2008) Bulky DNA lesions induced by reactive oxygen species. *Chem Res Toxicol*, **21**, 276-281.

56. Finkel, T. and Holbrook, N.J. (2000) Oxidants, oxidative stress and the biology of ageing. *Nature*, **408**, 239-247.

57. Pegg, A.E. (1990) Mammalian O6-alkylguanine-DNA alkyltransferase: regulation and importance in response to alkylating carcinogenic and therapeutic agents. *Cancer Res*, **50**, 6119-6129.

58. Sancar, A. (2003) Structure and function of DNA photolyase and cryptochrome blue-light photoreceptors. *Chem Rev*, **103**, 2203-2237.

59. Jiricny, J. (2006) The multifaceted mismatch-repair system. *Nat Rev Mol Cell Biol*, **7**, 335-346.

60. David, S.S., O'Shea, V.L. and Kundu, S. (2007) Base-excision repair of oxidative DNA damage. *Nature*, **447**, 941-950.

61. de Laat, W.L., Jaspers, N.G. and Hoeijmakers, J.H. (1999) Molecular mechanism of nucleotide excision repair. *Genes Dev*, **13**, 768-785.

62. Lieber, M.R. (2008) The mechanism of human nonhomologous DNA end joining. *J Biol Chem*, **283**, 1-5.

63. San Filippo, J., Sung, P. and Klein, H. (2008) Mechanism of eukaryotic homologous recombination. *Annu Rev Biochem*, **77**, 229-257.

64. Douki, T., Court, M., Sauvaigo, S., Odin, F. and Cadet, J. (2000) Formation of the main UV-induced thymine dimeric lesions within isolated and cellular DNA as measured by high performance liquid chromatography-tandem mass spectrometry. *J Biol Chem*, **275**, 11678-11685.

65. de Laat, W.L., Jaspers, N.G. and Hoeijmakers, J.H. (1999) Molecular mechanism of nucleotide excision repair. *Genes Dev.*, **13**, 768-785.

66. Hanawalt, P.C. (2002) Subpathways of nucleotide excision repair and their regulation. *Oncogene*, **21**, 8949-8956.

67. Lans, H., Marteijn, J.A. and Vermeulen, W. (2012) ATP-dependent chromatin remodeling in the DNA-damage response. *Epigenetics Chromatin*, **5**, 4.

68. Moser, J., Volker, M., Kool, H., Alekseev, S., Vrieling, H., Yasui, A., van Zeeland, A.A. and Mullenders, L.H. (2005) The UV-damaged DNA binding protein mediates efficient targeting of the nucleotide excision repair complex to UV-induced photo lesions. *DNA Repair (Amst)*, **4**, 571-582.

69. Aboussekhra, A., Biggerstaff, M., Shivji, M.K., Vilpo, J.A., Moncollin, V., Podust, V.N., Protic, M., Hubscher, U., Egly, J.M. and Wood, R.D. (1995)

Mammalian DNA nucleotide excision repair reconstituted with purified protein components. *Cell*, **80**, 859-868.

70. Sugasawa, K., Okamoto, T., Shimizu, Y., Masutani, C., Iwai, S. and Hanaoka, F. (2001) A multistep damage recognition mechanism for global genomic nucleotide excision repair. *Genes Dev*, **15**, 507-521.

71. Fousteri, M. and Mullenders, L.H. (2008) Transcription-coupled nucleotide excision repair in mammalian cells: molecular mechanisms and biological effects. *Cell Res*, **18**, 73-84.

72. Brueckner, F., Hennecke, U., Carell, T. and Cramer, P. (2007) CPD damage recognition by transcribing RNA polymerase II. *Science*, **315**, 859-862.

73. Sarker, A.H., Tsutakawa, S.E., Kostek, S., Ng, C., Shin, D.S., Peris, M., Campeau, E., Tainer, J.A., Nogales, E. and Cooper, P.K. (2005) Recognition of RNA polymerase II and transcription bubbles by XPG, CSB, and TFIIH: insights for transcription-coupled repair and Cockayne Syndrome. *Mol Cell*, **20**, 187-198.

74. Araujo, S.J., Tirode, F., Coin, F., Pospiech, H., Syvaoja, J.E., Stucki, M., Hubscher, U., Egly, J.M. and Wood, R.D. (2000) Nucleotide excision repair of DNA with recombinant human proteins: definition of the minimal set of factors, active forms of TFIIH, and modulation by CAK. *Genes Dev*, **14**, 349-359.

75. Staresincic, L., Fagbemi, A.F., Enzlin, J.H., Gourdin, A.M., Wijgers, N., Dunand-Sauthier, I., Giglia-Mari, G., Clarkson, S.G., Vermeulen, W. and Scharer, O.D. (2009) Coordination of dual incision and repair synthesis in human nucleotide excision repair. *EMBO J*, **28**, 1111-1120.

76. Sertic, S., Pizzi, S., Lazzaro, F., Plevani, P. and Muzi-Falconi, M. (2012) NER and DDR: classical music with new instruments. *Cell Cycle*, **11**, 668-674.

77. Kraemer, K.H., Patronas, N.J., Schiffmann, R., Brooks, B.P., Tamura, D. and DiGiovanna, J.J. (2007) Xeroderma pigmentosum, trichothiodystrophy and Cockayne syndrome: a complex genotype-phenotype relationship. *Neuroscience*, **145**, 1388-1396.

78. Lehmann, A.R. (2003) DNA repair-deficient diseases, xeroderma pigmentosum, Cockayne syndrome and trichothiodystrophy. *Biochimie*, **85**, 1101-1111.

79. Cleaver, J.E. (2005) Cancer in xeroderma pigmentosum and related disorders of DNA repair. *Nat Rev Cancer*, **5**, 564-573.

80. Tang, J.Y., Hwang, B.J., Ford, J.M., Hanawalt, P.C. and Chu, G. (2000) Xeroderma pigmentosum p48 gene enhances global genomic repair and suppresses UV-induced mutagenesis. *Mol Cell*, **5**, 737-744.

81. Pines, A., Backendorf, C., Alekseev, S., Jansen, J.G., de Gruijl, F.R., Vrieling, H. and Mullenders, L.H. (2009) Differential activity of UV-DDB in mouse keratinocytes and fibroblasts: impact on DNA repair and UV-induced skin cancer. *DNA Repair (Amst)*, **8**, 153-161.

82. Fitch, M.E., Nakajima, S., Yasui, A. and Ford, J.M. (2003) In vivo recruitment of XPC to UV-induced cyclobutane pyrimidine dimers by the DDB2 gene product. *J Biol Chem*, **278**, 46906-46910.

83. Scrima, A., Konickova, R., Czyzewski, B.K., Kawasaki, Y., Jeffrey, P.D., Groisman, R., Nakatani, Y., Iwai, S., Pavletich, N.P. and Thoma, N.H. (2008) Structural basis of UV DNA-damage recognition by the DDB1-DDB2 complex. *Cell*, **135**, 1213-1223.

84. Guzder, S.N., Habraken, Y., Sung, P., Prakash, L. and Prakash, S. (1995) Reconstitution of yeast nucleotide excision repair with purified Rad proteins, replication protein A, and transcription factor TFIIH. *J Biol Chem*, **270**, 12973-12976.

85. Mu, D., Park, C.H., Matsunaga, T., Hsu, D.S., Reardon, J.T. and Sancar, A. (1995) Reconstitution of human DNA repair excision nuclease in a highly defined system. *J Biol Chem*, **270**, 2415-2418.

86. Moggs, J.G., Yarema, K.J., Essigmann, J.M. and Wood, R.D. (1996) Analysis of incision sites produced by human cell extracts and purified proteins during nucleotide excision repair of a 1,3-intrastrand d(GpTpG)-cisplatin adduct. *J Biol Chem*, **271**, 7177-7186.

87. Yasuda, T., Sugasawa, K., Shimizu, Y., Iwai, S., Shiomi, T. and Hanaoka, F. (2005) Nucleosomal structure of undamaged DNA regions suppresses the non-specific DNA binding of the XPC complex. *DNA Repair (Amst)*, **4**, 389-395.

88. Wakasugi, M., Kawashima, A., Morioka, H., Linn, S., Sancar, A., Mori, T., Nikaido, O. and Matsunaga, T. (2002) DDB accumulates at DNA damage sites immediately after UV irradiation and directly stimulates nucleotide excision repair. *J Biol Chem*, **277**, 1637-1640.

89. Shiyanov, P., Nag, A. and Raychaudhuri, P. (1999) Cullin 4A associates with the UV-damaged DNA-binding protein DDB. *J Biol Chem*, **274**, 35309-35312.

90. Fischer, E.S., Scrima, A., Bohm, K., Matsumoto, S., Lingaraju, G.M., Faty, M., Yasuda, T., Cavadini, S., Wakasugi, M., Hanaoka, F. *et al.* (2011) The molecular basis of CRL4DDB2/CSA ubiquitin ligase architecture, targeting, and activation. *Cell*, **147**, 1024-1039.

91. Jackson, S. and Xiong, Y. (2009) CRL4s: the CUL4-RING E3 ubiquitin ligases. *Trends Biochem Sci*, **34**, 562-570.

92. Groisman, R., Polanowska, J., Kuraoka, I., Sawada, J., Saijo, M., Drapkin, R., Kisselev, A.F., Tanaka, K. and Nakatani, Y. (2003) The ubiquitin ligase activity in the DDB2 and CSA complexes is differentially regulated by the COP9 signalosome in response to DNA damage. *Cell*, **113**, 357-367.

93. Wang, H., Zhai, L., Xu, J., Joo, H.Y., Jackson, S., Erdjument-Bromage, H., Tempst, P., Xiong, Y. and Zhang, Y. (2006) Histone H3 and H4 ubiquitylation by the CUL4-DDB-ROC1 ubiquitin ligase facilitates cellular response to DNA damage. *Mol Cell*, **22**, 383-394.

94. Kapetanaki, M.G., Guerrero-Santoro, J., Bisi, D.C., Hsieh, C.L., Rapic-Otrin, V. and Levine, A.S. (2006) The DDB1-CUL4ADDB2 ubiquitin ligase is deficient in xeroderma pigmentosum group E and targets histone H2A at UV-damaged DNA sites. *Proc Natl Acad Sci U S A*, **103**, 2588-2593.

95. Sugasawa, K., Okuda, Y., Saijo, M., Nishi, R., Matsuda, N., Chu, G., Mori, T., Iwai, S., Tanaka, K. and Hanaoka, F. (2005) UV-induced ubiquitylation of XPC protein mediated by UV-DDB-ubiquitin ligase complex. *Cell*, **121**, 387-400.

96. Chen, X., Zhang, Y., Douglas, L. and Zhou, P. (2001) UV-damaged DNA-binding proteins are targets of CUL-4A-mediated ubiquitination and degradation. *J Biol Chem*, **276**, 48175-48182.

97. Nag, A., Bondar, T., Shiv, S. and Raychaudhuri, P. (2001) The xeroderma pigmentosum group E gene product DDB2 is a specific target of cullin 4A in mammalian cells. *Mol Cell Biol*, **21**, 6738-6747.

98. Liu, L., Lee, S., Zhang, J., Peters, S.B., Hannah, J., Zhang, Y., Yin, Y., Koff, A., Ma, L. and Zhou, P. (2009) CUL4A abrogation augments DNA damage response and protection against skin carcinogenesis. *Mol Cell*, **34**, 451-460.

99. Chen, X., Zhang, J., Lee, J., Lin, P.S., Ford, J.M., Zheng, N. and Zhou, P. (2006) A kinase-independent function of c-Abl in promoting proteolytic destruction of damaged DNA binding proteins. *Mol Cell*, **22**, 489-499.

100. El-Mahdy, M.A., Zhu, Q., Wang, Q.E., Wani, G., Praetorius-Ibba, M. and Wani, A.A. (2006) Cullin 4A-mediated proteolysis of DDB2 protein at DNA damage

sites regulates in vivo lesion recognition by XPC. *J Biol Chem*, **281**, 13404-13411.

101. Wang, Q.E., Wani, M.A., Chen, J., Zhu, Q., Wani, G., El-Mahdy, M.A. and Wani, A.A. (2005) Cellular ubiquitination and proteasomal functions positively modulate mammalian nucleotide excision repair. *Mol Carcinog*, **42**, 53-64.

102. Kopanja, D., Stoyanova, T., Okur, M.N., Huang, E., Bagchi, S. and Raychaudhuri, P. (2009) Proliferation defects and genome instability in cells lacking Cul4A. *Oncogene*, **28**, 2456-2465.

103. Stoyanova, T., Yoon, T., Kopanja, D., Mokyr, M.B. and Raychaudhuri, P. (2008) The xeroderma pigmentosum group E gene product DDB2 activates nucleotide excision repair by regulating the level of p21Waf1/Cip1. *Mol Cell Biol*, **28**, 177-187.

104. Stoyanova, T., Roy, N., Kopanja, D., Bagchi, S. and Raychaudhuri, P. (2009) DDB2 decides cell fate following DNA damage. *Proc Natl Acad Sci U S A*, **106**, 10690-10695.

105. Stoyanova, T., Roy, N., Kopanja, D., Raychaudhuri, P. and Bagchi, S. (2009) DDB2 (damaged-DNA binding protein 2) in nucleotide excision repair and DNA damage response. *Cell Cycle*, **8**, 4067-4071.

106. Hwang, B.J., Ford, J.M., Hanawalt, P.C. and Chu, G. (1999) Expression of the p48 xeroderma pigmentosum gene is p53-dependent and is involved in global genomic repair. *Proc Natl Acad Sci U S A*, **96**, 424-428.

107. Tan, T. and Chu, G. (2002) p53 Binds and activates the xeroderma pigmentosum DDB2 gene in humans but not mice. *Mol Cell Biol*, **22**, 3247-3254.

108. Neecke, H., Lucchini, G. and Longhese, M.P. (1999) Cell cycle progression in the presence of irreparable DNA damage is controlled by a Mec1- and Rad53-dependent checkpoint in budding yeast. *EMBO J*, **18**, 4485-4497.

109. Giannattasio, M., Lazzaro, F., Longhese, M.P., Plevani, P. and Muzi-Falconi, M. (2004) Physical and functional interactions between nucleotide excision repair and DNA damage checkpoint. *EMBO J*, **23**, 429-438.

110. Ray, A., Milum, K., Battu, A., Wani, G. and Wani, A.A. (2013) NER initiation factors, DDB2 and XPC, regulate UV radiation response by recruiting ATR and ATM kinases to DNA damage sites. *DNA Repair (Amst)*, **12**, 273-283.

111. Matsuda, N., Azuma, K., Saijo, M., Iemura, S., Hioki, Y., Natsume, T., Chiba, T. and Tanaka, K. (2005) DDB2, the xeroderma pigmentosum group E gene product,

is directly ubiquitylated by Cullin 4A-based ubiquitin ligase complex. *DNA Repair*, **4**, 537-545.

112. Tsuge, M., Masuda, Y., Kaneoka, H., Kidani, S., Miyake, K. and Iijima, S. (2013) SUMOylation of damaged DNA-binding protein DDB2. *Biochem. Biophys. Res. Commun.*, **438**, 26-31.

113. Cong, F., Tang, J., Hwang, B.J., Vuong, B.Q., Chu, G. and Goff, S.P. (2002) Interaction between UV-damaged DNA binding activity proteins and the c-Abl tyrosine kinase. *J. Biol. Chem.*, **277**, 34870-34878.

114. Zhao, Q., Barakat, B.M., Qin, S., Ray, A., El-Mahdy, M.A., Wani, G., Arafa el, S., Mir, S.N., Wang, Q.E. and Wani, A.A. (2008) The p38 mitogen-activated protein kinase augments nucleotide excision repair by mediating DDB2 degradation and chromatin relaxation. *J. Biol. Chem.*, **283**, 32553-32561.

115. Cai, Q., Fu, L., Wang, Z., Gan, N., Dai, X. and Wang, Y. (2014) a-N-Methylation of damaged DNA-binding protein 2 (DDB2) and its function in nucleotide excision repair. *J. Biol. Chem.*, **289**, 16046-16056.

116. Pines, A., Vrouwe, M.G., Marteijn, J.A., Typas, D., Luijsterburg, M.S., Cansoy, M., Hensbergen, P., Deelder, A., de Groot, A., Matsumoto, S. *et al.* (2012) PARP1 promotes nucleotide excision repair through DDB2 stabilization and recruitment of ALC1. *J. Cell Biol.*, **199**, 235-249.

117. Puumalainen, M.R., Lessel, D., Ruthemann, P., Kaczmarek, N., Bachmann, K., Ramadan, K. and Naegeli, H. (2014) Chromatin retention of DNA damage sensors DDB2 and XPC through loss of p97 segregase causes genotoxicity. *Nat Commun*, **5**, 3695.

118. Cazzalini, O., Perucca, P., Mocchi, R., Sommatis, S., Prosperi, E. and Stivala, L.A. (2014) DDB2 association with PCNA is required for its degradation after UV-induced DNA damage. *Cell Cycle*, **13**, 240-248.

119. Zhang, L., Lubin, A., Chen, H., Sun, Z. and Gong, F. (2012) The deubiquitinating protein USP24 interacts with DDB2 and regulates DDB2 stability. *Cell Cycle*, **11**, 4378-4384.

120. Kattan, Z., Marchal, S., Brunner, E., Ramacci, C., Leroux, A., Merlin, J.L., Domenjoud, L., Dauca, M. and Becuwe, P. (2008) Damaged DNA binding protein 2 plays a role in breast cancer cell growth. *PLoS One*, **3**, e2002.

121. Neale, M.J. and Keeney, S. (2006) Clarifying the mechanics of DNA strand exchange in meiotic recombination. *Nature*, **442**, 153-158.

122. Chapman, J.R., Taylor, M.R. and Boulton, S.J. (2012) Playing the end game: DNA double-strand break repair pathway choice. *Mol Cell*, **47**, 497-510.

123. Horejsi, Z., Falck, J., Bakkenist, C.J., Kastan, M.B., Lukas, J. and Bartek, J. (2004) Distinct functional domains of Nbs1 modulate the timing and magnitude of ATM activation after low doses of ionizing radiation. *Oncogene*, **23**, 3122-3127.

124. Riches, L.C., Lynch, A.M. and Gooderham, N.J. (2008) Early events in the mammalian response to DNA double-strand breaks. *Mutagenesis*, **23**, 331-339.

125. Matsuoka, S., Ballif, B.A., Smogorzewska, A., McDonald, E.R., 3rd, Hurov, K.E., Luo, J., Bakalarski, C.E., Zhao, Z., Solimini, N., Lerenthal, Y. *et al.* (2007) ATM and ATR substrate analysis reveals extensive protein networks responsive to DNA damage. *Science*, **316**, 1160-1166.

126. Stiff, T., O'Driscoll, M., Rief, N., Iwabuchi, K., Lobrich, M. and Jeggo, P.A. (2004) ATM and DNA-PK function redundantly to phosphorylate H2AX after exposure to ionizing radiation. *Cancer Res*, **64**, 2390-2396.

127. Lou, Z., Minter-Dykhouse, K., Franco, S., Gostissa, M., Rivera, M.A., Celeste, A., Manis, J.P., van Deursen, J., Nussenzweig, A., Paull, T.T. *et al.* (2006) MDC1 maintains genomic stability by participating in the amplification of ATM-dependent DNA damage signals. *Mol Cell*, **21**, 187-200.

128. Chapman, J.R. and Jackson, S.P. (2008) Phospho-dependent interactions between NBS1 and MDC1 mediate chromatin retention of the MRN complex at sites of DNA damage. *EMBO Rep*, **9**, 795-801.

129. Melander, F., Bekker-Jensen, S., Falck, J., Bartek, J., Mailand, N. and Lukas, J. (2008) Phosphorylation of SDT repeats in the MDC1 N terminus triggers retention of NBS1 at the DNA damage-modified chromatin. *J Cell Biol*, **181**, 213-226.

130. Kolas, N.K., Chapman, J.R., Nakada, S., Ylanko, J., Chahwan, R., Sweeney, F.D., Panier, S., Mendez, M., Wildenhain, J., Thomson, T.M. *et al.* (2007) Orchestration of the DNA-damage response by the RNF8 ubiquitin ligase. *Science*, **318**, 1637-1640.

131. Doil, C., Mailand, N., Bekker-Jensen, S., Menard, P., Larsen, D.H., Pepperkok, R., Ellenberg, J., Panier, S., Durocher, D., Bartek, J. *et al.* (2009) RNF168 binds and amplifies ubiquitin conjugates on damaged chromosomes to allow accumulation of repair proteins. *Cell*, **136**, 435-446.

132. Bunting, S.F., Callen, E., Wong, N., Chen, H.T., Polato, F., Gunn, A., Bothmer, A., Feldhahn, N., Fernandez-Capetillo, O., Cao, L. *et al.* (2010) 53BP1 inhibits homologous recombination in Brca1-deficient cells by blocking resection of DNA breaks. *Cell*, **141**, 243-254.

133. Cao, L., Xu, X., Bunting, S.F., Liu, J., Wang, R.H., Cao, L.L., Wu, J.J., Peng, T.N., Chen, J., Nussenzweig, A. *et al.* (2009) A selective requirement for 53BP1 in the biological response to genomic instability induced by Brca1 deficiency. *Mol Cell*, **35**, 534-541.

134. Zhang, F., Ma, J., Wu, J., Ye, L., Cai, H., Xia, B. and Yu, X. (2009) PALB2 links BRCA1 and BRCA2 in the DNA-damage response. *Curr Biol*, **19**, 524-529.

135. Sy, S.M., Huen, M.S. and Chen, J. (2009) PALB2 is an integral component of the BRCA complex required for homologous recombination repair. *Proc Natl Acad Sci U S A*, **106**, 7155-7160.

136. Zhang, F., Fan, Q., Ren, K. and Andreassen, P.R. (2009) PALB2 functionally connects the breast cancer susceptibility proteins BRCA1 and BRCA2. *Mol Cancer Res*, **7**, 1110-1118.

137. Bertram, M.J. and Pereira-Smith, O.M. (2001) Conservation of the MORF4 related gene family: identification of a new chromo domain subfamily and novel protein motif. *Gene*, **266**, 111-121.

138. Yochum, G.S. and Ayer, D.E. (2002) Role for the mortality factors MORF4, MRGX, and MRG15 in transcriptional repression via associations with Pf1, mSin3A, and Transducin-Like Enhancer of Split. *Mol Cell Biol*, **22**, 7868-7876.

139. Cai, Y., Jin, J., Tomomori-Sato, C., Sato, S., Sorokina, I., Parmely, T.J., Conaway, R.C. and Conaway, J.W. (2003) Identification of new subunits of the multiprotein mammalian TRRAP/TIP60-containing histone acetyltransferase complex. *J Biol Chem*, **278**, 42733-42736.

140. Doyon, Y., Selleck, W., Lane, W.S., Tan, S. and Cote, J. (2004) Structural and functional conservation of the NuA4 histone acetyltransferase complex from yeast to humans. *Mol Cell Biol*, **24**, 1884-1896.

141. Pardo, P.S., Leung, J.K., Lucchesi, J.C. and Pereira-Smith, O.M. (2002) MRG15, a novel chromodomain protein, is present in two distinct multiprotein complexes involved in transcriptional activation. *J Biol Chem*, **277**, 50860-50866.

142. Chen, M., Takano-Maruyama, M., Pereira-Smith, O.M., Gaufo, G.O. and Tominaga, K. (2009) MRG15, a component of HAT and HDAC complexes, is

essential for proliferation and differentiation of neural precursor cells. *J Neurosci Res*, **87**, 1522-1531.

143. Leung, J.K., Berube, N., Venable, S., Ahmed, S., Timchenko, N. and Pereira-Smith, O.M. (2001) MRG15 activates the B-myb promoter through formation of a nuclear complex with the retinoblastoma protein and the novel protein PAM14. *J Biol Chem*, **276**, 39171-39178.

144. Pena, A.N., Tominaga, K. and Pereira-Smith, O.M. (2011) MRG15 activates the cdc2 promoter via histone acetylation in human cells. *Exp Cell Res*, **317**, 1534-1540.

145. Chen, M., Tominaga, K. and Pereira-Smith, O.M. (2010) Emerging role of the MORF/MRG gene family in various biological processes, including aging. *Ann N Y Acad Sci*, **1197**, 134-141.

146. Garcia, S.N., Kirtane, B.M., Podlutsky, A.J., Pereira-Smith, O.M. and Tominaga, K. (2007) Mrg15 null and heterozygous mouse embryonic fibroblasts exhibit DNA-repair defects post exposure to gamma ionizing radiation. *FEBS Lett*, **581**, 5275-5281.

147. Tominaga, K., Kirtane, B., Jackson, J.G., Ikeno, Y., Ikeda, T., Hawks, C., Smith, J.R., Matzuk, M.M. and Pereira-Smith, O.M. (2005) MRG15 regulates embryonic development and cell proliferation. *Mol Cell Biol*, **25**, 2924-2937.

148. Hayakawa, T., Zhang, F., Hayakawa, N., Ohtani, Y., Shinmyozu, K., Nakayama, J. and Andreassen, P.R. (2010) MRG15 binds directly to PALB2 and stimulates homology-directed repair of chromosomal breaks. *J Cell Sci*, **123**, 1124-1130.

149. Sy, S.M., Huen, M.S. and Chen, J. (2009) MRG15 is a novel PALB2-interacting factor involved in homologous recombination. *J Biol Chem*, **284**, 21127-21131.

150. Stock, A., Clarke, S., Clarke, C. and Stock, J. (1987) N-terminal methylation of proteins: structure, function and specificity. *FEBS Lett*, **220**, 8-14.

151. Brosius, J. and Chen, R. (1976) The primary structure of protein L16 located at the peptidyltransferase center of Escherichia coli ribosomes. *FEBS Lett*, **68**, 105-109.

152. Chang, C.N., Schwartz, M. and Chang, F.N. (1976) Identification and characterization of a new methylated amino acid in ribosomal protein L33 of Escherichia coli. *Biochem Biophys Res Commun*, **73**, 233-239.

153. Wittmann-Liebold, B. and Pannenbecker, R. (1976) Primary structure of protein L33 from the large subunit of the Escherichia coli ribosome. *FEBS Lett*, **68**, 115-118.

154. Alix, J.H., Hayes, D., Lontie, J.F., Colson, C., Glatigny, A. and Lederer, F. (1979) Methylated amino acids in ribosomal proteins from Escherichia coli treated with ethionine and from a mutant lacking methylation of protein L11. *Biochimie*, **61**, 671-679.

155. Lederer, F., Alix, J.H. and Hayes, D. (1977) N-Trimethylalanine, a novel blocking group, found in E. coli ribosomal protein L11. *Biochem Biophys Res Commun*, **77**, 470-480.

156. Dognin, M.J. and Wittmann-Liebold, B. (1977) The primary structure of L11, the most heavily methylated protein from Escherichia coli ribosomes. *FEBS Lett*, **84**, 342-346.

157. Dognin, M.J. and Wittmann-Liebold, B. (1980) Identification of methylated amino acids during sequence analysis. Application to the Escherichia coli ribosomal protein L11. *Hoppe Seylers Z Physiol Chem*, **361**, 1697-1705.

158. Chen, R., Brosius, J. and Wittmann-Liebold, B. (1977) Occurrence of methylated amino acids as N-termini of proteins from Escherichia coli ribosomes. *J Mol Biol*, **111**, 173-181.

159. Brauer, D. and Wittmann-Liebold, B. (1977) The primary structure of the initiation factor IF-3 from Escherichia coli. *FEBS Lett*, **79**, 269-275.

160. Frost, L.S., Carpenter, M. and Paranchych, W. (1978) N-methylphenylalanine at the N-terminus of pilin isolated from Pseudomonas aeruginosa K. *Nature*, **271**, 87-89.

161. McKern, N.M., O'Donnell, I.J., Inglis, A.S., Stewart, D.J. and Clark, B.L. (1983) Amino acid sequence of pilin from Bacteroides nodosus (strain 198), the causative organism of ovine footrot. *FEBS Lett*, **164**, 149-153.

162. Hermodson, M.A., Chen, K.C. and Buchanan, T.M. (1978) Neisseria pili proteins: amino-terminal amino acid sequences and identification of an unusual amino acid. *Biochemistry*, **17**, 442-445.

163. Froholm, L.O. and Sletten, K. (1977) Purification and N-terminal sequence of a fimbrial protein from Moraxella nonliquefaciens. *FEBS Lett*, **73**, 29-32.

164. Marrs, C.F., Schoolnik, G., Koomey, J.M., Hardy, J., Rothbard, J. and Falkow, S. (1985) Cloning and sequencing of a Moraxella bovis pilin gene. *J Bacteriol*, **163**, 132-139.

165. Stock, A., Schaeffer, E., Koshland, D.E., Jr. and Stock, J. (1987) A second type of protein methylation reaction in bacterial chemotaxis. *J Biol Chem*, **262**, 8011-8014.

166. Desrosiers, R. and Tanguay, R.M. (1988) Methylation of Drosophila Histones at Proline, Lysine, and Arginine Residues during Heat-Shock. *Journal of Biological Chemistry*, **263**, 4686-4692.

167. Martinage, A., Briand, G., Vandorsselaer, A., Turner, C.H. and Sautiere, P. (1985) Primary Structure of Histone H2b from Gonads of the Starfish Asterias-Rubens - Identification of an N-Dimethylproline Residue at the Amino-Terminal. *European Journal of Biochemistry*, **147**, 351-359.

168. Medzihradszky, K.F., Zhang, X., Chalkley, R.J., Guan, S., McFarland, M.A., Chalmers, M.J., Marshall, A.G., Diaz, R.L., Allis, C.D. and Burlingame, A.L. (2004) Characterization of Tetrahymena histone H2B variants and posttranslational populations by electron capture dissociation (ECD) Fourier transform ion cyclotron mass spectrometry (FT-ICR MS). *Molecular & Cellular Proteomics*, **3**, 872-886.

169. Nomoto, M., Kyogoku, Y. and Iwai, K. (1982) N-Trimethylalanine, a novel blocked N-terminal residue of Tetrahymena histone H2B. *J Biochem*, **92**, 1675-1678.

170. Bonenfant, D., Coulot, M., Towbin, H., Schindler, P. and van Oostrum, J. (2006) Characterization of histone H2A and H2B variants and their post-translational modifications by mass spectrometry. *Molecular & Cellular Proteomics*, **5**, 541-552.

171. Henry, G.D., Dalgarno, D.C., Marcus, G., Scott, M., Levine, B.A. and Trayer, I.P. (1982) The Occurrence of Alpha-N-Trimethylalanine as the N-Terminal Amino-Acid of Some Myosin Light-Chains. *Febs Letters*, **144**, 11-15.

172. Henry, G.D., Trayer, I.P., Brewer, S. and Levine, B.A. (1985) The widespread distribution of alpha-N-trimethylalanine as the N-terminal amino acid of light chains from vertebrate striated muscle myosins. *Eur J Biochem*, **148**, 75-82.

173. Smith, G.M. and Pettigrew, G.W. (1980) Identification of N,N-Dimethylproline as the N-Terminal Blocking Group of Crithidia-Oncopelti Cytochrome-C557. *European Journal of Biochemistry*, **110**, 123-130.

174. Pettigrew, G.W. and Smith, G.M. (1977) Novel N-terminal protein blocking group identified as dimethylproline. *Nature*, **265**, 661-662.

175. Porras-Yakushi, T.R., Whitelegge, J.P. and Clarke, S. (2006) A novel SET domain methyltransferase in yeast: Rkm2-dependent trimethylation of ribosomal protein L12ab at lysine 10. *Journal of Biological Chemistry*, **281**, 35835-35845.

176. Sadaie, M., Shinmyozu, K. and Nakayama, J. (2008) A conserved SET domain methyltransferase, Set11, modifies ribosomal protein Rpl12 in fission yeast. *Journal of Biological Chemistry*, **283**, 7185-7195.

177. Carroll, A.J., Heazlewood, J.L., Ito, J. and Millar, A.H. (2008) Analysis of the Arabidopsis cytosolic ribosome proteome provides detailed insights into its components and their post-translational modification. *Mol Cell Proteomics*, **7**, 347-369.

178. Meng, F., Du, Y., Miller, L.M., Patrie, S.M., Robinson, D.E. and Kelleher, N.L. (2004) Molecular-level description of proteins from saccharomyces cerevisiae using quadrupole FT hybrid mass spectrometry for top down proteomics. *Anal Chem*, **76**, 2852-2858.

179. Chen, T., Muratore, T.L., Schaner-Tooley, C.E., Shabanowitz, J., Hunt, D.F. and Macara, I.G. (2007) N-terminal alpha-methylation of RCC1 is necessary for stable chromatin association and normal mitosis. *Nat Cell Biol*, **9**, 596-U203.

180. Tooley, C.E.S., Petkowski, J.J., Muratore-Schroeder, T.L., Balsbaugh, J.L., Shabanowitz, J., Sabat, M., Minor, W., Hunt, D.F. and Macara, I.G. (2010) NRMT is an alpha-N-methyltransferase that methylates RCC1 and retinoblastoma protein. *Nature*, **466**, 1125-U1144.

181. Dai, X., Otake, K., You, C., Cai, Q., Wang, Z., Masumoto, H. and Wang, Y. (2013) Identification of novel alpha-n-methylation of CENP-B that regulates its binding to the centromeric DNA. *J Proteome Res*, **12**, 4167-4175.

182. Bailey, A.O., Panchenko, T., Sathyan, K.M., Petkowski, J.J., Pai, P.J., Bai, D.L., Russell, D.H., Macara, I.G., Shabanowitz, J., Hunt, D.F. *et al.* (2013) Posttranslational modification of CENP-A influences the conformation of centromeric chromatin. *Proc Natl Acad Sci U S A*, **110**, 11827-11832.

183. Cai, Q., Fu, L., Wang, Z., Gan, N., Dai, X. and Wang, Y. (2014) alpha-N-methylation of damaged DNA-binding protein 2 (DDB2) and its function in nucleotide excision repair. *J Biol Chem*, **289**, 16046-16056.

184. Webb, K.J., Lipson, R.S., Al-Hadid, Q., Whitelegge, J.P. and Clarke, S.G. (2010) Identification of protein N-terminal methyltransferases in yeast and humans. *Biochemistry*, **49**, 5225-5235.

185. Petkowski, J.J., Schaner Tooley, C.E., Anderson, L.C., Shumilin, I.A., Balsbaugh, J.L., Shabanowitz, J., Hunt, D.F., Minor, W. and Macara, I.G. (2012) Substrate specificity of mammalian N-terminal alpha-amino methyltransferase NRMT. *Biochemistry*, **51**, 5942-5950.

186. Petkowski, J.J., Bonsignore, L.A., Tooley, J.G., Wilkey, D.W., Merchant, M.L., Macara, I.G. and Schaner Tooley, C.E. (2013) NRMT2 is an N-terminal monomethylase that primes for its homologue NRMT1. *Biochem J*, **456**, 453-462.

187. Villar-Garea, A., Forne, I., Vetter, I., Kremmer, E., Thomae, A. and Imhof, A. (2012) Developmental regulation of N-terminal H2B methylation in Drosophila melanogaster. *Nucleic Acids Res*, **40**, 1536-1549.

188. Shi, Y., Lan, F., Matson, C., Mulligan, P., Whetstine, J.R., Cole, P.A. and Casero, R.A. (2004) Histone demethylation mediated by the nuclear amine oxidase homolog LSD1. *Cell*, **119**, 941-953.

189. Lee, M.G., Wynder, C., Cooch, N. and Shiekhattar, R. (2005) An essential role for CoREST in nucleosomal histone 3 lysine 4 demethylation. *Nature*, **437**, 432-435.

190. Varshavsky, A. (1996) The N-end rule: functions, mysteries, uses. *Proc Natl Acad Sci U S A*, **93**, 12142-12149.

191. Tooley, J.G. and Schaner Tooley, C.E. (2014) New roles for old modifications: Emerging roles of N-terminal post-translational modifications in development and disease. *Protein Sci*.

192. Maurer-Stroh, S., Dickens, N.J., Hughes-Davies, L., Kouzarides, T., Eisenhaber, F. and Ponting, C.P. (2003) The Tudor domain 'Royal Family': Tudor, plant Agenet, Chromo, PWWP and MBT domains. *Trends Biochem Sci*, **28**, 69-74.

193. Kimura, Y., Kurata, Y., Ishikawa, A., Okayama, A., Kamita, M. and Hirano, H. (2013) N-Terminal methylation of proteasome subunit Rpt1 in yeast. *Proteomics*, **13**, 3167-3174.

194. Alamgir, M., Eroukova, V., Jessulat, M., Xu, J. and Golshani, A. (2008) Chemical-genetic profile analysis in yeast suggests that a previously uncharacterized open reading frame, YBR261C, affects protein synthesis. *BMC Genomics*, **9**, 583.

195. Kaiser, S., Park, Y.K., Franklin, J.L., Halberg, R.B., Yu, M., Jessen, W.J., Freudenberg, J., Chen, X., Haigis, K., Jegga, A.G. *et al.* (2007) Transcriptional recapitulation and subversion of embryonic colon development by mouse colon tumor models and human colon cancer. *Genome Biol*, **8**, R131.

196. Sabates-Bellver, J., Van der Flier, L.G., de Palo, M., Cattaneo, E., Maake, C., Rehrauer, H., Laczko, E., Kurowski, M.A., Bujnicki, J.M., Menigatti, M. *et al.* (2007) Transcriptome profile of human colorectal adenomas. *Mol Cancer Res*, **5**, 1263-1275.

197. Brune, V., Tiacci, E., Pfeil, I., Doring, C., Eckerle, S., van Noesel, C.J., Klapper, W., Falini, B., von Heydebreck, A., Metzler, D. *et al.* (2008) Origin and pathogenesis of nodular lymphocyte-predominant Hodgkin lymphoma as revealed by global gene expression analysis. *J Exp Med*, **205**, 2251-2268.

198. Sperger, J.M., Chen, X., Draper, J.S., Antosiewicz, J.E., Chon, C.H., Jones, S.B., Brooks, J.D., Andrews, P.W., Brown, P.O. and Thomson, J.A. (2003) Gene expression patterns in human embryonic stem cells and human pluripotent germ cell tumors. *Proc Natl Acad Sci U S A*, **100**, 13350-13355.

199. Finak, G., Bertos, N., Pepin, F., Sadekova, S., Souleimanova, M., Zhao, H., Chen, H., Omeroglu, G., Meterissian, S., Omeroglu, A. *et al.* (2008) Stromal gene expression predicts clinical outcome in breast cancer. *Nat Med*, **14**, 518-527.

200. Zhang, J., Yang, P.L. and Gray, N.S. (2009) Targeting cancer with small molecule kinase inhibitors. *Nat Rev Cancer*, **9**, 28-39.

201. Hochegger, H., Takeda, S. and Hunt, T. (2008) Cyclin-dependent kinases and cell-cycle transitions: does one fit all? *Nat Rev Mol Cell Biol*, **9**, 910-916.

202. Lim, S. and Kaldis, P. (2013) Cdks, cyclins and CKIs: roles beyond cell cycle regulation. *Development*, **140**, 3079-3093.

203. Chen, X., Niu, H., Chung, W.H., Zhu, Z., Papusha, A., Shim, E.Y., Lee, S.E., Sung, P. and Ira, G. (2011) Cell cycle regulation of DNA double-strand break end resection by Cdk1-dependent Dna2 phosphorylation. *Nat Struct Mol Biol*, **18**, 1015-1019.

204. Huertas, P., Cortes-Ledesma, F., Sartori, A.A., Aguilera, A. and Jackson, S.P. (2008) CDK targets Sae2 to control DNA-end resection and homologous recombination. *Nature*, **455**, 689-692.

205. Blagosklonny, M.V. (2004) Flavopiridol, an inhibitor of transcription: implications, problems and solutions. *Cell Cycle*, **3**, 1537-1542.

206. Sedlacek, H.H. (2001) Mechanisms of action of flavopiridol. *Crit Rev Oncol Hematol*, **38**, 139-170.

207. Gao, M. and Karin, M. (2005) Regulating the regulators: control of protein ubiquitination and ubiquitin-like modifications by extracellular stimuli. *Mol Cell*, **19**, 581-593.

208. Luger, K., Mader, A.W., Richmond, R.K., Sargent, D.F. and Richmond, T.J. (1997) Crystal structure of the nucleosome core particle at 2.8 A resolution. *Nature*, **389**, 251-260.

209. Campos, E.I. and Reinberg, D. (2009) Histones: annotating chromatin. *Annu Rev Genet*, **43**, 559-599.

210. Tse, C., Sera, T., Wolffe, A.P. and Hansen, J.C. (1998) Disruption of higher-order folding by core histone acetylation dramatically enhances transcription of nucleosomal arrays by RNA polymerase III. *Mol Cell Biol*, **18**, 4629-4638.

211. Dorigo, B., Schalch, T., Bystricky, K. and Richmond, T.J. (2003) Chromatin fiber folding: requirement for the histone H4 N-terminal tail. *J Mol Biol*, **327**, 85-96.

212. Shogren-Knaak, M., Ishii, H., Sun, J.M., Pazin, M.J., Davie, J.R. and Peterson, C.L. (2006) Histone H4-K16 acetylation controls chromatin structure and protein interactions. *Science*, **311**, 844-847.

213. Sun, Y., Jiang, X., Xu, Y., Ayrapetov, M.K., Moreau, L.A., Whetstine, J.R. and Price, B.D. (2009) Histone H3 methylation links DNA damage detection to activation of the tumour suppressor Tip60. *Nat Cell Biol*, **11**, 1376-1382.

214. Fraga, M.F., Ballestar, E., Villar-Garea, A., Boix-Chornet, M., Espada, J., Schotta, G., Bonaldi, T., Haydon, C., Ropero, S., Petrie, K. *et al.* (2005) Loss of acetylation at Lys16 and trimethylation at Lys20 of histone H4 is a common hallmark of human cancer. *Nature Genetics*, **37**, 391-400.

215. Wagner, E.J. and Carpenter, P.B. (2012) Understanding the language of Lys36 methylation at histone H3. *Nat Rev Mol Cell Biol*, **13**, 115-126.

216. Edmunds, J.W., Mahadevan, L.C. and Clayton, A.L. (2008) Dynamic histone H3 methylation during gene induction: HYPB/Setd2 mediates all H3K36 trimethylation. *EMBO J*, **27**, 406-420.

217. Li, F., Mao, G., Tong, D., Huang, J., Gu, L., Yang, W. and Li, G.M. (2013) The histone mark H3K36me3 regulates human DNA mismatch repair through its interaction with MutSalpha. *Cell*, **153**, 590-600.

218. Pfister, S.X., Ahrabi, S., Zalmas, L.P., Sarkar, S., Aymard, F., Bachrati, C.Z., Helleday, T., Legube, G., La Thangue, N.B., Porter, A.C. *et al.* (2014) SETD2-

dependent histone H3K36 trimethylation is required for homologous recombination repair and genome stability. *Cell Rep*, **7**, 2006-2018.

219. Carvalho, S., Vitor, A.C., Sridhara, S.C., Martins, F.B., Raposo, A.C., Desterro, J.M., Ferreira, J. and de Almeida, S.F. (2014) SETD2 is required for DNA double-strand break repair and activation of the p53-mediated checkpoint. *Elife*, **3**, e02482.

220. Aymard, F., Bugler, B., Schmidt, C.K., Guillou, E., Caron, P., Briois, S., Iacovoni, J.S., Daburon, V., Miller, K.M., Jackson, S.P. *et al.* (2014) Transcriptionally active chromatin recruits homologous recombination at DNA double-strand breaks. *Nat Struct Mol Biol*, **21**, 366-374.

Chapter 2. α-N-Methylation of Damaged DNA-Binding Protein 2 (DDB2) and Its Function in Nucleotide Excision Repair

Introduction

Nucleotide excision repair (NER), a versatile DNA repair pathway that eliminates a wide variety of helix-distorting DNA lesions, including ultraviolet (UV) light-induced cyclobutane pyrimidine dimer (CPD) and pyrimidine(6-4)pyrimidone photoproducts (6-4PPs), as well as bulky DNA adducts induced by numerous environmental carcinogens (1). There are two subpathways of NER, i.e., GG-NER and transcription-coupled NER (TC-NER), which operates throughout the entire genome and removes lesions from transcribed strand of active genes, respectively (1,2).

DDB2 is normally present as a heterodimer known as UV-DDB, which comprises of DDB1 (p127) and DDB2 (p48) (3). UV-DDB serves as a GG-NER factor for the detection of UV-induced DNA damage in chromatin, where DDB2's binding to damaged DNA precedes the recruitment of XPC to chromatin (4). XP-E cells and Chinese hamster ovary cells lacking UV-DDB exhibit a defect in the repair of CPDs, but not 6-4PPs (4,5), and overexpression of DDB2 in Chinese hamster ovary cells can increase UV resistance (6). Furthermore, DDB2 regulates ATM/ATR activation and decides cell fate by coordinating with XPC (7) and stimulating the proteasomal degradation of p21 (8), respectively.

Protein α-N-methylation is a type of post-translational modification that is conserved from E. coli to man (9), and a number of proteins were found to be α-N-

methylated in eukaryotic cells. In this context, α-N-methylation of histone H2B was observed in several organisms (10-15). Other eukaryotic proteins known to be α-N-methylated include human RCC1, SET, retinoblastoma protein (Rb), etc. (16-27). Recently, the long-sought α-N-methyltransferase in human and yeast have been discovered (17,20). The human α-N-methyltransferase NRMT (also known as NTMT1) recognizes a common N-terminal sequence motif of XPK ('X' represents S, P or A) (17). Lately, the recognition motif of NRMT was further expanded based on an in vitro peptide methylation assay (18). Considering that DDB2 harbors an N-terminal APK motif, we reason that DDB2 might constitute an NRMT substrate and be α-N-methylated in cells.

Herein we report our identification and characterization of α-N-methylation of DDB2. We demonstrated that NRMT could catalyze the α-N-methylation of DDB2 in vitro and in human cells, and this methylation promoted DDB2's nuclear localization, facilitated DDB2's recruitment to CPD foci, augmented CPD repair efficiency, enabled ATM activation, and conferred the resistance of human cells toward UV damage. Furthermore, results from our study expanded the function of protein α-N-methylation to DNA repair.

Materials and Methods

Cell culture conditions

The HEK293T human embryonic kidney epithelial cells were purchased from ATCC. AA8 and GM01389 cells were kindly provided by Dr. Michael M. Seidman

(National Institute of Aging). HEK293T cells were cultured in Dulbecco's modified Eagle's medium (ATCC), and AA8 and GM01389 cells were cultured in α Minimum Essential Medium (αMEM, ATCC). The media contained 10% (v/v, for HEK293T and AA8 cells) or 15% (v/v, for GM01389 cells) fetal bovine serum (Invitrogen), 100 units/ml penicillin, and 100 μg/ml streptomycin. The cells were cultured at 37°C in 5% CO_2 atmosphere.

Constructs

The expression plasmid for NRMT-His_6 was kindly provided by Dr. Ian Macara (17). The human DDB2 open-reading frame was amplified to introduce a 5' XbaI restriction site and a 3' BamHI site, and subcloned into a modified mammalian expression vector pRK7 in which three tandem repeats of the FLAG epitope tag (DYKDDDK) were inserted between BamHI and EcoRI sites to give pRK7-DDB2-3×FLAG. DDB2-K4Q mutant was amplified from pRK7-DDB2-3×FLAG plasmid using site-directed mutagenesis. DDB2-His_6 was generated by subcloning DDB2 coding sequence with 5' SacI, N-terminal X-factor cleavage site (IEGR) and 3'NotI into E. coli expression vector pET28a.

Preparation of recombinant proteins

NRMT-His_6 and DDB2-His_6 were expressed in Rosetta (DE3) pLysS E. coli strain after growth at 37°C in Luria broth supplemented with 2% (v/v) ethanol to an optical density at 600 nm of approximately 0.8, followed by induction with 0.5 mM isopropylthiogalactopyranoside at room temperature overnight for NRMT-His_6, and at

37°C for 4 hr for DDB2-His_6. The proteins were then purified by using Talon affinity resin (Clontech) following the manufacturer's recommended procedures. pRK7-DDB2-3×FLAG was transfected into HEK293T cells using Lipofectamine 2000 (Invitrogen) and the resulting C-terminally FLAG-tagged DDB2 was purified by using Anti-FLAG M2 affinity beads (Sigma).

siRNA knockdown

Control and human NRMT SMARTpool siRNA were obtained from Thermo Scientific. Sequences of NRMT SMARTpool siRNA were GCGAGGUGAUAGAAGACGA, AGGUGGAUAUGGUCGACAU, UGAGGGAAGGCCCGAACAA and GGACUGUGGAGCUGGCAUU. HEK293T cells were cultured in 6-well plates in antibiotic-free medium at a density of 5×10^5 cells per well for 24 hrs, and transfected with 100 pmol siRNA using Lipofectamine 2000 (Invitrogen). Cells were harvested 48 hr later for RT-PCR analysis.

Real-time quantitative RT-PCR - Total RNA was isolated using the Total RNA Kit I (Omega). cDNA was generated by using M-MLV reverse transcriptase (Promega) and an $oligo(dT)_{16}$ primer. Real-time quantitative RT-PCR for evaluating the extent of siRNA knockdown was performed by using the iQ SYBR Green Supermix kit (Bio-Rad) and gene-specific primers for NRMT or the control gene GAPDH. The primers were 5'-GCCCTCCCTTCCTCTTCC-3' and 5'-CCAACCACGGCTCTACTCA -3' for NRMT, and 5'-TTTGTCAAGCTCATTTCCTGGTATG-3' and 5'-TCTCTTCCTCTTGTGCTCTTGCTG -3' for GAPDH.

In vitro methylation assay

Purified NRMT-His_6 (0.3 μg) was incubated with 1 μg X-factor-cleaved DDB2-His_6 or synthetic N-terminal peptide of DDB2 (Genemed Synthesis, Inc.) with 100 μM S-adenosyl-L-methionine (S-AdoMet) as the methyl donor and brought to 50 μL with methyltransferase buffer (50 mM Tris, 50 mM potassium acetate, pH 8.0). Reactions were continued at 30°C for 2 hr.

LC-MS/MS analysis

The FLAG-tagged DDB2 was isolated using affinity purification with anti-FLAG M2 beads. The sample was subsequently reduced, alkylated and digested with Glu-C at an enzyme:protein ratio of 1:20 (w/w) at room temperature overnight. Peptide mixtures were subjected to online LC-MS/MS analysis with an EASY-nLC II that is coupled with an LTQ Orbitrap Velos mass spectrometer equipped with a nanoelectrospray ionization source (Thermo, San Jose, CA) following similar procedures as described previously (28). The separation was conducted by using a homemade trapping column (150 μm × 50 mm) and a separation column (75 μm ×120 mm), packed with ReproSil-Pur C18-AQ resin (3 μm in particle size, Dr. Maisch HPLC GmbH, Germany). Peptide samples were initially loaded onto the trapping column with a solvent mixture of 0.1% formic acid in CH_3CN/H_2O (2:98, v/v) at a flow rate of 4.0 μL/min. The peptides were then separated with a 90-min linear gradient of 2-40% acetonitrile in 0.1% formic acid and at a flow rate of 220 nL/min. The mass spectrometer was operated in the positive-ion mode, and the spray voltage was 1.8 kV. The data were acquired in a data-dependent scan mode where

one full-scan MS was followed with 20 MS/MS scans. To obtain high-quality MS/MS, the data were also collected in selected-ion monitoring mode where the fragmentations of the protonated ions of the unmodified and mono-, di- or tri-methylated forms of the N-terminal peptide of DDB2 were monitored. All the MS/MS data were manually analyzed.

Fluorescence microscopy

The AA8 and GM01389 cells transiently expressing the wild-type or K4Q mutant of DDB2 were grown on glass coverslips, and irradiated with UV-C light at 40 J/m^2 through a 5-μm isopore polycarbonate filter (Millipore). After the irradiation, the membrane was removed, and the cells were incubated at 37°C for 30 min. The cells were subsequently fixed with 4% (w/v) paraformaldehyde, permeated using 0.5% (v/v) Triton X-100 in PBS, washed with PBS, and the DNA was denatured by incubation in 2 M HCl for 5 min. Cells were then incubated in a solution containing 20% (v/v) goat serum, 0.3% (v/v) Triton X-100, and 5% (w/v) bovine serum albumin (BSA) to block non-specific binding. Primary anti-FLAG (Cell Signaling) and anti-CPD (Kamiya Biomedical Company) antibodies and secondary antibodies (Invitrogen) were subsequently added and incubated at 4°C for overnight and then at room temperature for 1 hr. After the incubation, the coverslips were washed with PBS and mounted onto microscope slides in ProLong Gold Antifade Reagent with DAPI (Invitrogen). Images were captured with a Leica TCS SP2/UV confocal microscope (Leica Microsystems).
Colonogenic Survival assay - For survival assay, GM01389 cells, at 24 hr following transfection with pRK7-DDB2-3×FLAG, pRK7-DDB2-K4Q-3×FLAG or empty control, were plated in 6-well plates in triplicate at densities of 200-2000 cells per well. The cells

were subsequently exposed to various doses of UV-C light and the cells were attached to the plates immediately afterwards. Cell colonies grown for 10-14 days (29) were then fixed using 6% (v/v) glutaraldehyde and stained with 0.5% (w/v) crystal violet. Colonies containing at least 50 cells were counted under a microscope.

Nuclear fractionation and Western blot

HEK293T cells transiently expressing the wild- type DDB2 or DDB2-K4Q were collected immediately, or at 30 min, after irradiation with 40 J/m^2 UV-C light. The nuclear and cytoplasmic fractions were obtained using NE-PER Nuclear and Cytoplasmic extraction kit (Thermo Scientific) following the manufacturer's recommended procedures. Antibodies that specifically recognized histone H3 and FLAG epitope tag were purchased from Cell Signaling and used at 1:10000 dilution. Antibody that specifically recognized human actin (abcam) was used at 1:5000 dilution. For ATM activation, antibodies that specifically recognized human ATM or phospho-ATM (Ser1981), and human CHK1 or phospho-CHK1 (Ser345) were purchased from Cell Signaling and used at 1:1000 dilution. Horseradish peroxidase-conjugated secondary goat anti-rabbit antibody (abcam) was used at a 1:10000 dilution.

Flow cytometry-based DNA repair assay

The CPD repair assay was performed following similar procedures as described previously (30). The GM01389 cells were plated in 6-well plates at a density of 3×10^5 cells/well, after 16 hr, plasmids for overexpressing wild-type DDB2 or DDB2-K4Q mutant and the empty control were transfected individually into the plated GM01389

cells. At 28 hr after transfection, the DMEM medium was replaced with 1×PBS buffer and the cells were irradiated with UV-C light at 10 J/m^2. After the irradiation, PBS buffer was removed and fresh medium with 200 ng/ml nocodazole was added to the cells. At various time intervals following UV irradiation, the cells were washed with PBS, resuspended in 125 μL PBS and fixed by adding 375 μL pre-chilled 100% ethanol at -20 °C for at least 1 hr. The cells were subsequently permeated and denatured with 0.5% (v/v) Triton X-100 in 2 N HCl in ddH_2O at room temperature for 15 min. Cells were washed trice with PBS and resuspended in 200 μL PBS with 100 μg/ml RNase at 37 °C for 1 hr. After that, cells were blocked in blocking buffer, which contained 5% (v/v) bovine serum albumin and 0.3% (v/v) Triton X-100 in PBS, at room temperature for 20 min. Cells were then resupended in the blocking buffer containing mouse anti-CPD antibody (Kamiya Biomedical Company, 1:1000 dilution) at room temperature for 45 min and then at 4°C overnight. Cell pellets were subsequently washed thrice with washing buffer, which contained 0.3% (v/v) Triton X-100 in PBS, and then resupended in Alexa Fluor 647 Goat anti-Mouse antibody (1:200 dilution, Invitrogen) at room temperature for 1 hr. Pellets were again washed thrice with washing buffer then resuspended in sorting buffer (1×PBS, 1 mM EDTA, 25 mM HEPES, 1% FBS, v/v, pH 7.0) for flow cytometry analysis (BD FACS Aria I).

Results

Human DDB2 is mono-, di- and tri-methylated on the α-amino group of its N-terminal alanine residue

We first assessed whether DDB2 can be α-N-methylated. To this end, we expressed the C-terminally FLAG-tagged DDB2 in HEK293T cells and purified the protein from the cell lysate using anti-FLAG M2 beads (Figure 2.1a). Glu-C digestion of the resulting protein yields the N-terminal peptide of APKKRPE. From our MS result, we were able to identify doubly charged ions of the unmodified as well as the mono-, di- and tri-methylated forms of the peptide $_1$APKKRPE$_7$ at *m/z* values of 413.2481, 420.2558, 427.2634, and 434.2742, respectively (Figure 2.2a). As depicted in Figure 2.2 b-d and 2.3a, we observed the y_2-y_6 ions for the mono- and di-methylated peptide, and the y_2, y_3-y_5 ions for tri-methylated peptide. These ions display the same *m/z* values as those for the corresponding unmodified peptide. In addition, we observed the b_2+Me, b_3+Me and b_5+Me ions in the MS/MS of the monomethylated peptide, as well as the b_2+2Me, b_3+2Me, b_5+2Me ions and neutral loss of an $NH(CH_3)_2$ in the MS/MS for the dimethylated peptide (Figure 2.2c&d). On the other hand, the MS/MS for the corresponding trimethylated peptide displays the b_2+3Me, b_3+3Me, b_4+3Me, b_5+3Me ions and a fragment ion arising from the elimination of an $N(CH_3)_3$ (Figure 2.2a). The

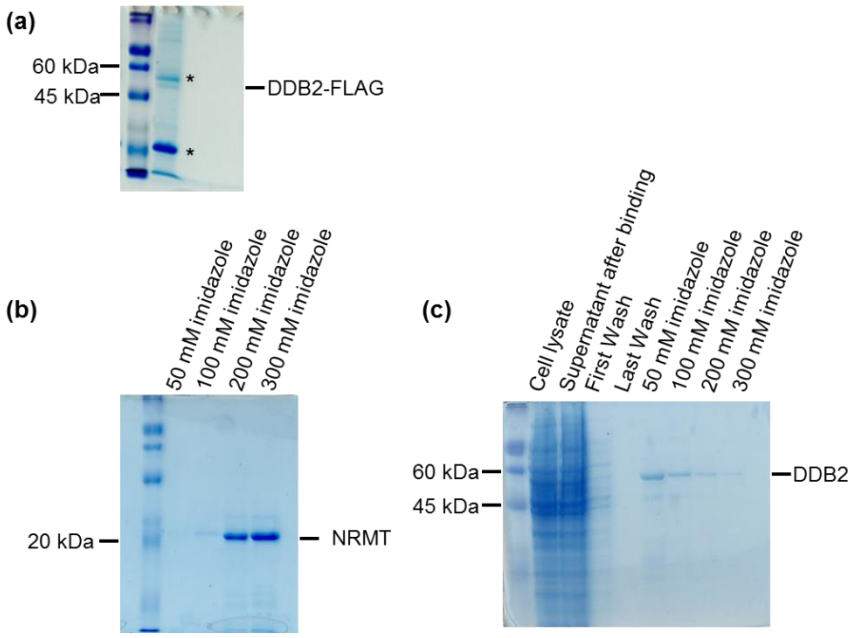

Figure 2. 1. SDS-PAGE characterizations of recombinant DDB2 and NRMT. Shown as the image for SDS-PAGE gels for the C-terminally FLAG-tagged DDB2 isolated from HEK293T cells (a), and NRMT-His_6 (b) and DDB2-His_6 (c) purified from *E. coli* Rosetta (DE3) pLysS cells. * indicates antibody heavy and light chains.

observation of the y_6+Me ion for the trimethylated peptide (Figure 2.3a) is perhaps attributed to the methyl group migration prior to amide bond cleavage during collisional activation, as observed previously (31). To further confirm this, we acquired the MS/MS/MS arising from the further fragmentation of the y_6+Me ion found in the MS/MS of the trimethylated peptide (Figure 2.3b). The observation of the b_2, b_2+Me, b_3+Me, b_4+Me and b_5+Me+H_2O ions, but not the b_3, b_4, or b_5+H_2O ion, demonstrated that the methyl group is migrated to the third lysine, or one of the two residues on the N-terminal portion (proline or lysine). In this regard, the ion of *m/z* 639.6 found in Figure 2.3b may be potentially attributed to the y_5-H_2O ion; the observation of the b_5+H_2O, but not the y_5-H_2O ion in the MS/MS/MS for the y_6 ion observed for the dimethylated peptide (Figure A1) suggested that the ion of *m/z* 639.6 can only be assigned to the b_5+Me+H_2O ion. Together, the above results provide solid evidence for supporting the mono-, di- and tri-methylation of the N-terminus of DDB2.

NRMT can catalyze the α-N-methylation of DDB2 in human cells and in vitro

Considering that NRMT can catalyze the α-N-methylation of RCC1 and several other human proteins carrying the conserved N-terminal XPK motif, we asked whether this enzyme can also induce the α-N-methylation of DDB2, which harbors an N-terminal APK motif. To this end, we knocked down the expression of NRMT in HEK293T cells by using siRNA and co-transfected the cells with NRMT siRNA together with the plasmid for expressing the C-terminally FLAG-tagged DDB2. Quantitative real-time PCR and Western blot results showed that NRMT knockdown efficiency was greater than 80% (Figure 2.4a and 2.4b). We then estimated the extent of N-terminal methylation

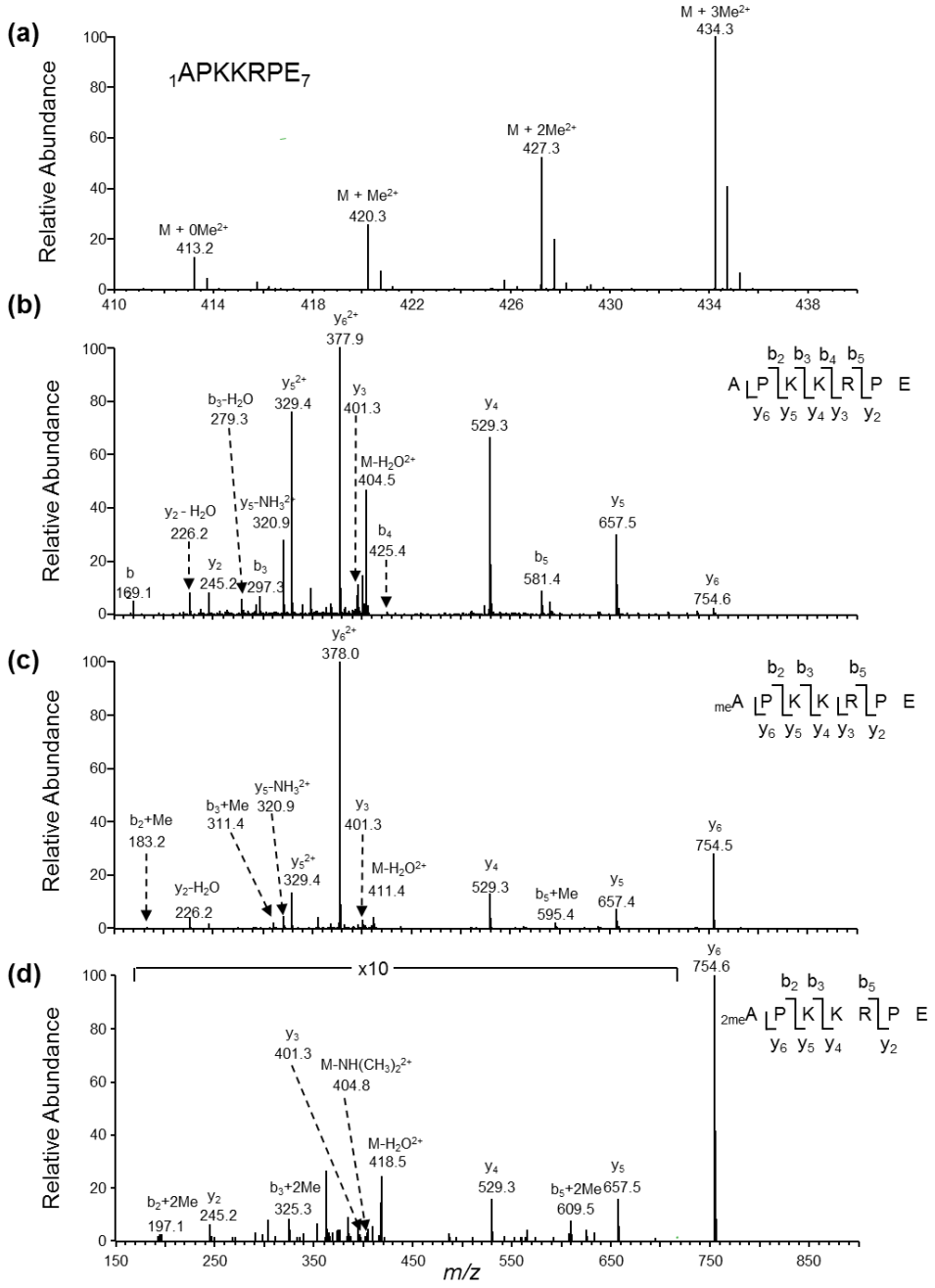

Figure 2. 2. ESI-MS and MS/MS characterizations of α-N-methylation of DDB2 isolated from HEK293T cells. (a) ESI-MS showing the presence of unmodified as well as mono-, di-, tri-α-N-methylated forms of the peptide $_1$APKKRPE$_7$ of C-terminally FLAG-tagged DDB2 isolated from HEK293T cells. (b-d) ESI-MS/MS of unmodified (b) as well as mono- (c), di-methylated (d) forms of the peptide $_1$APKKRPE$_7$. A region of the spectrum in Fig. 2.2d was amplified to visualize better the peaks for some fragment ions of low abundance.

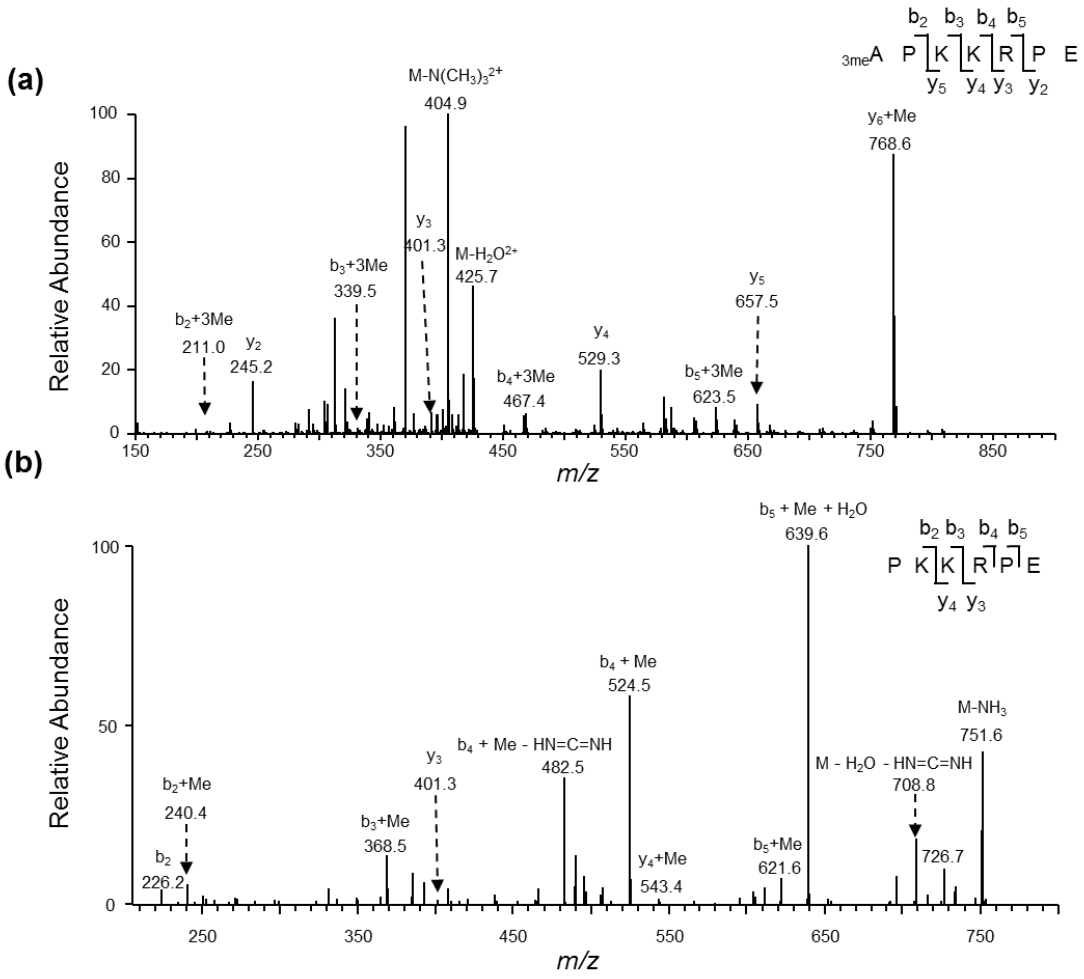

Figure 2. 3. MS/MS and MS/MS/MS characterizations of the α-N-trimethylated peptide of DDB2. (a) ESI-MS/MS of tri-methylated form of the peptide $_1$APKKRPE$_7$ arising from the Glu-C digestion of C-terminally FLAG-tagged DDB2 isolated from HEK293T cells. (b) MS/MS/MS of y_6+Me ion found in the MS/MS of the tri-methylated form of the peptide $_1$APKKRPE$_7$.

based on the relative abundances of precursor ions for the methylated and unmodified peptides of the C-terminally FLAG-tagged DDB2 isolated from HEK293T cells. Following NRMT knockdown, there is a significant reduction in the level of α-N-methylation in DDB2 relative to that observed for DDB2 isolated from cells treated with control, non-targeting siRNA (Figure 2.4c). In this regard, it is worth noting that methylation may alter the ionization efficiency of the N-terminal peptide. Thus, the absolute methylation levels may differ from those estimated from the relative ion abundances; nevertheless, the method still offers a valid comparison about the relative levels of methylation of DDB2 isolated from cells with or without NRMT knockdown. We next examined whether NRMT could catalyze the α-N-methylation of DDB2 *in vitro.* To this end, we generated the recombinant His_6-tagged NRMT and DDB2 (Figure 2.1b-c). To remove the initial methionine, we generated the recombinant DDB2 protein that is fused with a His_6-tag and Factor X (a protease) recognition sequence on the N-terminus. Cleavage with Factor X renders the second residue of DDB2 (i.e., alanine) exposed for α-N-methylation. LC-MS/MS analysis of the Glu-C digestion mixture of the *in vitro* methylated DDB2 revealed the presence of mono-, di-, and tri-methylated N-terminal peptide (Figure A2b&c), and the absence of methylated N-terminal peptide in the samples without the addition of NRMT (Figure A2a).

To assess whether the folding of DDB2 is required for the α-N-methylation, we also incubated the peptide containing N-terminal 12 amino acids of DDB2 (without the initial methionine) with NRMT together with *S*-AdoMet *in vitro.* Our MS and MS/MS

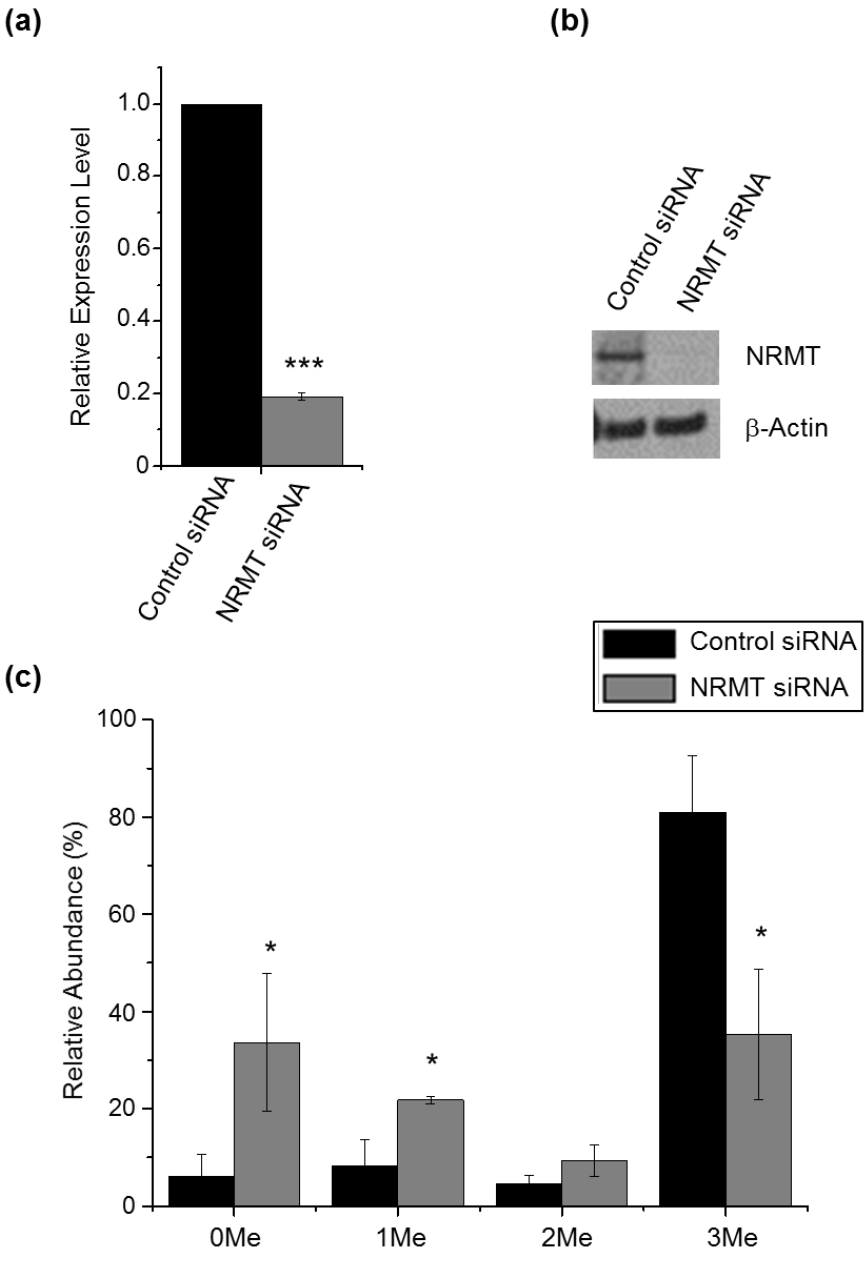

Figure 2. 4. NRMT can catalyze the α-N-methylation of DDB2 in cells. (a) Relative mRNA level of NRMT by real-time PCR using GAPDH as control; (b) Relative level of NRMT protein by Western analysis using GAPDH as control; (c) Relative abundances of different methylation forms of N-terminal peptide APKKRPE of DDB2 isolated from HEK293T cells treated with control and NRMT siRNA, as determined by semi-quantitative MS analysis. The results represent the mean and standard deviation of results obtained from three independent experiments. "*", $P < 0.05$; the P values were calculated by using unpaired two-tailed t-test.

results revealed unequivocally the mono-, di-, and tri-methylation of the N-terminus of the peptide $_{1}$APKKRPETQKTS$_{12}$ (Figure 2.5b, Figure A3). As expected, we only observed the unmodified form of the peptide when NRMT was not included in the reaction (Figure 2.5a). Together, we conclude that NRMT can catalyze the α-N-methylation of DDB2.

The proline and lysine in the 'APK' motif are important for the α-N-methylation of DDB2

In light of the importance of the XPK motif in α-N-methylation, we also performed *in vitro* methylation assay with the 12-amino acid peptide variants $_{1}$AAKKRPETQKTS$_{12}$ and $_{1}$APQKRPETQKTS$_{12}$, where the P and K in the XPK motif were mutated to A and Q, respectively. As displayed in Figure 2.5c-e, relative to the wild-type sequence, the methylation level for $_{1}$AAKKRPETQKTS$_{12}$ is profoundly decreased, whereas $_{1}$APQKRPETQKTS$_{12}$ was predominantly unmethylated (The MS/MS results are shown in Figures A4-A5). Hence, we constructed a plasmid allowing for the expression of C-terminally FLAG-tagged DDB2-K4Q mutant and examined whether the mutant protein can be methylated in cells. In keeping with the *in vitro* result, LC-MS/MS analysis showed that the unmodified peptide APQKRPE could be readily detected in the Glu-C digestion mixture of the DDB2-K4Q mutant isolated from HEK293T cells; however, the corresponding methylated peptides were below the detection limit (Figure A6). In this vein, it was observed previously that the K4Q mutant of RCC1 or CENP-B could not be methylated on the N-termini by NRMT (16,26).

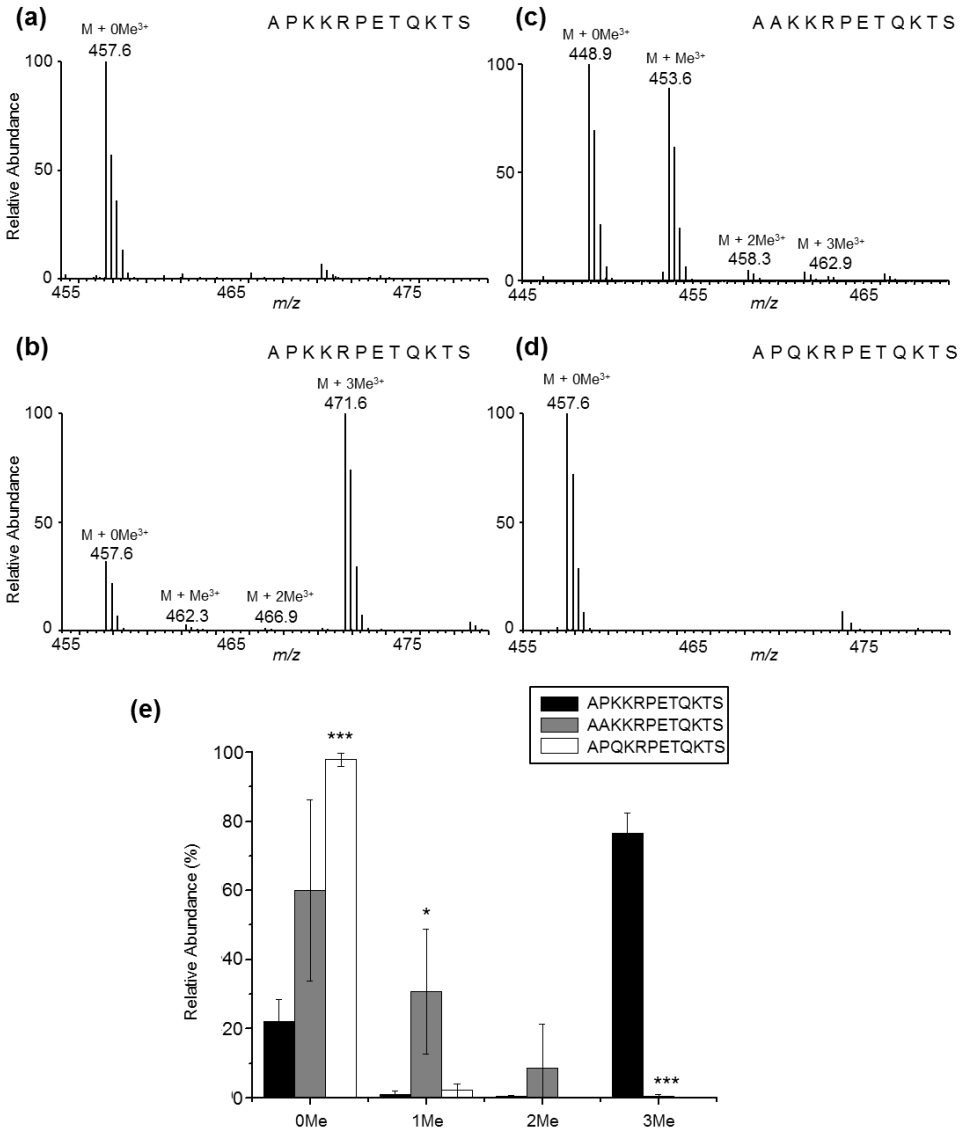

Figure 2. 5. NRMT can catalyze the α-N-methylation of DDB2 in vitro. (a) ESI-MS of unmodified forms of the peptide 1APKKRPETQKTS12 without addition of NRMT; (b) ESI-MS of unmodified, mono-, di-, tri-α-N-methylated forms of the peptide $_1$APKKRPETQKTS$_{12}$ with addition of NRMT; (c) ESI-MS of unmodified, mono-, di-, tri-α-N-methylated forms of the peptide DDB2-P3A, i.e., $_1$AAKKRPETQKTS$_{12}$, with the addition of NRMT; (d) ESI-MS of unmodified, mono-, di-, tri-α-N-methylated forms of the peptide DDB2-K4Q, i.e., $_1$APQKRPETQKTS$_{12}$, with the addition of NRMT; (e) Relative abundances of different methylation forms of N-terminal 12 amino acids of DDB2, DDB2-P3A, DDB2-K4Q as determined by semi-quantitative MS analysis. The results represent the mean and standard deviation of results obtained from three independent experiments. "*", $P < 0.05$; "***", $P < 0.001$. The P values were calculated by using unpaired two-tailed t-test.

α-N-methylation affects DDB2's nuclear localization and its recruitment to CPD foci

Previous studies showed that DDB2 is rapidly recruited to CPD foci in cells following exposure to UV irradiation (32). We reason that α-N-trimethylation of DDB2 may affect its intracellular localization and its binding to damaged DNA. In this regard, α-N-methylation of DDB2 may promote its nuclear localization by facilitating its interaction with other nuclear proteins which can recognize this methylation mark, and there are many cellular protein readers that can recognize the side chains of methylated lysine and arginine (33). To test this, we transfected HEK293T cells with FLAG-tagged DDB2 and DDB2-K4Q expression vectors, and examined the distribution of the wild-type and mutant DDB2 in the cytoplasmic and nuclear fractions before and after treatment with UV-C light. Our results demonstrated that, with or without UV-C light exposure, the methylation-defective mutant displayed a reduced presence in the nuclear fraction than wild-type DDB2 (Figure 2.6a).

We next examined whether deficient α-N-methylation affects DDB2's recruitment to CPD foci. To this end, we transfected FLAG-tagged DDB2 and DDB2-K4Q expression vectors into AA8 Chinese hamster ovary (CHO) cells which do not express endogenous UV-DDB (32). As shown in Figure 2.6b-c, immunofluorescence analyses using anti-FLAG and anti-CPD antibodies revealed that 97.4% of CPD foci co-localized with DDB2 foci in cells transfected with wild-type DDB2 construct, whereas only 61.5% of the CPD foci co-localized with DDB2 foci in AA8 cells transfected with the plasmid for DDB2-K4Q. To further strengthen this finding, we conducted similar

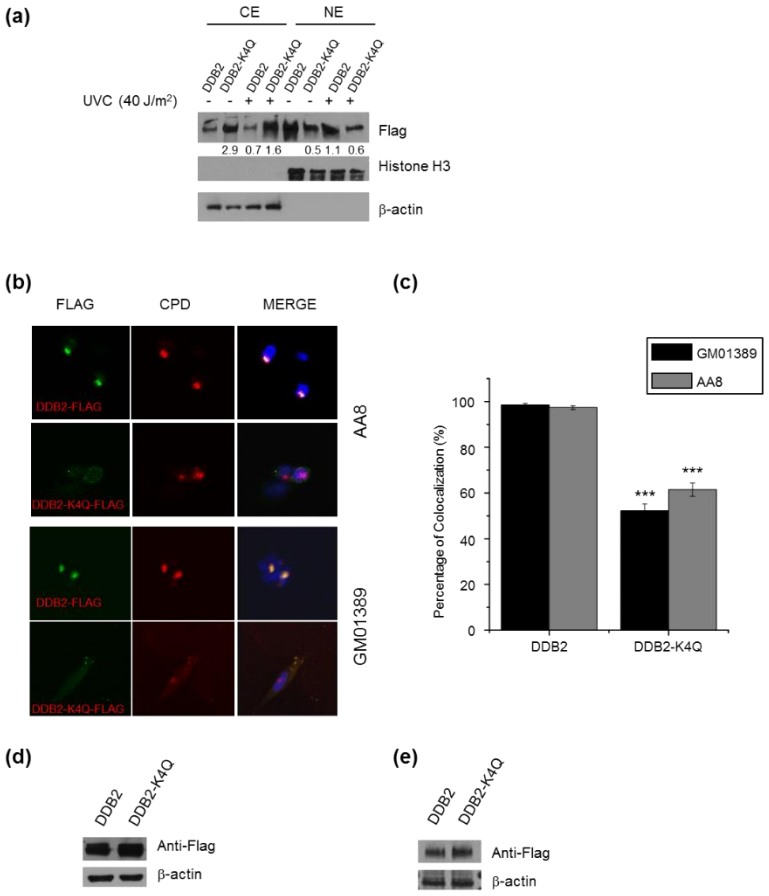

Figure 2. 6. α-N-methylation is important for DDB2's nuclear localization and recruitment to DNA damage foci. (a) Western blot revealed the less nuclear localization and more cytoplamic localization of DDB2-K4Q than wild-type DDB2 in HEK293T cells with or without exposure to UV-C light. β-actin was used as a loading control for the cytoplasmic extract (CE), and histone H3 was used as a loading control for the nuclear extract (NE). (b) Representative images for monitoring the co-localization of transfected wild-type DDB2 and DDB2-K4Q to CPD foci in AA8 and GM01389 cells; (c) Percentage of CPD foci that are co-localized with DDB2 foci (%). In cells transfected with the wild-type DDB2 construct, almost all CPD foci have colocalization with DDB2 foci, whereas only a portion of CPD foci bear colocalization with DDB2 foci in cells transfected with the DDB2-K4Q plasmid. The results represent the mean and standard deviation of results obtained from three biological replicates, and approximately 100 cells were counted in each replicate. "***", $P < 0.001$. The P values were calculated by using unpaired two-tailed t-test. (d-e) Western blot analysis of wild-type DDB2 and DDB2-K4Q in whole-cell extracts of AA8 (d) and GM01389 (e) cells transfected with the corresponding DDB2 constructs. β-actin was used as a loading control.

experiments using human XPE cells (GM01389) which do not carry a functional DDB2. Figure 6b&c displayed that 98.5% of CPD foci co-localized with DDB2 foci in GM01389 cells transfected with wild-type DDB2 construct, whereas only 52.2% of the CPD foci co-localized with DDB2 foci in cells transfected with the plasmid for DDB2-K4Q. In this vein, it is worth noting that wild-type DDB2 and DDB2-K4Q mutant were expressed at similar levels in GM01389 and AA8 cells, as shown by Western analysis (Figure 2.6d-e). Thus, the above results demonstrated that α-N-methylation plays a significant role in DDB2's recruitment to CPD foci.

α-N-methylation of DDB2 facilitates CPD repair in GM01389 cells

Viewing that the methylation-defective mutant of DDB2 exhibited diminished nuclear localization and reduced recruitment to CPD foci, we next examined whether the α-N-methylation of DDB2 plays a role in CPD repair using a flow cytometry-based method (30). Our results showed that, approximately 70% of CPD was removed in GM01389 cells transfected with wild-type DDB2 construct, whereas only about 39% of the CPD was repaired in cells transfected with the DDB2-K4Q plasmid at 48 hr following UV-C exposure (Figure 2.7). Thus, α-N-methylation enhances CPD repair in human cells.

α-N-methylation of DDB2 promotes ATM activation in GM01389 cells

DDB2, as an early UV damage recognition factor, was previously shown to be crucial for ATM recruitment to DNA damage sites and for its activation (7). On the

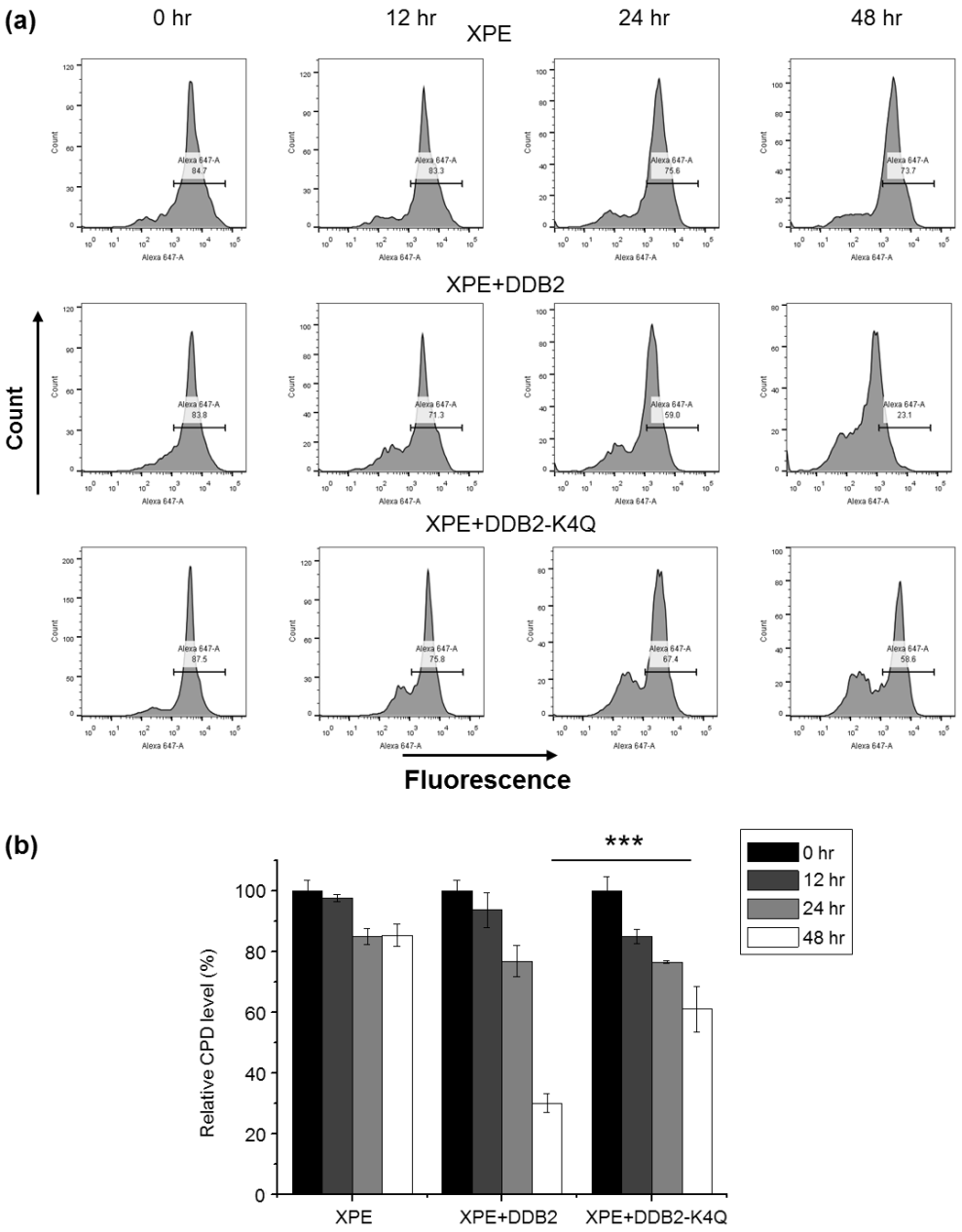

Figure 2. 7. α-N-methylation of DDB2 stimulates CPD repair in human cells. (a) Flow cytometry results showing the level of CPD in GM01389 with empty control, wild-type DDB2 and DDB2-K4Q at various time intervals (0, 12, 24, and 48 hr) after irradiation with 10 J/m^2 UV-C light. (c) Quantitative results showing that CPD was repaired more efficiently in GM01389 cells with transient expression of wild-type DDB2 than those with DDB2-K4Q. The results represent the mean and standard deviation of data obtained from three biological replicates. "***", $P < 0.001$. The *P* values were calculated by using unpaired two-tailed t-test.

grounds that diminished α-N-trimethylation resulted in reduced recruitment of DDB2 to DNA damage sites, we reason that defective α-N-trimethylation may also compromise the recruitment and activation of downstream DNA damage response factors including ATM. Hence, we assessed ATM activation by monitoring the phosphorylation levels of ATM-S1981 and CHK1-S345 using Western analysis. It turned out that the overexpression of wild-type DDB2, but not its K4Q mutant, can significantly enhance the phosphorylation levels of ATM-S1981 and CHK1-S345 after UVC damage (Figure 2.8a). We also knocked down the expression of NRMT in HEK293T cells using siRNA and monitored how ATM activation is affected by the resulting reduced α-N-trimethylation of DDB2. Together, our results showed that NRMT knockdown indeed led to diminished phosphorylation of ATM-S1981 and CHK1-S345 (Figure 2.8b). In this context, it is worth noting that the reduced ATM activation may also be attributed to the diminished methylation of other NRMT substrates that may also play an important role in ATM activation. Therefore, our results supported that α-N-methylation of DDB2 is important for ATM activation.

α-N-methylation is crucial for cellular resistance toward UV light

Reduced recruitment of DDB2 to CPD sites and diminished ATM activation could result in compromised repair of CPD lesions, which may convey elevated sensitivity of cells to UV light. To test this, we assessed the viability of GM01389 cells by employing clonogenic survival assays. Our results showed that the proliferating ability of GM01389 cells is enhanced substantially in cells complement with wild-type DDB2,

but not the DDB2-K4Q mutant (Figure 2.8c). These results support that α-N-methylation of DDB2 can protect cells from cytotoxic effects conferred by UV damage.

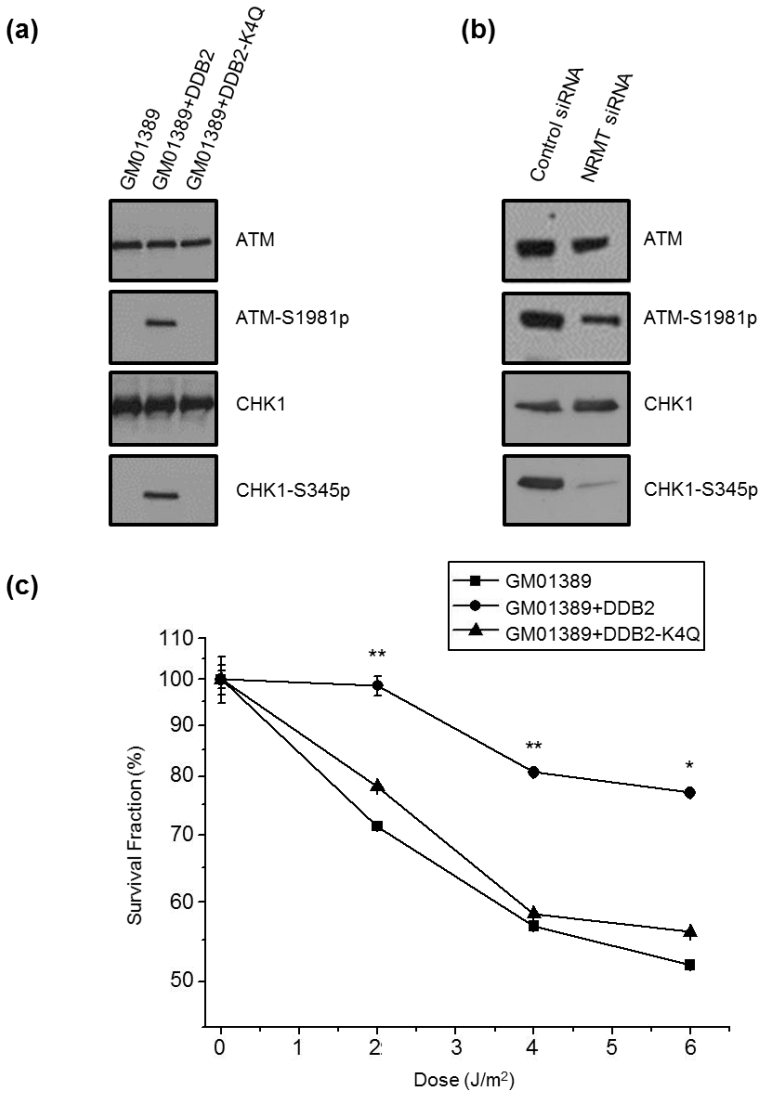

Figure 2. 8. α-N-methylation of DDB2 is important for ATM activation and for cellular resistance toward UV irradiation. (a) 30 mins after irradiation with 25 J/m^2 UV-C light, ATM autophosphorylation (ATM-S1981p) and CHK1 phosphorylation (CHK1-S345) were increased in GM01389 cells complemented with wild-type DDB2 but not α-N-methylation-defective DDB2-K4Q mutant. (b) After siRNA-induced knockdown of NRMT, ATM autophosphorylation (ATM-S1981p) and CHK1 phosphorylation (CHK1-S345) were reduced relative to control siRNA knockdown in HEK293T cells at 30 mins after irradiation with 25 J/m^2 UV-C light. (c) α-N-methylation is important for cellular resistance toward UV-induced cytotoxicity. Cellular sensitivity toward UV-C light as measured by clonogenic survival assay. The results represent the mean and standard deviation of results obtained from three independent experiments. "*", $P < 0.05$; "**", $P < 0.01$. The P values were calculated by using unpaired two-tailed t-test.

Discussion

We found that DDB2 can be α-N-methylated by NRMT in human cells and *in vitro*. In addition, *in vitro* methylation assay demonstrated that changing the proline in the 'XPK' motif to an alanine reduces markedly the α-N-methylation of the protein, whereas mutating the lysine in the motif to a glutamine abolishes the methylation. The availability of the DDB2-K4Q mutant defective in α-N-methylation allows us to examine the biological function of α-N-methylation. Our results illustrated that α-N-methylation of DDB2 facilitates DDB2's localization to DNA damage site, perhaps through enhancing the binding activity of DDB2 to DNA and/or by promoting its nuclear localization. In addition, α-N-methylation of DDB2 plays an important role in ATM activation and it confers resistance of human cells toward UV damage.

The functions of phosphorylation and ubiquitination of DDB2 have been extensively studied. UV-DDB associates tightly with CUL4-ROC1 complex which exhibits ubiquitin ligase activity (34). Following UV irradiation, UV-DDB complex localizes to UV-damage-enriched mononucleosome fraction and DDB2 is subsequently polyubiquitinated (35). Polyubiquitination of DDB2 reduces its binding affinity to DNA damage sites and is speculated to facilitate the handover of the lesion to XPC (36). In addition, DDB2 can be phosphorylated by c-Abl protein tyrosine kinase and this phosphorylation suppresses DDB2's binding toward UV-damaged DNA (37). On the other hand, p38 MAPK, a serine/threonine protein kinase, can facilitate the recruitment of NER factors XPC and TFIIH to UV-induced DNA damage sites by phosphorylating DDB2 (38).

Unlike methylation on the side chains of arginine and lysine residues, which have attracted great attention because these modifications on the N-terminal tails of core histones play a crucial role in chromatin structure and function (39), the biological functions of α-N-methylation for most eukaryotic proteins, except for RCC1 (16), CENP-A (27) and CENP-B (26), remain undefined. In this vein, α-N-methylation of RCC1 was shown to be important for spindle pole assembly, and the RCC1 mutants deficient in N-terminal α-methylation bind much more weakly to chromatin during mitosis, which induces a spindle pole defect (16). α-N-trimethylation of CENP-B can enhance its binding to the CENP-B box on human α-satellite DNA and mouse centromeric minor satellite DNA (26). On the grounds that trimethylation introduces a quaternary ammonium ion, a permanent cation (9), to the N-terminus of the protein, α-N-trimethylation may enhance the binding of the protein to DNA through electrostatic interaction between the protein N-terminus and phosphate groups in DNA. Therefore, a similar principle may account for the observations made in our study. In addition, α-N-methylation may also affect the function of DDB2 by modulating its interaction with other cellular proteins and by altering its intracellular location. Further investigations are required to exploit the mechanism underlying the observed biological functions of DDB2 introduced by α-N-methylation.

In conclusion, we uncovered a novel type of post-translational modification for DDB2, identified the enzyme involved in this methylation and revealed the role of this

methylation in repair of UV-induced CPD lesions. Our results also expanded the function of protein α-N-methylation to DNA repair.

References

1. de Laat, W.L., Jaspers, N.G. and Hoeijmakers, J.H. (1999) Molecular mechanism of nucleotide excision repair. *Genes Dev.*, **13**, 768-785.

2. Hanawalt, P.C. (2002) Subpathways of nucleotide excision repair and their regulation. *Oncogene*, **21**, 8949-8956.

3. Keeney, S., Chang, G.J. and Linn, S. (1993) Characterization of a human DNA damage binding protein implicated in xeroderma pigmentosum E. *J. Biol. Chem.*, **268**, 21293-21300.

4. Moser, J., Volker, M., Kool, H., Alekseev, S., Vrieling, H., Yasui, A., van Zeeland, A.A. and Mullenders, L.H. (2005) The UV-damaged DNA binding protein mediates efficient targeting of the nucleotide excision repair complex to UV-induced photo lesions. *DNA Repair*, **4**, 571-582.

5. Tang, J.Y., Hwang, B.J., Ford, J.M., Hanawalt, P.C. and Chu, G. (2000) Xeroderma pigmentosum p48 gene enhances global genomic repair and suppresses UV-induced mutagenesis. *Mol. Cell*, **5**, 737-744.

6. Sun, N.K., Lu, H.P. and Chao, C.C. (2002) Overexpression of damaged-DNA-binding protein 2 (DDB2) potentiates UV resistance in hamster V79 cells. *Chang Gung Med J*, **25**, 723-733.

7. Ray, A., Milum, K., Battu, A., Wani, G. and Wani, A.A. (2013) NER initiation factors, DDB2 and XPC, regulate UV radiation response by recruiting ATR and ATM kinases to DNA damage sites. *DNA Repair (Amst)*, **12**, 273-283.

8. Stoyanova, T., Roy, N., Kopanja, D., Bagchi, S. and Raychaudhuri, P. (2009) DDB2 decides cell fate following DNA damage. *Proc Natl Acad Sci U S A*, **106**, 10690-10695.

9. Stock, A., Clarke, S., Clarke, C. and Stock, J. (1987) N-terminal methylation of proteins: structure, function and specificity. *Febs Lett*, **220**, 8-14.

10. Xiong, L., Adhvaryu, K.K., Selker, E.U. and Wang, Y. (2010) Mapping of lysine methylation and acetylation in core histones of Neurospora crassa. *Biochemistry*, **49**, 5236-5243.

11. Medzihradszky, K.F., Zhang, X., Chalkley, R.J., Guan, S., McFarland, M.A., Chalmers, M.J., Marshall, A.G., Diaz, R.L., Allis, C.D. and Burlingame, A.L. (2004) Characterization of Tetrahymena histone H2B variants and posttranslational populations by electron capture dissociation (ECD) Fourier

transform ion cyclotron mass spectrometry (FT-ICR MS). *Mol Cell Proteomics*, **3**, 872-886.

12. Nomoto, M., Kyogoku, Y. and Iwai, K. (1982) N-Trimethylalanine, a novel blocked N-terminal residue of *Tetrahymena* histone H2B. *J. Biochem.*, **92**, 1675-1678.

13. Bonenfant, D., Coulot, M., Towbin, H., Schindler, P. and van Oostrum, J. (2006) Characterization of histone H2A and H2B variants and their post-translational modifications by mass spectrometry. *Mol Cell Proteomics*, **5**, 541-552.

14. Desrosiers, R. and Tanguay, R.M. (1988) Methylation of *Drosophila* histones at proline, lysine, and arginine residues during heat-shock. *J. Biol. Chem.*, **263**, 4686-4692.

15. Martinage, A., Briand, G., Vandorsselaer, A., Turner, C.H. and Sautiere, P. (1985) Primary structure of histone H2b from gonads of the starfish *Asterias-rubens* - Identification of an N-dimethylproline residue at the amino-terminal. *Eur J Biochem*, **147**, 351-359.

16. Chen, T., Muratore, T.L., Schaner-Tooley, C.E., Shabanowitz, J., Hunt, D.F. and Macara, I.G. (2007) N-terminal α-methylation of RCC1 is necessary for stable chromatin association and normal mitosis. *Nat Cell Biol*, **9**, 596-603.

17. Tooley, C.E., Petkowski, J.J., Muratore-Schroeder, T.L., Balsbaugh, J.L., Shabanowitz, J., Sabat, M., Minor, W., Hunt, D.F. and Macara, I.G. (2010) NRMT is an α-N-methyltransferase that methylates RCC1 and retinoblastoma protein. *Nature*, **466**, 1125-1128.

18. Petkowski, J.J., Schaner Tooley, C.E., Anderson, L.C., Shumilin, I.A., Balsbaugh, J.L., Shabanowitz, J., Hunt, D.F., Minor, W. and Macara, I.G. (2012) Substrate specificity of mammalian N-terminal α-amino methyltransferase NRMT. *Biochemistry*, **51**, 5942-5950.

19. Henry, G.D., Dalgarno, D.C., Marcus, G., Scott, M., Levine, B.A. and Trayer, I.P. (1982) The occurrence of α-N-trimethylalanine as the N-terminal amino-acid of some myosin light-chains. *Febs Lett*, **144**, 11-15.

20. Webb, K.J., Lipson, R.S., Al-Hadid, Q., Whitelegge, J.P. and Clarke, S.G. (2010) Identification of protein N-terminal methyltransferases in yeast and humans. *Biochemistry*, **49**, 5225-5235.

21. Porras-Yakushi, T.R., Whitelegge, J.P. and Clarke, S. (2006) A novel SET domain methyltransferase in yeast: Rkm2-dependent trimethylation of ribosomal protein L12ab at lysine 10. *J. Biol. Chem.*, **281**, 35835-35845.

22. Sadaie, M., Shinmyozu, K. and Nakayama, J. (2008) A conserved SET domain methyltransferase, Set11, modifies ribosomal protein Rpl12 in fission yeast. *J. Biol. Chem.*, **283**, 7185-7195.

23. Carroll, A.J., Heazlewood, J.L., Ito, J. and Millar, A.H. (2008) Analysis of the *Arabidopsis* cytosolic ribosome proteome provides detailed insights into its components and their post-translational modification. *Mol Cell Proteomics*, **7**, 347-369.

24. Smith, G.M. and Pettigrew, G.W. (1980) Identification of *N,N*-dimethylproline as the N-terminal blocking group of *Crithidia-oncopelti* cytochrome-C557. *Eur J Biochem*, **110**, 123-130.

25. Meng, F., Du, Y., Miller, L.M., Patrie, S.M., Robinson, D.E. and Kelleher, N.L. (2004) Molecular-level description of proteins from *Saccharomyces cerevisiae* using quadrupole FT hybrid mass spectrometry for top down proteomics. *Anal. Chem.*, **76**, 2852-2858.

26. Dai, X., Otake, K., You, C., Cai, Q., Wang, Z., Masumoto, H. and Wang, Y. (2013) Identification of novel alpha-n-methylation of CENP-B that regulates its binding to the centromeric DNA. *J Proteome Res*, **12**, 4167-4175.

27. Bailey, A.O., Panchenko, T., Sathyan, K.M., Petkowski, J.J., Pai, P.J., Bai, D.L., Russell, D.H., Macara, I.G., Shabanowitz, J., Hunt, D.F. *et al.* (2013) Posttranslational modification of CENP-A influences the conformation of centromeric chromatin. *Proc Natl Acad Sci U S A*, **110**, 11827-11832.

28. Zhang, F., Dai, X. and Wang, Y. (2012) 5-Aza-2'-deoxycytidine induced growth inhibition of leukemia cells through modulating endogenous cholesterol biosynthesis. *Mol Cell Proteomics*, **11**, M111 016915.

29. Ziv, Y., Bielopolski, D., Galanty, Y., Lukas, C., Taya, Y., Schultz, D.C., Lukas, J., Bekker-Jensen, S., Bartek, J. and Shiloh, Y. (2006) Chromatin relaxation in response to DNA double-strand breaks is modulated by a novel ATM- and KAP-1 dependent pathway. *Nature Cell Biology*, **8**, 870-876.

30. Rouget, R., Auclair, Y., Loignon, M., Affar el, B. and Drobetsky, E.A. (2008) A sensitive flow cytometry-based nucleotide excision repair assay unexpectedly reveals that mitogen-activated protein kinase signaling does not regulate the

removal of UV-induced DNA damage in human cells. *J Biol Chem*, **283**, 5533-5541.

31. Xiong, L., Ping, L., Yuan, B. and Wang, Y. (2009) Methyl group migration during the fragmentation of singly charged ions of trimethyllysine-containing peptides: precaution of using MS/MS of singly charged ions for interrogating peptide methylation. *J. Am. Soc. Mass Spectrom.*, **20**, 1172-1181.

32. Hwang, B.J., Toering, S., Francke, U. and Chu, G. (1998) p48 Activates a UV-damaged-DNA binding factor and is defective in xeroderma pigmentosum group E cells that lack binding activity. *Mol. Cell Biol.*, **18**, 4391-4399.

33. Patel, D.J. and Wang, Z. (2013) Readout of epigenetic modifications. *Annu. Rev. Biochem.*, **82**, 81-118.

34. Groisman, R., Polanowska, J., Kuraoka, I., Sawada, J., Saijo, M., Drapkin, R., Kisselev, A.F., Tanaka, K. and Nakatani, Y. (2003) The ubiquitin ligase activity in the DDB2 and CSA complexes is differentially regulated by the COP9 signalosome in response to DNA damage. *Cell*, **113**, 357-367.

35. Matsuda, N., Azuma, K., Saijo, M., Iemura, S., Hioki, Y., Natsume, T., Chiba, T. and Tanaka, K. (2005) DDB2, the xeroderma pigmentosum group E gene product, is directly ubiquitylated by Cullin 4A-based ubiquitin ligase complex. *DNA Repair*, **4**, 537-545.

36. Sugasawa, K., Okuda, Y., Saijo, M., Nishi, R., Matsuda, N., Chu, G., Mori, T., Iwai, S., Tanaka, K. and Hanaoka, F. (2005) UV-induced ubiquitylation of XPC protein mediated by UV-DDB-ubiquitin ligase complex. *Cell*, **121**, 387-400.

37. Cong, F., Tang, J., Hwang, B.J., Vuong, B.Q., Chu, G. and Goff, S.P. (2002) Interaction between UV-damaged DNA binding activity proteins and the c-Abl tyrosine kinase. *J. Biol. Chem.*, **277**, 34870-34878.

38. Zhao, Q., Barakat, B.M., Qin, S., Ray, A., El-Mahdy, M.A., Wani, G., Arafa el, S., Mir, S.N., Wang, Q.E. and Wani, A.A. (2008) The p38 mitogen-activated protein kinase augments nucleotide excision repair by mediating DDB2 degradation and chromatin relaxation. *J. Biol. Chem.*, **283**, 32553-32561.

39. Jenuwein, T. and Allis, C.D. (2001) Translating the histone code. *Science*, **293**, 1074-1080.

Chapter 3. Identification and Functional Characterizations of Serine 26 Phosphorylation in DDB2

Introduction

DDB2 (p48), normally present together with DDB1 (p127) as a heterodimer known as ultraviolet-damaged DNA binding protein (UV-DDB) (1-3), functions in nucleotide excision repair (NER) (4). NER eliminates a wide array of helix-distorting DNA lesions, including UV light-induced cyclobutane pyrimidine dimer (CPD) and pyrimidine(6-4)pyrimidone photoproducts (6-4PPs), as well as bulky DNA adducts induced by numerous environmental carcinogens (5). Xeroderma pigmentosum (XP) is a rare recessive genetic disease due to mutations in one of the eight genes, XPA through XPG, which lead to defective NER, and XPV, which gives rise to compromised translesion synthesis (6). Among them, the *XPE* gene encodes DDB2, and XPE cells display deficiencies in the repair of CPDs, but not 6-4PPs (4,7). XPE patients manifest hypersensitivity to sunlight and are susceptible to developing skin cancer (6). GM01389 cells, which carry a mutant DDB2 with an L350P substitution and the deletion of N349, are deficient in DDB activity; transfection wild-type DDB2 to hamster cells could restore the DDB and DNA repair activities (8). Meanwhile, cultured hamster cells, which express DDB1, but not DDB2, fail to repair CPD and are hypersensitive to UV light (9,10). Along this line, *Ddb2*$^{-/-}$ mice are susceptible to UV-induced skin carcinogenesis, and the skin tissues of these mice display a significantly reduced initial rate of removal of

CPD lesions following UV exposure (11). Recently, DDB2 was also reported to regulate ATM/ATR activation by coordinating with XPC (12).

Post-translational modification (PTM) is a common mechanism for regulating proteins' structure, interaction, localization and function. DDB2 is extensively modified by various types of PTMs, which encompass phosphorylation, α-N-methylation, SUMOylation, ubiquitination, and poly(ADP-ribosyl)ation (13-18); however, in most cases it remains yet unestablished which particular amino acid residues were modified. Mass spectrometry (MS) has been widely used as an analytical strategy to identify PTMs. In this context, MS could facilitate the unambiguous determination of the types and sites of PTMs. In the present study, we found that the ectopically expressed DDB2 is phosphorylated at S26 in HEK293T cells by Cdks. We also revealed that this phosphorylation promotes DDB2's nuclear localization and recruitment to CPD foci, facilitates DDB2 degradation via the proteasomal pathway, enables ATM activation, enhances CPD repair, and conveys cellular resistance toward UVC light.

Materials and Methods Materials

Cell culture conditions

The HEK293T cells were purchased from ATCC. GM01389 cells were kindly provided by Dr. Michael M. Seidman (National Institute of Aging). HEK293T and GM01389 cells were cultured in Dulbecco's modified Eagle's medium (ATCC) and α Minimum Essential Medium (αMEM, ATCC), respectively. The media contained 10% (for HEK293T) or 15% (for GM01389 cells) fetal bovine serum (Invitrogen), 100

units/ml penicillin, and 100 μg/ml streptomycin. The cells were cultured at 37°C in 5% CO_2 atmosphere.

Constructs

The pRK7-DDB2-3×FLAG plasmid was constructed previously (17), and the DDB2-S26A mutant construct was amplified from the pRK7-DDB2-3×FLAG plasmid using site-directed mutagenesis.

LC-MS/MS analysis

The FLAG-tagged DDB2 was isolated using affinity purification with anti-FLAG M2 beads (Sigma). The sample was subsequently reduced, alkylated and digested with trypsin at an enzyme: protein ratio of 1:50 (w/w) at room temperature overnight. The resulting peptide mixture was subjected to online LC-MS/MS analysis with an EASY-nLC II that was interfaced with an LTQ Orbitrap Velos mass spectrometer equipped with a nanoelectrospray ionization source (Thermo, San Jose, CA) following similar procedures as described previously (19). The separation was conducted by using a homemade trapping column (150 μm × 50 mm) and a separation column (75 μm ×120 mm), packed with ReproSil-Pur C18-AQ resin (3 μm in particle size, Dr. Maisch HPLC GmbH, Germany). Peptide samples were initially loaded onto the trapping column with a solvent mixture of 0.1% formic acid in CH_3CN/H_2O (2:98, v/v) at a flow rate of 4.0 μl/min. The peptides were then separated using a 90-min linear gradient of 2-40% acetonitrile in 0.1% formic acid and at a flow rate of 220 nl/min. The mass spectrometer was operated in the positive-ion mode, and the spray voltage was 1.8 kV. The data were

acquired in a data-dependent scan mode where one full-scan MS was followed with 20 MS/MS scans. To obtain high-quality MS/MS, the data were also collected in selected-ion monitoring mode where the fragmentation of the $[M+2H]^{2+}$ ions of the unmodified and phosphorylated forms of the peptide SRSPLELEPEAK from DDB2 were monitored. The MS/MS data were manually analyzed.

Fluorescence microscopy

The GM01389 cells transfected with the expression plasmids for the wild-type DDB2, DDB2-S26A or empty control were grown on glass coverslips, and irradiated with UV-C light at 40 J/m^2 through a 5-μm isopore polycarbonate filter (Millipore). After the irradiation, the membrane was removed, and the cells recovered at 37°C for 30 min. The cells were subsequently fixed with 4% paraformaldehyde, permeated using 0.5% Triton X-100 in PBS, washed with PBS, and the DNA was denatured by incubation with 2 M HCl for 5 min. The cells were then incubated in a solution containing 20% goat serum, 0.3% Triton X-100, and 5% bovine serum albumin (BSA) at room temperature for 1 hr to block non-specific binding. Primary anti-FLAG (Cell Signaling) and anti-CPD (Kamiya Biomedical Company) antibodies and secondary antibodies (Invitrogen) were subsequently added and incubated at 4°C for overnight and then at room temperature for 1 hr. After the incubation, the coverslips were washed with PBS and mounted onto microscope slides in ProLong Gold Antifade Reagent with DAPI (Invitrogen). Images were captured with a Leica TCS SP2/UV confocal microscope (Leica Microsystems).

Western blot

To examine the localization of DDB2, HEK293T cells transiently expressing the wild-type DDB2 or DDB2-S26A were collected immediately, or at 30 min, after irradiation with 40 J/m^2 UV-C light. The nuclear and cytoplasmic fractions were prepared using NE-PER Nuclear and Cytoplasmic extraction kit (Thermo Scientific) following the manufacturer's recommended procedures. The lysate was separated by SDS-PAGE, and the proteins transferred to a nitrocellulose membrane (Whatman) in transfer buffer (10 mM $NaHCO_3$, 3 mM Na_2CO_3, and 20% methanol). The membrane was blocked in 5% (w/v) blocking-grade milk (Bio-Rad), 0.1% (v/v) Tween-20 in PBS for 6 hr. Antibodies that specifically recognized histone H3 and FLAG epitope tag (Cell Signaling) were used at 1:10000 dilution. Antibody that specifically recognized human actin (abcam) and ubiquitin (Cell Signaling) were used at 1:5000 dilution. For ATM activation, antibodies that specifically recognized human ATM or phospho-ATM (Ser1981), and human CHK1 and phospho-CHK1 (Ser345) (Cell Signaling) were used at 1:1000 dilution. Horseradish peroxidase-conjugated secondary goat anti-rabbit antibody (abcam) and goat anti-mouse antibody (Santa Cruz) were used at a 1:10000 dilution. The secondary antibody was detected using ECL Advance Western Blotting Detection Kit (GE Healthcare) and visualized with Hyblot CL autoradiography film (Denville Scientific, Inc., Metuchen, NJ).

Colonogenic survival assay

For survival assay, GM01389 cells, at 24 hr following transfection with pRK7-DDB2-3×FLAG, pRK7-DDB2-S26A-3×FLAG or empty control, were plated in 6-well

plates in triplicate at densities of 200-2000 cells per well. After 6 hr, the cells were exposed with various doses of UV-C light. Cell colonies grown for 10-14 days (20) were then fixed using 6% (v/v) glutaraldehyde and stained with 0.5% (w/v) crystal violet. Colonies containing at least 50 cells were counted under a microscope.

Flow cytometry-based DNA repair assay

The CPD repair assay was performed following previously described procedures (17,21). The GM01389 cells were plated in 6-well plates at a density of 3×10^5 cells/well and, after 16 hr, plasmids for overexpressing wild-type DDB2 or DDB2-S26A mutant were transfected individually into the plated GM01389 cells. At 28 hr following transfection, the DMEM medium was replaced with 1×PBS buffer and the cells irradiated with UV-C light at 10 J/m^2. After the irradiation, PBS buffer was removed and fresh medium containing 200 ng/ml nocodazole was added to the cells. At various time intervals following UV irradiation, the cells were washed with PBS, resuspended in 125 μl PBS and fixed by adding 375 μl pre-chilled (-20°C) ethanol and incubating for at least 1 hr. The cells were subsequently permeated and denatured with 0.5% (v/v) Triton X-100 in 2 N HCl at room temperature for 15 min. The cells were washed thrice with PBS and resuspended in 200 μl PBS with 100 μg/ml RNase A at 37°C for 1 hr. The cells were subsequently blocked in blocking buffer, which contained 5% (v/v) bovine serum albumin and 0.3% (v/v) Triton X-100 in PBS, at room temperature for 20 min. The cells were then resuspended in the blocking buffer containing mouse anti-CPD antibody (1:1000 dilution) at room temperature for 45 min and then at 4°C overnight. Cell pellets were subsequently washed thrice with washing buffer, which contained 0.3% (v/v) Triton

X-100 in PBS, and then resuspended in Alexa Fluor 647 Goat anti-Mouse antibody (1:200 dilution, Invitrogen) at room temperature for 1 hr. The cell pellets were washed again with the washing buffer for three times and resuspended in sorting buffer (1×PBS, 1 mM EDTA, 25 mM HEPES, 1% FBS, v/v, pH 7.0) for flow cytometry analysis (BD FACS Aria I).

Results

Serine 26 of DDB2 is phosphorylated in human cells

DDB2 was previously observed to be phosphorylated by p38 mitogen-activated protein kinase (MAPK) and c-Abl protein tyrosine kinase (15,16), though the phosphorylation sites have not yet been identified. We recently constructed a plasmid for expressing C-terminally FLAG-tagged DDB2 in HEK293T cells (17). Aside from α-N-methylation (17), our LC-MS/MS analysis of the tryptic digestion mixture of DDB2 also led to the identification of a phosphorylated peptide SRSPLELEPEAK with the underlined S26 being phosphorylated. As shown in Figure 3.1, the MS/MS of the $[M + 2H]^{2+}$ ion of the phosphorylated peptide SRSPLELEPEAK revealed the presence of b_2, y_2, y_4-y_5 and y_9 ions, which exhibit the same m/z values as the corresponding fragment ions observed in the MS/MS of the $[M + 2H]^{2+}$ ion of the unmodified peptide. Additionally, b_3, b_6, b_8, b_{10}, b_{11} and y_{10} ions found in the MS/MS of the $[M + 2H]^{2+}$ ion of the phosphorylated peptide bear a phosphorylated amino acid residue. These results provide unambiguous evidence to support the phosphorylation of S26 in DDB2.

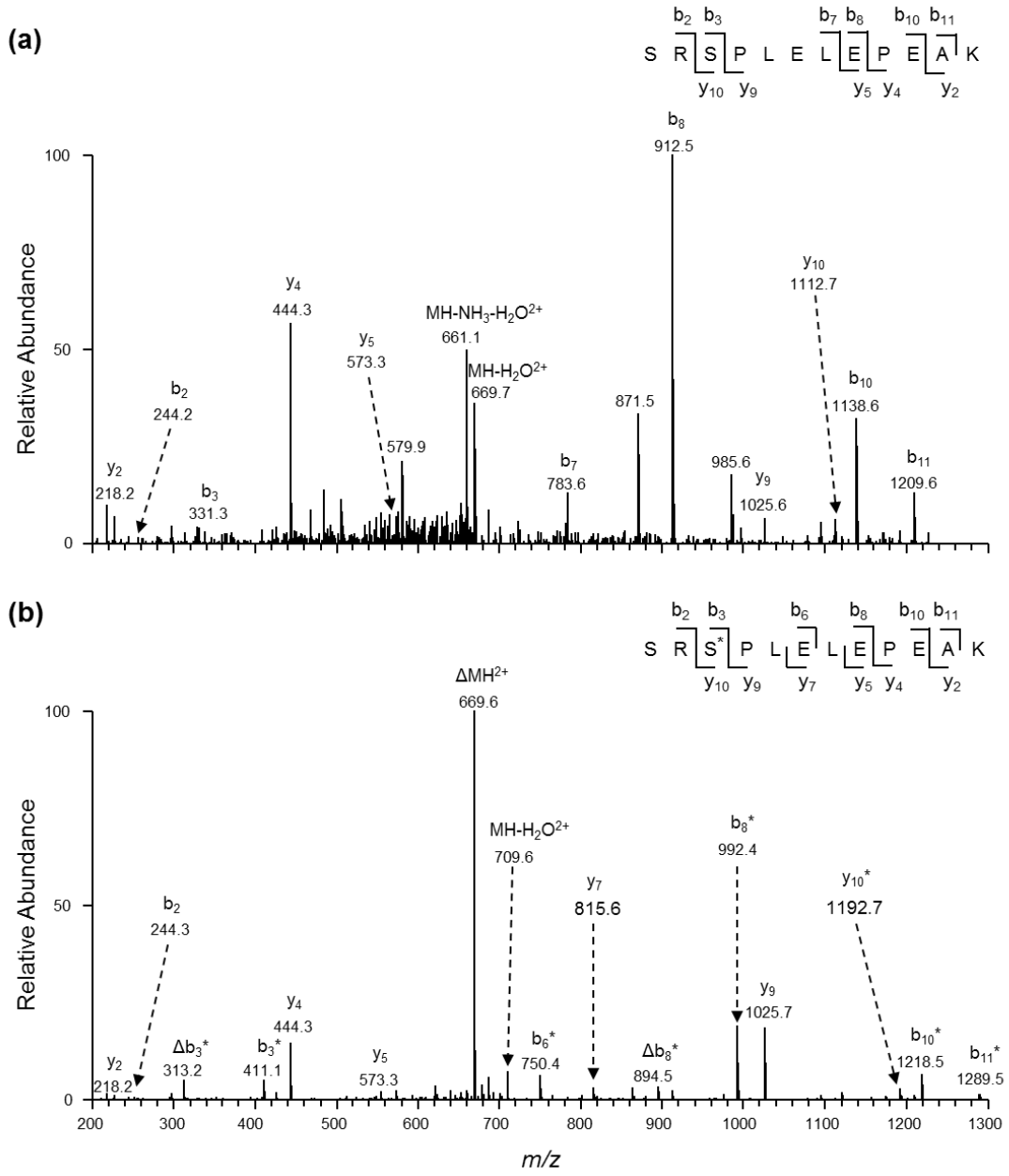

Figure 3. 1. ESI-MS/MS of the $[M+2H]^{2+}$ ions of (a) the unmodified $_{24}$SRSPLELEPEAK$_{35}$ and (b) monophosphorylated $_{24}$SRSPLELEPEAK$_{35}$ from the tryptic digestion mixture of C-terminally FLAG-tagged DDB2 isolated from HEK293T cells. Asterisk (*) and triangle (Δ) designate those ions bearing a phosphate group and carrying a neutral loss of H3PO4, respectively.

Viewing that S26 precedes a proline residue and can be specifically phosphorylated by kinases including p38 MAPK and Cdks (22), we assessed whether the level of the S26 phosphorylation can be altered upon treatment with inhibitors of these kinases. Our results showed that upon treatment with flavopiridol, a Cdk inhibitor, the ratio of signal intensity for the phosphorylated/unmodified peptide was reduced by more than 80%; however, there is no substantial decline in the level of this phosphorylation upon treatment with SB203580, a p38 MAPK inhibitor (Figure 3.2a&b). These results demonstrated that the phosphorylation of S26 in DDB2 is mediated by Cdks.

To assess whether S26 phosphorylation of DDB2 is altered upon UVC light exposure, we examined the phosphorylation level of S26 in DDB2 in HEK293T cells irradiated with 40 J/m^2 UVC light. Our LC-MS/MS results revealed no appreciable change in the phosphorylation level of S26 in cells upon exposure to UV light (Figure 3.2c).

S26 phosphorylation is required for DDB2's recruitment to CPD foci

To examine the function of S26 phosphorylation, we first asked whether deficiency in this phosphorylation affects DDB2's recruitment to CPD foci. To test this, we transiently transfected GM01389 cells, which do not carry functional DDB2, with expression vectors for FLAG-tagged DDB2 and a phosphorylation-deficient mutant of DDB2, i.e., DDB2-S26A. Immunofluorescence analyses using anti-FLAG and anti-CPD antibodies revealed that 98.5% of CPD foci co-localized with DDB2 foci in GM01389 cells complemented with wild-type DDB2, whereas only 1.5% of the CPD foci co-localized with DDB2 foci in cells reconstituted with DDB2-S26A (Figure 3.3a, b). In this context, it is worth noting that wild-type DDB2 and DDB2-S26A mutant were expressed

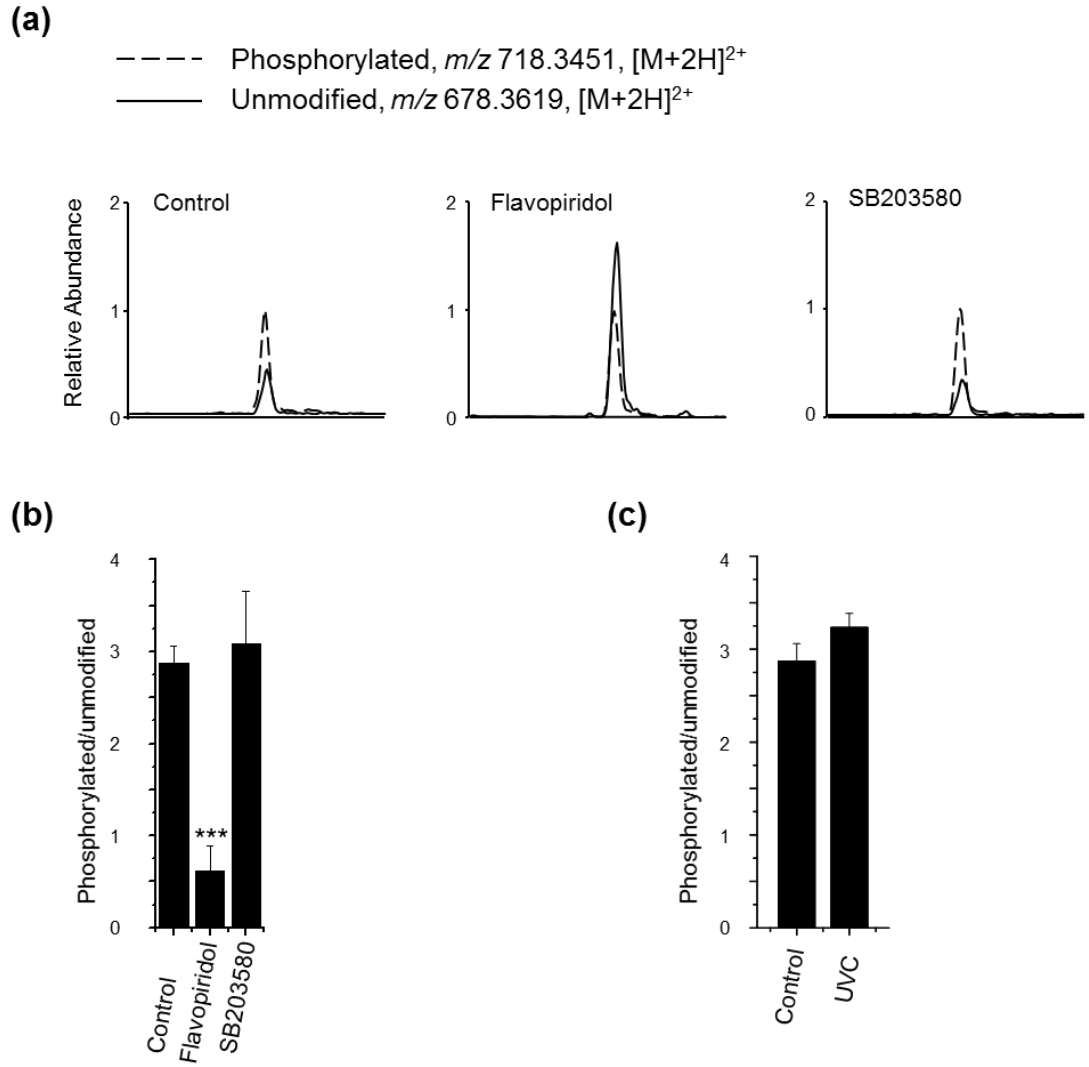

Figure 3. 2. S26 phosphorylation of DDB2 is mediated by Cdks, but not p38 MAPK. (a) Selected-ion chromatogram for monitoring the $[M+2H]^{2+}$ ions of the unmodified (m/z 678.3619) and monophosphorylated (m/z 718.3451) peptide 24SRSPLELEPEAK35 from the tryptic digestion of FLAG-tagged DDB2 isolated from HEK293T cells without any treatment, treated with 1 μM flavopiridol for 6 hr, or treated with 10 μM SB203580 for 30 min. (b) Relative levels of phosphorylation of S26 in DDB2 in HEK293T cells under various treatment conditions as described in (a). (c) Relative levels of S26 phosphorylation of DDB2 in HEK293T cells without treatment or exposed with 40 J/m2 UV-C light. The results represent the mean and standard deviation of results obtained from three independent experiments. "***", $P < 0.001$. The *P* values were calculated by using unpaired two-tailed t-test.

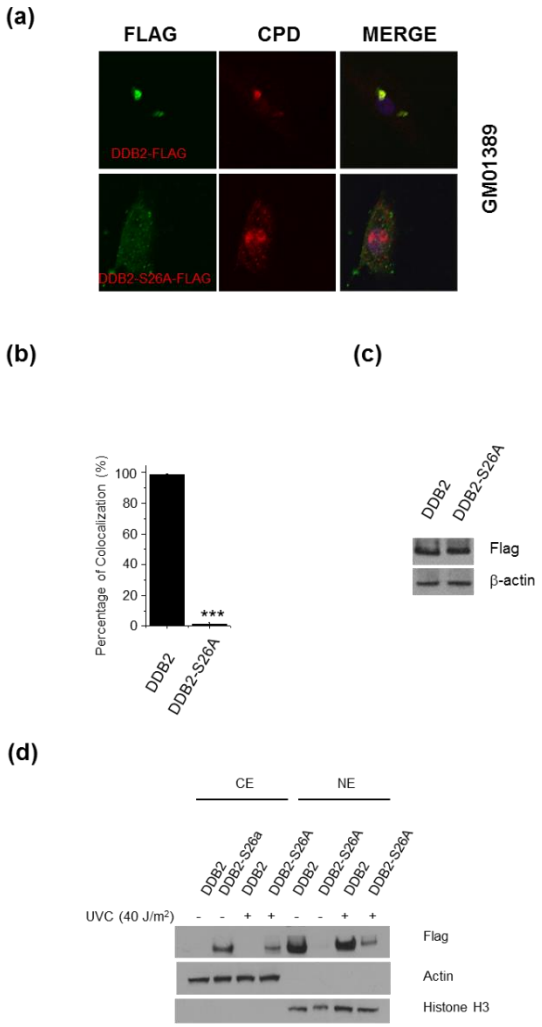

Figure 3. 3. S26 phosphorylation of DDB2 plays a significant role in its recruitment to DNA damage foci. (a) Representative images for monitoring the co-localization of transfected wild-type DDB2 and DDB2-S26A to CPD foci in GM01389 cells; (b) The percentage of CPD foci that are co-localized with DDB2 foci. In cells transfected with the DDB2-S26A construct, almost no DDB2 foci co-localized with CPD foci, whereas almost all DDB2 foci displayed co-localization with CPD foci in cells transfected with the wild-type DDB2 plasmid. The results represent the mean and standard deviation of results obtained from three biological replicates, and approximately 100 cells were counted in each replicate. "***", $P < 0.001$. The P values were calculated by using unpaired two-tailed Student's t-test. (c) Western blot analysis of wild-type DDB2 and DDB2-S26A in whole-cell extracts of GM01389 cells transfected with the corresponding DDB2 constructs. β-actin was used as a loading control. (d) Western blot revealed the attenuated nuclear localization of DDB2-S26A relative to wild-type DDB2 in HEK293T cells with or without exposure to UV-C light. β-actin and histone H3 were employed as loading controls for the cytoplasmic extract (CE) and nuclear extract (NE), respectively.

at similar levels in GM01389 cells, as shown by Western blot analysis (Figure 3.3c). Additionally, our immunofluorescence assay results showed more diffused distribution of DDB2-S26A (Figure 3.3a). Consistent with these findings, our Western blot result demonstrated that, with or without UV-C light exposure, the phosphorylation-defective mutant displayed a reduced presence in the nuclear fraction relative to wild-type DDB2 (Figure 3.3d). Thus, the above results demonstrated that S26 phosphorylation plays a pivotal role in DDB2's nuclear localization and recruitment to CPD foci.

S26 phosphorylation of DDB2 is indispensable for CPD repair in GM01389 cells

Transfection of DDB2 into hamster cells can enhance the repair of CPDs (7), and the above results demonstrated that the phosphorylation-defective mutant of DDB2 exhibited diminished recruitment to CPD foci. Thus, we also asked whether the phosphorylation of DDB2 also plays a role in CPD repair by using a flow cytometry-based method (21). As expected, GM01389 cells displayed very little repair of the CPD lesion (Figure 3.4a, b). On the other hand, significant repair (by 70%) of CPD was observed at 48 hr in GM01389 cells complemented with wild-type DDB2, but not DDB2-S26A (Figure 3.4a, b). These results demonstrated that the repair of CPD in human cells necessitates S26 phosphorylation.

Cross-talk between S26 phosphorylation and polyubiquitination

Protein phosphorylation is a very important signaling event which can promote or inhibit protein polyubiquitination (23,24). Polyubiquitination of DDB2 is known to initiate its degradation after UV irradiation, which enables XPC recruitment (25,26). We

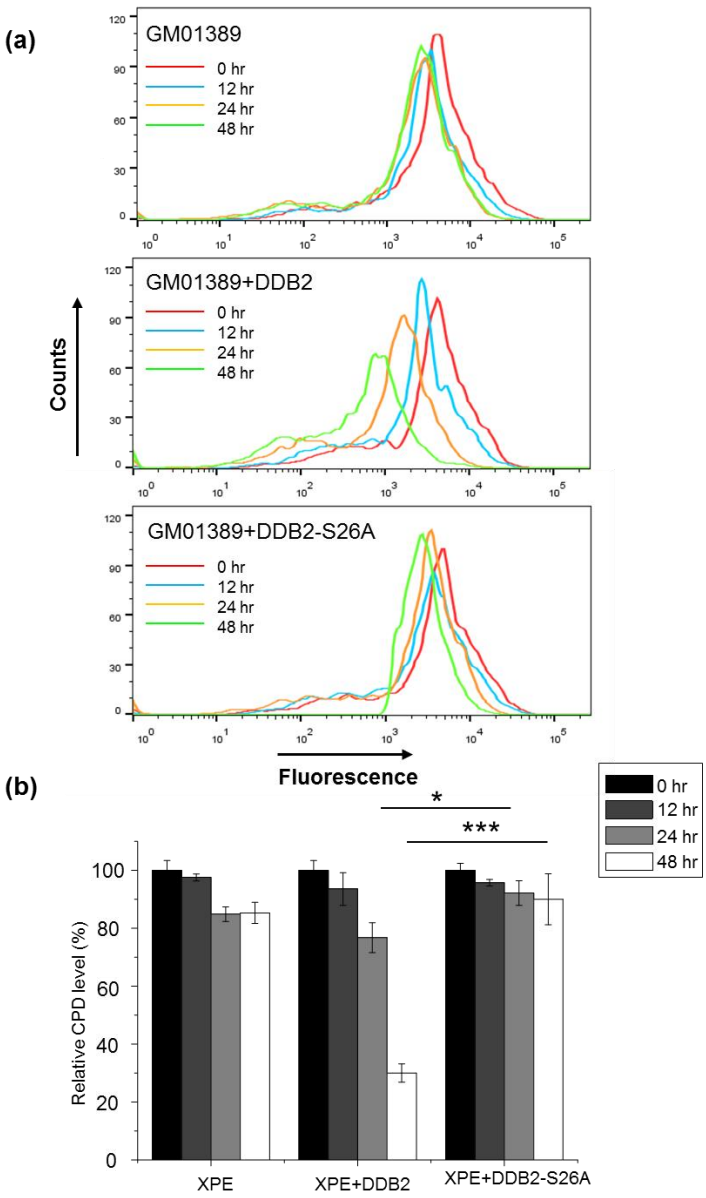

Figure 3. 4. S26 phosphorylation of DDB2 promotes CPD repair in GM01389 cells. (a) Flow cytometry results showing the levels of CPD in GM01389 cells reconstituted with empty control vector, wild-type DDB2 and DDB2-S26A at various time intervals (0, 12, 24, and 48 hr) after irradiation with 10 J/m^2 UV-C light. (b) Quantitative analysis of CPD repair efficiency in GM01389 cells with transient expression of empty control, wild-type DDB2 and DDB2-S26A. The results represent the mean and standard deviation of results obtained from three biological replicates. "*", $P < 0.05$; "***", $P < 0.001$. The P values were calculated by using unpaired two-tailed Student's t-test.

hypothesize that the newly identified S26 phosphorylation may also alter polyubiquitination of DDB2. Our results indeed revealed more pronounced degradation for wild-type DDB2 than DDB2-S26A after irradiation with 40 J/m^2 UV light (Figure 5a). Considering that DDB2 degradation is known to be mediated by Cul4A through the ubiquitin-proteasome pathway (27-29), we treated cells with a proteasome inhibitor, MG132, and examined the degradation of wild-type DDB2 and DDB2-S26A after UV exposure. It turned out that, after UV irradiation, more pronounced polyubiquitination was observed for the wild-type DDB2 than the S26A mutant (Figure 3.5b). Together, these results supported that the phosphorylation of S26 in DDB2 positively regulates the polyubiquitination and proteasomal degradation of DDB2.

S26 phosphorylation of DDB2 facilitates ATM activation in GM01389 cells

DDB2, as an early UV damage recognition factor, was previously found to be crucial for ATM recruitment to DNA damage sites and for its activation (12). Viewing that defective S26 phosphorylation resulted in diminished recruitment of DDB2 to DNA damage sites, we reason that the reduced phosphorylation at S26 may also compromise the recruitment and activation of DNA damage response factors including ATM. Hence, we examined ATM activation by monitoring the phosphorylation levels of ATM-S1981 and CHK1-S345 with Western blot analysis. Our results (Figure 3.5c) demonstrated that reconstitution with wild-type DDB2, but not its S26A mutant, significantly enhanced the phosphorylation of ATM-S1981 and CHK1-S345 following UV damage. Thus, S26 phosphorylation of DDB2 is important for ATM activation.

S26 phosphorylation of DDB2 confers cellular resistance toward UV damage

We reason that the diminished ATM activation, abolished recruitment of DDB2 to CPD sites, and compromised repair of CPD lesions observed for the phosphorylation-defective mutant of DDB2 may also confer elevated sensitivity of cells toward UV light exposure. To test this, we assessed the viability of GM01389 cells and the same cells complemented with wild-type DDB2 or DDB2-S26A by employing the clonogenic survival assay. Our results showed that the proliferating ability of GM01389 cells is enhanced substantially in cells reconstituted with wild-type DDB2, but not DDB2-S26A (Figure 3.5d). Thus, phosphorylation of S26 in DDB2 can protect cells from the cytotoxic effects of UV damage.

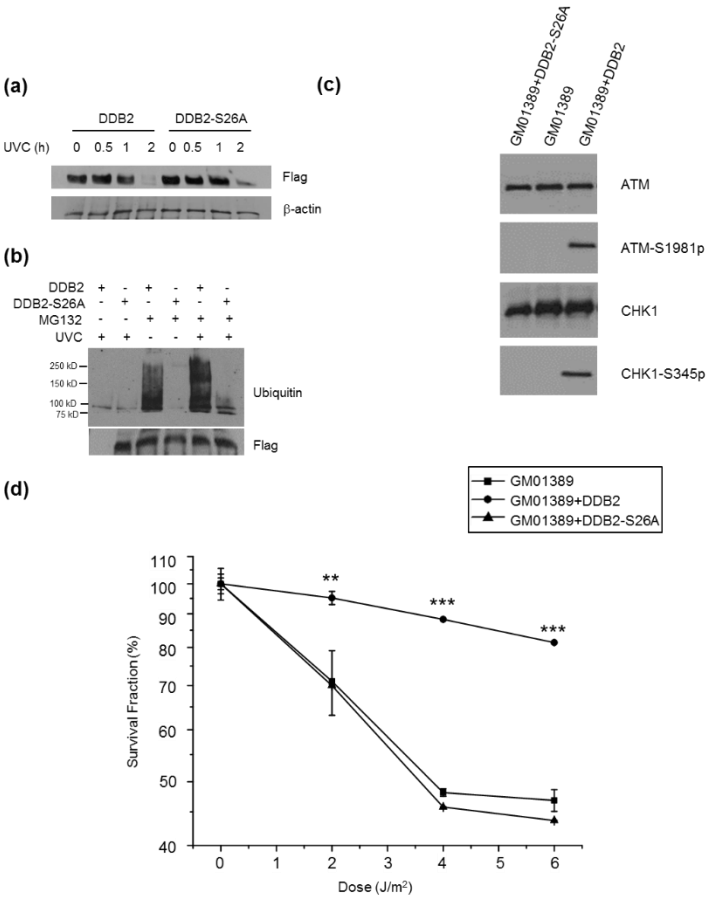

Figure 3. 5. S26 phosphorylation of DDB2 stimulates the proteasomal degradation of DDB2, promotes ATM activation and enhances cellular resistance toward UV irradiation. (a) HEK293T cells transfected with FLAG-tagged wild-type DDB2 or S26A mutant were irradiated with 40 J/m^2 UV-C light, and recovered in fresh DMEM medium for the indicated periods of time. The level of wild-type DDB2 is diminished more rapidly than the S26A mutant. (b) HEK293T cells transfected with FLAG-tagged wild-type DDB2 or S26A mutant were pretreated with 10 μM MG132 for 2 hr before exposure to 40 J/m^2 UV-C light. The cells were then recovered for another 2 hr. Cell lysates were immunoprecipitated with anti-FLAG M2 beads and analyzed by anti-ubiquitin and anti-FLAG antibody. (c) At 30 min after irradiation with 25 J/m^2 UV-C light, GM01389 cells complemented with wild-type DDB2, but not the phosphorylation-defective DDB2-S26A mutant, exhibited increased ATM autophosphorylation (ATM-S1981p) and CHK1 phosphorylation (CHK1-S345). (d) Clonogenic survival assay revealed that S26 phosphorylation of DDB2 enhanced cellular resistance toward UV-induced cytotoxicity. The data represent the mean and standard deviation of results obtained from three independent experiments. "**", $P < 0.01$; "***", $P < 0.001$. The P values were calculated by using unpaired two-tailed Student's t-test.

Discussion

NER, a central cellular repair pathway for protecting cells against the carcinogenic effects of UV light from the sun, operates through two subpathways, i.e., global-genome NER and transcription-coupled NER, which repair DNA damage throughout the entire genome and those DNA lesions situated on the transcribed strand of active genes, respectively (1,2).

DDB2, as a component of the UV-DDB complex, which exhibits high binding affinity toward UV-induced DNA lesions including CPD and 6-4 PP (10,30,31), is the initial factor of GG-NER involved in the detection of UV-induced DNA damage in chromatin. Following UV damage, DDB1, an E3 ubiquitin ligase, becomes tightly associated with the CUL4-RBX1 complex toward ubiquitinating XPC and DDB2 (13,32). Polyubiquitination of DDB2, but not XPC, reduces its binding affinity to DNA damage sites (25,26). Additionally, DDB2 can be phosphorylated by p38 MAPK and SUMOylated by PIASγ, which can facilitate NER (14,16). By contrast, c-Abl protein tyrosine kinase phosphorylates DDB2 and suppresses DDB2's binding toward UV-damaged DNA (15). DDB2 is comprised of the N-terminal helix-loop-helix motif (residues 101-136) and the 7-bladed WD40 β-propeller domain (residues 137-455) (33). Most mutations in *XPE* gene affect the interaction of DDB2 with DNA or DDB1. For instance, Lys244Glu and Arg273His mutations abolished DDB2's DNA binding capability, whereas Leu350Pro mutation combined with the deletion of Asn349, as observed in GM01389 cells, disrupted DDB2's binding toward DDB1 (8,34-36). Although a previous proteome-wide phosphorylation site mapping study detected S26

phosphorylation of DDB2 in HeLa cells (37), no experiments were conducted to assess how this phosphorylation affects DDB2's function.

In the present study, we found that S26 in DDB2 is also phosphorylated in HEK293T cells and this phosphorylation involves Cdks. We also demonstrated that this phosphorylation is indispensable for the recruitment of DDB2 to UV-induced CPD sites, for ATM activation and for promoting CPD repair. Moreover, we found that these functions of S26 phosphorylation may reside in its role on the ubiquitination and proteasomal degradation of DDB2. Together, our study provides important insights into the function of S26 phosphorylation in DDB2. Considering the critical roles of Cdks in cell cycle progression (38), further studies are needed to reveal the identities of Cdk(s) involved in this phosphorylation and the regulatory mechanism of this phosphorylation.

References

1. Hanawalt, P.C. (2002) Subpathways of nucleotide excision repair and their regulation. *Oncogene*, **21**, 8949-8956.

2. de Laat, W.L., Jaspers, N.G. and Hoeijmakers, J.H. (1999) Molecular mechanism of nucleotide excision repair. *Genes Dev.*, **13**, 768-785.

3. Kamileri, I., Karakasilioti, I. and Garinis, G.A. (2012) Nucleotide excision repair: new tricks with old bricks. *Trends Genet.*, **28**, 566-573.

4. Moser, J., Volker, M., Kool, H., Alekseev, S., Vrieling, H., Yasui, A., van Zeeland, A.A. and Mullenders, L.H. (2005) The UV-damaged DNA binding protein mediates efficient targeting of the nucleotide excision repair complex to UV-induced photo lesions. *DNA Repair*, **4**, 571-582.

5. Petit, C. and Sancar, A. (1999) Nucleotide excision repair: from *E. coli* to man. *Biochimie*, **81**, 15-25.

6. Cleaver, J.E. (2005) Cancer in xeroderma pigmentosum and related disorders of DNA repair. *Nat. Rev. Cancer*, **5**, 564-573.

7. Tang, J.Y., Hwang, B.J., Ford, J.M., Hanawalt, P.C. and Chu, G. (2000) Xeroderma pigmentosum p48 gene enhances global genomic repair and suppresses UV-induced mutagenesis. *Mol. Cell*, **5**, 737-744.

8. Nichols, A.F., Itoh, T., Graham, J.A., Liu, W., Yamaizumi, M. and Linn, S. (2000) Human damage-specific DNA-binding protein p48. Characterization of XPE mutations and regulation following UV irradiation. *J. Biol. Chem.*, **275**, 21422-21428.

9. Puumalainen, M.R., Lessel, D., Ruthemann, P., Kaczmarek, N., Bachmann, K., Ramadan, K. and Naegeli, H. (2014) Chromatin retention of DNA damage sensors DDB2 and XPC through loss of p97 segregase causes genotoxicity. *Nat. Commun.*, **5**, 3695.

10. Hwang, B.J., Toering, S., Francke, U. and Chu, G. (1998) p48 Activates a UV-damaged-DNA binding factor and is defective in xeroderma pigmentosum group E cells that lack binding activity. *Mol. Cell. Biol.*, **18**, 4391-4399.

11. Yoon, T., Chakrabortty, A., Franks, R., Valli, T., Kiyokawa, H. and Raychaudhuri, P. (2005) Tumor-prone phenotype of the DDB2-deficient mice. *Oncogene*, **24**, 469-478.

12. Ray, A., Milum, K., Battu, A., Wani, G. and Wani, A.A. (2013) NER initiation factors, DDB2 and XPC, regulate UV radiation response by recruiting ATR and ATM kinases to DNA damage sites. *DNA Repair*, **12**, 273-283.

13. Matsuda, N., Azuma, K., Saijo, M., Iemura, S., Hioki, Y., Natsume, T., Chiba, T. and Tanaka, K. (2005) DDB2, the xeroderma pigmentosum group E gene product, is directly ubiquitylated by Cullin 4A-based ubiquitin ligase complex. *DNA Repair*, **4**, 537-545.

14. Tsuge, M., Masuda, Y., Kaneoka, H., Kidani, S., Miyake, K. and Iijima, S. (2013) SUMOylation of damaged DNA-binding protein DDB2. *Biochem. Biophys. Res. Commun.*, **438**, 26-31.

15. Cong, F., Tang, J., Hwang, B.J., Vuong, B.Q., Chu, G. and Goff, S.P. (2002) Interaction between UV-damaged DNA binding activity proteins and the c-Abl tyrosine kinase. *J. Biol. Chem.*, **277**, 34870-34878.

16. Zhao, Q., Barakat, B.M., Qin, S., Ray, A., El-Mahdy, M.A., Wani, G., Arafa el, S., Mir, S.N., Wang, Q.E. and Wani, A.A. (2008) The p38 mitogen-activated protein kinase augments nucleotide excision repair by mediating DDB2 degradation and chromatin relaxation. *J. Biol. Chem.*, **283**, 32553-32561.

17. Cai, Q., Fu, L., Wang, Z., Gan, N., Dai, X. and Wang, Y. (2014) α-N-Methylation of damaged DNA-binding protein 2 (DDB2) and its function in nucleotide excision repair. *J. Biol. Chem.*, **289**, 16046-16056.

18. Pines, A., Vrouwe, M.G., Marteijn, J.A., Typas, D., Luijsterburg, M.S., Cansoy, M., Hensbergen, P., Deelder, A., de Groot, A., Matsumoto, S. *et al.* (2012) PARP1 promotes nucleotide excision repair through DDB2 stabilization and recruitment of ALC1. *J. Cell Biol.*, **199**, 235-249.

19. Zhang, F., Dai, X. and Wang, Y. (2012) 5-Aza-2'-deoxycytidine induced growth inhibition of leukemia cells through modulating endogenous cholesterol biosynthesis. *Mol. Cell. Proteomics*, **11**, M111 016915.

20. Ziv, Y., Bielopolski, D., Galanty, Y., Lukas, C., Taya, Y., Schultz, D.C., Lukas, J., Bekker-Jensen, S., Bartek, J. and Shiloh, Y. (2006) Chromatin relaxation in response to DNA double-strand breaks is modulated by a novel ATM- and KAP-1 dependent pathway. *Nat. Cell Biol.*, **8**, 870-876.

21. Rouget, R., Auclair, Y., Loignon, M., Affar el, B. and Drobetsky, E.A. (2008) A sensitive flow cytometry-based nucleotide excision repair assay unexpectedly reveals that mitogen-activated protein kinase signaling does not regulate the

removal of UV-induced DNA damage in human cells. *J. Biol. Chem.*, **283**, 5533-5541.

22. Chang, E.J., Begum, R., Chait, B.T. and Gaasterland, T. (2007) Prediction of cyclin-dependent kinase phosphorylation substrates. *PLoS One*, **2**, e656.

23. Gao, M. and Karin, M. (2005) Regulating the regulators: control of protein ubiquitination and ubiquitin-like modifications by extracellular stimuli. *Mol. Cell*, **19**, 581-593.

24. Hunter, T. (2007) The age of crosstalk: phosphorylation, ubiquitination, and beyond. *Mol. Cell*, **28**, 730-738.

25. El-Mahdy, M.A., Zhu, Q., Wang, Q.E., Wani, G., Praetorius-Ibba, M. and Wani, A.A. (2006) Cullin 4A-mediated proteolysis of DDB2 protein at DNA damage sites regulates in vivo lesion recognition by XPC. *J. Biol. Chem.*, **281**, 13404-13411.

26. Sugasawa, K., Okuda, Y., Saijo, M., Nishi, R., Matsuda, N., Chu, G., Mori, T., Iwai, S., Tanaka, K. and Hanaoka, F. (2005) UV-induced ubiquitylation of XPC protein mediated by UV-DDB-ubiquitin ligase complex. *Cell*, **121**, 387-400.

27. Chen, X., Zhang, Y., Douglas, L. and Zhou, P. (2001) UV-damaged DNA-binding proteins are targets of CUL-4A-mediated ubiquitination and degradation. *J. Biol. Chem.*, **276**, 48175-48182.

28. Nag, A., Bondar, T., Shiv, S. and Raychaudhuri, P. (2001) The xeroderma pigmentosum group E gene product DDB2 is a specific target of cullin 4A in mammalian cells. *Mol. Cell. Biol.*, **21**, 6738-6747.

29. Rapic-Otrin, V., McLenigan, M.P., Bisi, D.C., Gonzalez, M. and Levine, A.S. (2002) Sequential binding of UV DNA damage binding factor and degradation of the p48 subunit as early events after UV irradiation. *Nucleic Acids Res.*, **30**, 2588-2598.

30. Treiber, D.K., Chen, Z. and Essigmann, J.M. (1992) An ultraviolet light-damaged DNA recognition protein absent in xeroderma pigmentosum group E cells binds selectively to pyrimidine (6-4) pyrimidone photoproducts. *Nucleic Acids Res.*, **20**, 5805-5810.

31. Wittschieben, B.O., Iwai, S. and Wood, R.D. (2005) DDB1-DDB2 (xeroderma pigmentosum group E) protein complex recognizes a cyclobutane pyrimidine dimer, mismatches, apurinic/apyrimidinic sites, and compound lesions in DNA. *J. Biol. Chem.*, **280**, 39982-39989.

32. Groisman, R., Polanowska, J., Kuraoka, I., Sawada, J., Saijo, M., Drapkin, R., Kisselev, A.F., Tanaka, K. and Nakatani, Y. (2003) The ubiquitin ligase activity in the DDB2 and CSA complexes is differentially regulated by the COP9 signalosome in response to DNA damage. *Cell*, **113**, 357-367.

33. Scrima, A., Konickova, R., Czyzewski, B.K., Kawasaki, Y., Jeffrey, P.D., Groisman, R., Nakatani, Y., Iwai, S., Pavletich, N.P. and Thoma, N.H. (2008) Structural basis of UV DNA-damage recognition by the DDB1-DDB2 complex. *Cell*, **135**, 1213-1223.

34. Tang, J. and Chu, G. (2002) Xeroderma pigmentosum complementation group E and UV-damaged DNA-binding protein. *DNA Repair*, **1**, 601-616.

35. Wittschieben, B.O. and Wood, R.D. (2003) DDB complexities. *DNA Repair*, **2**, 1065-1069.

36. Rapic-Otrin, V., Kuraoka, I., Nardo, T., McLenigan, M., Eker, A.P., Stefanini, M., Levine, A.S. and Wood, R.D. (1998) Relationship of the xeroderma pigmentosum group E DNA repair defect to the chromatin and DNA binding proteins UV-DDB and replication protein A. *Mol. Cell. Biol.*, **18**, 3182-3190.

37. Sugiyama, N., Masuda, T., Shinoda, K., Nakamura, A., Tomita, M. and Ishihama, Y. (2007) Phosphopeptide enrichment by aliphatic hydroxy acid-modified metal oxide chromatography for nano-LC-MS/MS in proteomics applications. *Mol. Cell. Proteomics*, **6**, 1103-1109.

38. Nurse, P. (2000) A long twentieth century of the cell cycle and beyond. *Cell*, **100**, 71-78.

Chapter 4. α-N-Methylation of MRG15 Facilitates H3K36me3-H4K16Ac Crosstalk and ATM Activation through Chromatin Recruitment and Allosteric Regulation of TIP60

Introduction

The package of genomic DNA into chromatin in eukaryotic cells imposes a physical barrier that the DNA repair machinery must overcome prior to accessing DNA damage sites, and multiple lines of evidence support that post-translational modifications (PTMs) of core histones and DNA damage response proteins play an essential role in establishing a conducive chromatin environment for DNA repair (1,2). In this vein, acetylation of lysine 16 in histone H4 (H4K16Ac) and ubiquitination of lysine 120 in histone H2B result in decompaction of the 30 nm chromatin fiber and create a biochemically accessible chromatin environment for DNA repair (3-7).

MRG15, a member of the highly conserved MORF4-related gene (MRG) family of proteins (8), plays an important role in maintaining genomic integrity, as manifested by the embryonically lethal phenotype of *Mrg15*$^{-/-}$ mice (9). MRG15 can interact with PALB2 (10,11), a tumor suppressor protein that physically and functionally links with BRCA1 and BRCA2 in the BRCA complex and plays a crucial role in repairing DNA double strand breaks (DSBs) and interstrand cross-link lesions through the homologous recombination (HR) pathway (12). In addition, MRG15 was found in several distinct protein complexes that are important in chromatin remodeling, transcription regulation and cell proliferation (13,14), including the histone deacetylase (15) and TIP60-

containing histone acetyltransferase (HAT) complexes (16,17). However, it remains unexplored whether and how MRG15 and TIP60 directly interact with each other.

Apart from the side chains of arginine and lysine residues, protein methylation also occurs on the N-terminal α-amino group of some proteins (18-21). This methylation is conserved from *Escherichia coli* to man (18); however, the functions of protein α-N-methylation remain poorly understood (19-22). Recent studies showed that N-terminal Xaa-Pro-Lys N-methyltransferase 1 (NTMT1) can catalyze the α-N-methylation of proteins harboring an N-terminal Xaa-Pro-Lys (XPK) motif (after the removal of the initiator methionine) (20,23). Considering that MRG15 contains an N-terminal APK motif, we reason that MRG15 may constitute a substrate for NTM1A and this methylation may modulate its function in DNA repair.

In the present study, we observed, for the first time, that MRG15 can be α-N-methylated. We also found that the α-N-methylated N-terminus of MRG15 facilitates the recruitment of TIP60 to chromatin through its interaction with the chromo domain of TIP60, and it also serves as an allosteric regulator to stimulate TIP60's enzymatic activity. Furthermore, we found that this chromo domain recognition of α-N-methylation of MRG15 is indispensible for H4K16 acetylation, DNA damage-induced ATM activation, HR repair and cellular resistance toward genotoxic agents that induce DNA DSBs and interstrand cross-links. Moreover, we uncovered a novel crosstalk between H3K36me3 and H4K16Ac in human cells, and we defined MRG15 as the molecular determinant for this crosstalk.

Materials and Methods

Cell culture

HEK293T human embryonic kidney epithelial cells and HeLa cells were purchased from ATCC (Manassas, VA). U2OS cells harboring a chromosomally integrated copy of DR-GFP reporter were provided by Prof. Jeremy M. Stark (24). HeLa cells stably expressing SETD2 shRNA (HeLa-shSETD2) or control scrambled shRNA (HeLa-shScr) and UOK121 and UOK143 clear cell renal cell carcinoma (ccRCC) cells were provided by Prof. Guomin Li (25). HEK293T, UOK121 and UOK143 cells were cultured in Dulbecco's modified Eagle's medium (ATCC). HeLa, HeLa-shSETD2 and HeLa-shScr cells were cultured in RPMI1640 medium. All culture media contained 10% fetal bovine serum (Invitrogen), 100 unit/mL penicillin, and 100 μg/mL streptomycin. The cells were cultured in a humidified atmosphere with 5% CO_2 at 37°C.

Constructs

The expression plasmid for NTM1A-His_6 was kindly provided by Prof. Ian G. Macara (20), and the plasmids for expressing HA-TIP60, HA-TIP60-W26A and HA-TIP60-Y47A were generously provided by Prof. Yingli Sun (26). The human MRG15 open-reading frame was amplified to introduce a 5' XbaI restriction site and a 3' BamHI site, and subcloned into a modified mammalian expression vector pRK7 in which three tandem repeats of the FLAG epitope tag (DYKDDDK) were inserted between the BamHI and EcoRI sites to give pRK7-MRG15-3×FLAG. MRG15-K4Q and MRG15-Y46AW49A mutants were amplified from pRK7-MRG15-3×FLAG plasmid using site-

directed mutagenesis. MRG15-His_6 was generated by subcloning human MRG15 coding sequence (containing amino acids 2-323) with 5' SacI, N-terminal X-factor cleavage site (IEGR) and 3' NotI into *E. coli* expression vector pET28a.

FLAG-tagged MRG15 isolation, digestion, and LC-MS/MS analysis

The pRK7-MRG15-3×FLAG plasmid was transfected into HEK293T cells using Lipofectamine 2000. The cells were collected at 48 hr later using trypsin-EDTA solution (ATCC), washed with PBS, lysed in CellLytic lysis buffer (Sigma) containing a protease inhibitor cocktail (Sigma). The resulting C-terminally FLAG-tagged MRG15 was purified by using anti-FLAG M2 affinity beads (Sigma). The sample was subsequently reduced, alkylated, and digested with Glu-C at an enzyme/protein ratio of 1:20 (w/w) at room temperature overnight. Peptide mixtures were subjected to online LC-MS/MS analysis with an EASY-nLC II that was coupled with an LTQ Orbitrap Velos mass spectrometer equipped with a nanoelectrospray ionization source (Thermo, San Jose, CA) following similar procedures as previously described (27). The separation was conducted by using a homemade trapping column (150 μm × 50 mm) and a separation column (75 μm ×120 mm), packed with ReproSil-Pur C18-AQ resin (3 μm in particle size, Dr. Maisch HPLC GmbH, Germany). Peptide samples were initially loaded onto the trapping column with a solvent mixture of 0.1% formic acid in CH_3CN/H_2O (2:98, v/v) at a flow rate of 4.0 μL/min. The peptides were then separated using a 90-min linear gradient of 2-40% acetonitrile in 0.1% formic acid and at a flow rate of 220 nL/min. The mass spectrometer was operated in the positive-ion mode, and the spray voltage was 1.8 kV. The data were acquired in a data-dependent scan mode where one full-scan MS was

followed with 20 MS/MS scans. To obtain high-quality MS/MS, the data were also collected in selected-ion monitoring mode where the fragmentations of the protonated ions of the unmodified and mono-, di- or tri-methylated forms of the N-terminal peptide of MRG15 were monitored. All the MS/MS data were manually analyzed.

For assessing how α-N-methylation of MRG15 is affected by genotoxic agents, HEK293T cells were treated with 100 ng/mL neocarzinostatin (NCS, Sigma) or 2 μM mitomycin C (MMC) for 1 hr at 47 hr after transfection with C-terminally FLAG-tagged MRG15 plasmid, or treated with 30 μM cisplatin for 5 hr at 43 hr after the plasmid transfection. After the treatments, the FLAG-tagged MRG15 proteins was again isolated and processed for LC-MS/MS analysis.

siRNA knockdown

Control siRNA, 3' UTR-MRG15 siRNA and human NTM1A SMARTpool siRNA were obtained from Thermo Scientific. Sequence of 3' UTR-MRG15 siRNA was 5′-GGGAUAUGCUGUAGAGUGUTT-3′ (3′-UTR: 1393-1411) (10). Sequences of NTM1A SMARTpool siRNA were GCGAGGUGAUAGAAGACGA, AGGUGGAUAUGGUCGACAU, UGAGGGAAGGCCCGAACAA and GGACUGUGGAGCUGGCAUU. HEK293T cells were cultured in 6-well plates in antibiotic-free medium at a density of 5×10^5 cells per well for 24 hr, and transfected with 100 pmol siRNA using Lipofectamine 2000 (Invitrogen).

Real-time quantitative RT-PCR

At 48 hr after siRNA transfection, cells were harvested for real-time quantitative RT-PCR analysis. Total RNA was isolated using Total RNA Kit I (Omega). cDNA was generated by using M-MLV reverse transcriptase (Promega) and an oligo$(dT)_{16}$ primer. Real-time quantitative RT-PCR for evaluating the efficiency of siRNA knockdown was performed by using the iQ SYBR Green Supermix kit (Bio-Rad) and *GAPDH* was used as an internal control. The primers were 5'-TGGATGAGAAGAGCCTTGC -3' and 5'-CAGGAGGAGCCACTTCATAAT -3' for *MRG15*, 5'-GCCCTCCCTTCCTCTTCC-3' and 5'-CCAACCACGGCTCTACTCA -3' for *NTM1A*, and 5'-TTTGTCAAGCTCATTTCCTGGTATG-3' and 5'-TCTCTTCCTCTTGTGCTCTTGCTG -3' for *GAPDH*.

DSB repair assays

U2OS cells with a chromosomally integrated copy of DR-GFP plasmid (24) were transfected with 3' UTR-MRG15 siRNA or non-targeting control siRNA. The HeLa-shScr, HeLa-shSETD2, UOK121 and UOK143 cells were seeded in six-well plates at the same density and transfected with pDRGFP plasmid. At 24 hr after transfection, pCBASce I plasmid (1 μg/well) (24), which allows for the expression of I-SceI, was transfected into the cells alone or in combination with pRK7-MRG15-3×FLAG, or its K4Q or Y46AW49A mutant (2 μg/well). Cells without I-SceI transfection were used as negative control. Three days after the transfection with I-SceI, the cells were washed with PBS and stored in a sorting buffer (1×PBS, 1 mM EDTA, 25 mM HEPES, 1% FBS, pH 7.0) for flow cytometry analysis (BD FACS Aria I).

Clonogenic survival assay

UOK cells and HeLa cells were plated in 6-well plates in triplicate at densities of 200-4000 cells per well. At 6 hr later, the cells were treated with different doses of NCS, MMC or γ rays. Cell colonies grown for 10-14 days were then fixed using 6% (v/v) glutaraldehyde and stained with 0.5% (w/v) crystal violet (28). Colonies containing at least 50 cells were counted under a microscope.

Isolation of chromatin-bound proteins

Chromatin-associated proteins were isolated as previously described (29). Briefly, the cells were lysed with cytoplasmic lysis buffer (10 mM Tris-HCl, pH 8.0, 0.34 M sucrose, 3 mM $CaCl_2$, 2 mM $MgCl_2$, 0.1 mM EDTA, 1 mM DTT, 0.5% NP-40, protease inhibitor cocktail) for 30 min on ice, and the intact nuclei were subsequently pelleted by centrifugation at 5000 rpm for 2 min. Nuclei were lysed with nuclear lysis buffer (20 mM HEPES, pH 7.9, 1.5 mM $MgCl_2$, 1 mM EDTA, 150 mM KCl, 0.1% NP-40, 1 mM DTT, 10% glycerol, protease inhibitor cocktail) by homogenization. After centrifugation at 14000 rpm for 30 min, the chromatin-enriched pellet fraction was incubated in a chromatin incubation buffer (20 mM HEPES, pH 7.9, 1.5 mM $MgCl_2$, 150 mM KCl, 10% glycerol, protease inhibitor cocktail and 0.15 unit/μl benzonase, Sigma) on ice for 2 hr. Debris was then removed by centrifugation at 5000 rpm for 2 min and the supernatant collected as the chromatin fraction.

Core histone extraction

Core histones were extracted from cultured human cells following previously described procedures (30). Briefly, cell pellets were washed with a 5-mL lysis buffer containing 0.25 M sucrose, 10 mM $MgCl_2$, 0.5 mM PMSF, 50 mM Tris (pH 7.4) and 0.5% Triton X-100. The pellets were then resuspended in 5 mL of the same buffer and kept at 4ºC overnight. The histones were extracted from the cell lysis mixture with 0.4 M sulfuric acid by incubating at 4ºC for at least 4 hr with continuous vortexing, precipitated with cold acetone, centrifuged, dried and redissolved in water.

Western blot

The cell lysates were separated by SDS-PAGE, and the proteins were transferred to a nitrocellulose membrane (Whatman) in transfer buffer (10 mM $NaHCO_3$, 3 mM Na_2CO_3, and 20% methanol). The membrane was blocked in PBS containing 5% (w/v) blocking-grade milk (Bio-Rad) and 0.1% (v/v) Tween-20 for 6 hr. Antibodies that specifically recognized histone H3, FLAG epitope tag (Cell Signaling) and human actin (abcam) were used at 1:10000 dilution. Antibodies that specifically recognized human ATM or phospho-ATM (Ser1981), and human CHK1 and phospho-CHK1 (Ser345), human CHK2 or phospho-CHK3 (T68), human trimethylated H3 (lysine 36), human H4 and acetylated H4 (lysine 16) (Cell Signaling) were used at 1:1000 dilution. Horseradish peroxidase-conjugated secondary goat anti-rabbit antibody (abcam) and goat anti-mouse antibody (Santa Cruz) were used at a 1:10000 dilution. The secondary antibody was detected using ECL Advance Western Blotting Detection Kit (GE Healthcare) and

visualized with Hyblot CL autoradiography film (Denville Scientific, Inc., Metuchen, NJ).

Histone acetyltransferase (HAT) assay

HA-TIP60 was purified from HEK293T cells by using anti-HA magnetic beads (Thermo Scinentific) following the manufacturer's recommended procedures and dialyzed in HAT buffer (50 mM Tris-HCl, pH 8.0, 10% glycerol, 0.1 mM EDTA and 1 mM DTT). The HAT reaction contained 0.5 μg HA-TIP60, 1 μg histone H4 and 100 μM acetyl-coenzyme A in a 60 μL HAT buffer, without or with 0.5 μg N-terminal peptide of MRG15 $_{1}$APKQDPKPKFQE$_{12}$, which was treated with NTM1A in the presence or absence of *S*-adenosyl-L-methionine (details provided in the Supplementary Materials). The reaction mixture was then analyzed by Western blot.

Results

MRG15 could be α-N-methylated in human cells by N-terminal Xaa-Pro-Lys N-methyltransferase 1 (NTMT1)

Considering that MRG15 harbors an N-terminal consensus XPK motif which can be recognized and α-N-methylated by human NTMT1 (20), we reasoned that MRG15 may be α-N-methylated by NTMT1. To explore this possibility, we first examined whether MRG15 can be α-N-methylated in human cells. We expressed the C-terminally FLAG-tagged MRG15 in HEK293T cells, isolated it from the cell lysate by using anti-FLAG M2 beads, and digested it with Glu-C. LC-MS and MS/MS analysis of the peptide

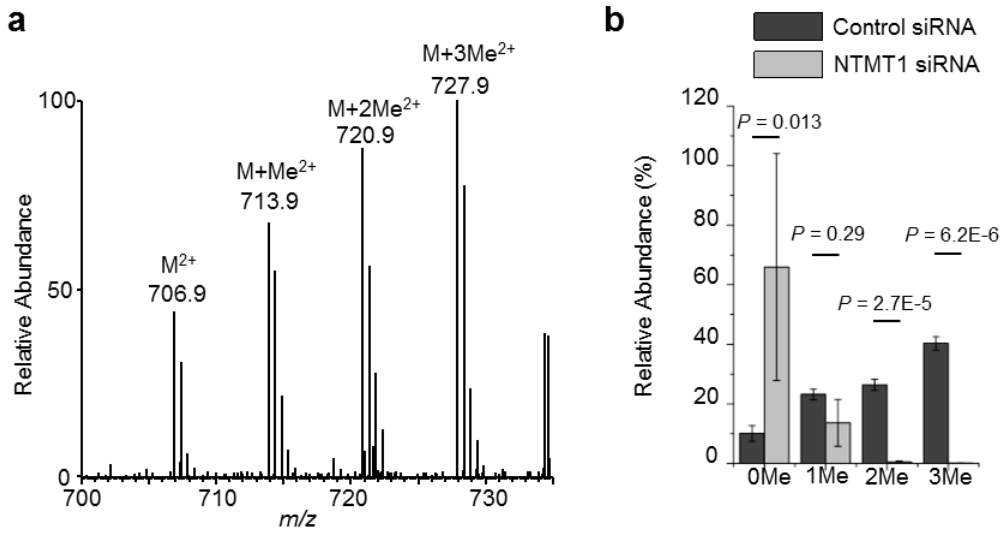

Figure 4. 1. NTMT1 catalyzes the α-N-methylation of MRG15. (a) Positive-ion ESI-MS of the N-terminal peptide APKQDPKPKFQE of MRG15 isolated from HEK293T cells. (b) Relative abundances of different methylation forms of N-terminal peptide APKQDPKPKFQE of MRG15 isolated from HEK293T cells with control and NTMT1 siRNA demonstrated that NTMT1 can catalyze the α-N-methylation of MRG15 in cells. The level of methylation was quantified by dividing the signal intensity for the doubly charged ion of the specific methylated form of the aforementioned N-terminal peptide by the total signal intensities for the doubly charged ion of the unmethylated and all methylated forms of the N-terminal peptide. The results represent mean and standard deviation of data acquired from three independent experiments. The *P* values were calculated by using unpaired two-tailed Student's t-test.

mixture revealed the α-N-methylation of MRG15 (Figure 4.1&B1), where we observed the doubly charged ions of the unmodified along with the mono-, di- and tri-methylated forms of the peptide $_{1}$APKQDPKPKFQE$_{12}$ in the MS (Figure 4.1a). The MS/MS and MS/MS/MS results further supported that the methylation occurs on the N-terminal alanine residue (Figures B1&B2). In this respect, the MS/MS for the trimethylated peptide displays the y_2, y_5 and y_7-y_{10} ions, but not the y_{11} ion, which is inadequate to support the α-N-trimethylation of this peptide (Figure B1d). The MS/MS/MS arising from the further fragmentation of the b_5+3Me ion observed in the MS/MS showed the presence of the y_4 ion, together with the neutral loss of an $N(CH_3)_3$ from the precursor ion (Figure B2), thereby supporting unequivocally the α-N-trimethylation of this peptide.

We next asked whether MRG15 is an NTMT1 substrate. Toward this end, we assessed how siRNA-mediated depletion of NTMT1 alters the α-N-methylation level of MRG15. Our results showed that the siRNA treatment led to a marked reduction in the expression of NTMT1 at both the mRNA and protein levels, which is accompanied with nearly complete loss of di- and tri-methylation of the α-amino group of MRG15 (Figure 4.1b&B3). We also conducted an *in-vitro* methylation assay with the use of recombinant NTMT1, and our LC-MS results revealed that NTM1A is able to catalyze the α-N-methylation of recombinant MRG15 and a synthetic N-terminal peptide of MRG15, $_{1}$APKQDPKPKFQE$_{12}$ (Figure B4&B5a,b). Together, the above results support that NTMT1 catalyzes the α-N-methylation of MRG15 both *in vitro* and in human cells.

α-N-methylation of MRG15 promotes the chromatin localization and allosterically stimulates the enzymatic activity of TIP60, which are indispensible for H4K16 acetylation and DNA damage-induced ATM activation

MRG15 is known to interact with TIP60 and MOF histone acetyltransferases (13,16,31), which mediates H4K16 acetylation (32,33). However, it remains undefined whether and how MRG15 and TIP60 directly interact with each other. Viewing that chromo domain is known to interact with the side chains of methylated lysine and arginine and TIP60, we hypothesized that TIP60 might be capable of binding, through its chromo domain, with the α-N-methylated N-terminal tail of MRG15. Indeed, our results showed that wild-type MRG15 can interact with TIP60; however, MRG15-K4Q, which loses its consensus recognition sequence for NTMT1 and is defective in α-N-methylation (Figure B5c,d,e&S6), failed to do so (Figure 4.2a). In this vein, we found that wild-type MRG15 and its K4Q mutant were expressed at similar levels (Figure B7a). In addition, the interaction between MRG15 and TIP60 requires an intact chromo domain of the latter, as manifested by the observation that the mutation of tyrosine 47 (TIP60-Y47A) in the chromo domain of TIP60, but not tryptophan 26 (TIP60-W26A) outside of the chromo domain (26), abolishes this interaction (Figure 4.2b). These results support that the interaction between MRG15 and TIP60 necessitates the α-N-methylation of the former and the presence of a functional chromo domain of the latter.

We also assessed how this interaction affects TIP60's chromatin localization and H4K16 acetylation. Our results showed that the siRNA-mediated depletion of endogenous MRG15 led to a substantial decline in chromatin-bound TIP60, and this

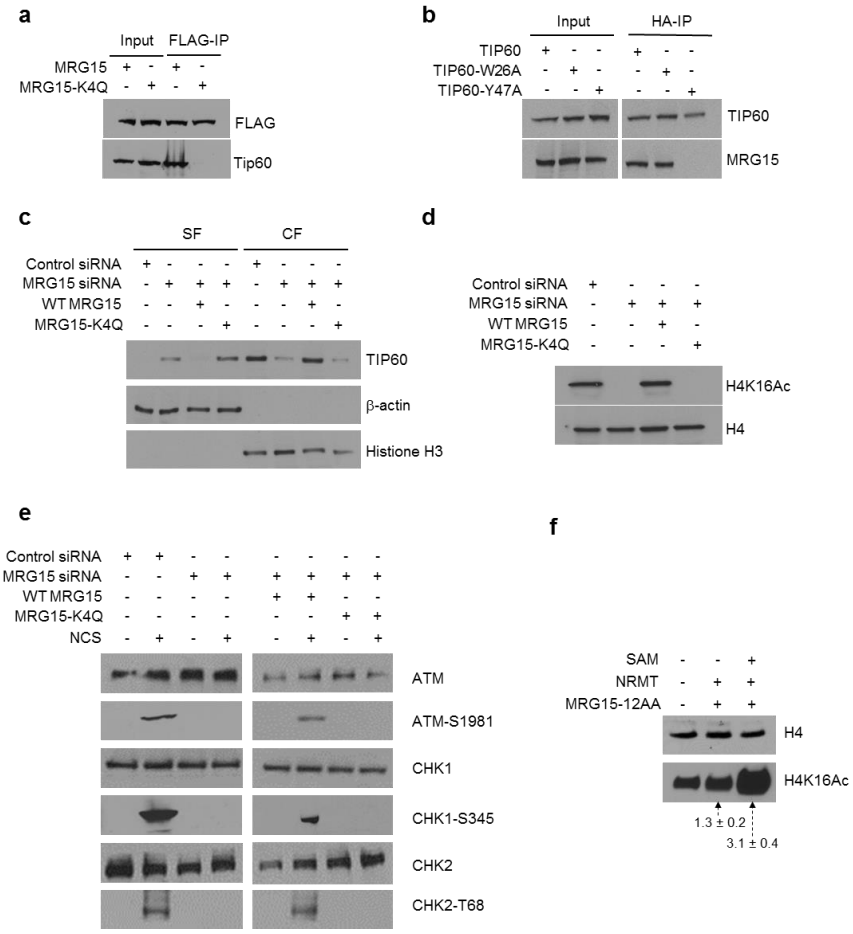

Figure 4. 2. NTMT1 α-N-methylation of MRG15 plays an important role in histone H4K16 acetylation and NCS-induced ATM activation. (a) C-terminally FLAG-tagged wild-type MRG15, but not MRG15-K4Q, could allow for the pull-down of TIP60 histone acetyltransferase. (b) HA-tagged wild-type TIP60 and TIP60-W26A, but not TIP60-Y47A, led to the pull-down of MRG15 by anti-HA magnetic beads. (c) α-N-methylation of MRG15 facilitates the recruitment of TIP60 to chromatin. Western blot results revealed that the reduction in chromatin-occupied MRG15 in HEK293T cells emanating from MRG15 depletion could be rescued by reconstituting the cells with the plasmid for expressing wild-type MRG15, but not MRG15-K4Q. β-actin and histone H3 were used as loading controls for the soluble (SF) and chromatin (CF) fractions, respectively. (d) α-N-methylation of MRG15 facilitated the TIP60-mediated H4K16 acetylation. Core histone extracts were used for the Western blot. (e) α-N-methylation of MRG15 is important for NCS-induced ATM activation. (f) α-N-methylated N-terminal peptide of MRG15 stimulates allosterically the enzymatic activity of TIP60. The relative level of H4K16Ac as compared to the control case in the first lane is labeled under the H4K16Ac band, the results represent the mean and standard deviation obtained from two biological replicates. Histone H4 was used as the loading control.

reduction could be fully restored by complementing cells with wild-type MRG15, but not its methylation-defective mutant (MRG15-K4Q, Figure 4.2c). In line with the reduced chromatin localization of TIP60, our Western result showed that the siRNA-induced depletion of MRG15 led to nearly complete loss of H4K16Ac, and this elimination of H4K16 acetylation could be rescued entirely by reconstituting cells with wild-type MRG15, but not MRG15-K4Q (Figure 4.2d).

Considering that H4K16Ac is important for decompacting the 30 nm chromatin fiber (34) and modulating ATM activation (35), we next asked how defective α-N-methylation of MRG15 affects DNA damage-induced ATM activation by monitoring the phosphorylation of S1981 in ATM, S345 in CHK1 and T68 in CHK2, which are known ATM targets (36-38). In line with the above findings on H4K16Ac, our results demonstrated that the ATM activation induced by neocarzinostatin (NCS), a radiomimetic agent, is abolished in MRG15-depleted cells, and this loss of ATM activation can be rescued completely by wild-type MRG15, but not MRG15-K4Q (Figure 4.2e).

Our above results showed that the siRNA-mediated depletion of MRG15 led to almost complete abrogation of H4K16 acetylation and DNA damage-triggered ATM activation, whereas only partial loss in chromatin localization of TIP60 was observed, suggesting that other mechanism(s) might regulate H4K16 acetylation. Considering that H3K9me3 was previously found to allosterically stimulate the acetyltransferase activity of TIP60 (26), we reason that α-N-methylation, aside from enhancing the recruitment of TIP60 to chromatin, may also increase the enzymatic activity of TIP60 via an allosteric

mechanism. To explore this possibility, we conducted an *in-vitro* histone acetyltransferase assay to assess the effect of α-N-methylation of an N-terminal peptide of MRG15 on the enzymatic activity of TIP60 by employing recombinant human histone H4 as a substrate. Our results showed that the N-terminal peptide of MRG15 methylated by NTM1A enhanced the enzymatic activity of TIP60 by ~3 fold, whereas the corresponding unmethylated peptide failed to do so (Figure 4.2f&Figure B8). Together, the above findings supported an essential role of α-N-methylation of MRG15 in H4K16 acetylation and ATM activation, and this function of α-N-methylation involves its participation in the interaction between MRG15 and TIP60, together with the allosteric stimulation of the enzymatic activity of the latter.

α-N-methylation of MRG15 promotes HR-mediated repair of DNA DSBs and renders cells resistant to ionizing radiation and interstrand cross-linking agent

MRG15 was previously shown to function in HR repair and in the cellular resistance towards exposure to ionizing radiation and interstrand cross-linking agents (10). Having established the indispensible role of α-N-methylation of MRG15 in stimulating H4K16 acetylation and DNA damage-induced ATM activation, we next assessed the functions of this methylation in HR repair by employing U2OS cells with a chromosomally integrated DR-GFP construct (24,39). Our results revealed that the siRNA-mediated depletion of endogenous MRG15 led to diminished efficiency in HR repair, which could be fully restored by complementing cells with siRNA-resistant

construct for wild-type MRG15, but not MRG15-K4Q (Figure 4.3a), supporting that α-N-methylation of MRG15 is essential for its function in HR repair.

In agreement with the importance of α-N-methylation in MRG15's role in HR repair, we found that treatment of HEK293T cells with NCS or mitomycin C (MMC) led to significant elevations in the levels of α-N-trimethylation of MRG15 (Figure 4.3e). In addition, clonogenic survival assay revealed that the elevated sensitivity toward NCS, ionizing radiation, and MMC in MRG15-depleted HeLa cells could be restored by ectopic expression of wild-type MRG15, but not MRG15-K4Q (Figure 4.3b-d). Cumulatively, these results showed that α-N-methylation of MRG15 stimulates HR repair and confers cellular protection from the cytotoxic effects of agents that induce interstrand cross-links and DSBs in DNA.

The chromo domain of MRG15 interacts with H3K36me3 in cells

Having demonstrated the importance of α-N-methylation of MRG15 in the recruitment of TIP60 to chromatin and in ATM activation, we next assessed the mechanism of recruitment of MRG15 to chromatin. In this vein, MRG15 was previously shown to interact with H3K36me3 *in-vitro* (40). Thus, we hypothesized that this interaction may facilitate the recruitment of MRG15 to chromatin. To test this, we first assessed the interaction between the chromo domain of MRG15 and H3K36me3 in living cells. Our pull-down assay using the C-terminally FLAG-tagged MRG15 showed that MRG15 can bind to H3K36me3. Furthermore, this binding is greatly diminished for an MRG15 variant where a tyrosine and a tryptophan in the aromatic cage of the chromo

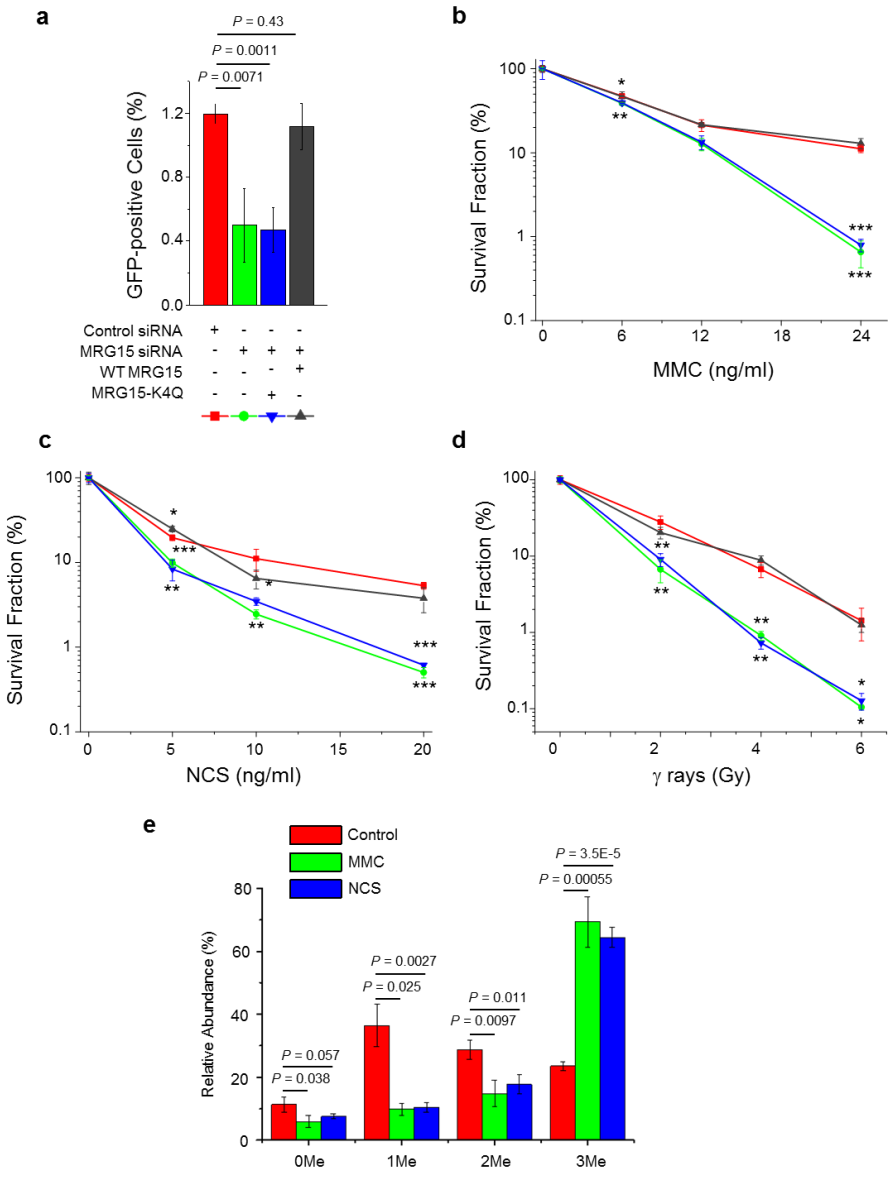

Figure 4. 3. α-N-methylation of MRG15 functions in homologous recombination repair. (a) Diminished HR repair in U2OS-DR-GFP cells emanating from siRNA-induced knockdown of endogenous MRG15 can be fully rescued by complementing cells with siRNA-resistant construct for expressing wild-type MRG15, but not MRG15-K4Q. (b)-(d) The hypersensitivity to MMC (b), NCS (c), and γ-ray (d) in HeLa cells arising from MRG15 knockdown could be restored by transfecting cells with the plasmid for expressing wild-type MRG15, but not MRG15-K4Q. (e) Treatment with MMC and NCSled to elevated trimethylation on the N-terminus of MRG15. The results represent mean and standard deviation of data acquired from three independent experiments. The *P* values were calculated by using unpaired two-tailed Student's t-test.

domain (40) were mutated to alanines (i.e., MRG15-Y46AW49A, Figure 4.4a). To further examine this interaction, we employed anti-MRG15 antibody to pull down endogenous MRG15 from HeLa-shScr and HeLa-shSETD2 cells (25) and assessed the levels of histone H3 and H3K36me3 in the pull-down mixtures using Western analysis. Our results showed that the loss of SETD2 abolished the pull-down of histone H3 and, not surprisingly, H3K36me3 (Figure 4.4b), demonstrating that the endogenous interaction between MRG15 and histone H3 requires the SETD2-mediated H3K36 trimethylation. Along this line, previous Western blot result showed that SETD2 was highly depleted in HeLa-shSETD2 cells (25). Moreover, we found that N-terminus of chromatin-bound MRG15 is primarily trimethylated (Figure 4.4c), suggesting that chromatin binding of MRG15 may promote its α-N-methylation. Along this line, it is worth noting that NTMT1-GFP was found to be primarily nuclear (20).

The interaction between the chromo domain of MRG15 and H3K36me3 plays an important role in the recruitment of TIP60 to chromatin, and is essential for H4K16 acetylation and DNA damage-induced ATM activation

We next asked how the interaction between the chromo domain of MRG15 and H3K36me3 impacts the recruitment of TIP60 to chromatin. Results from our chromatin fractionation assay revealed that the chromatin occupancy of TIP60 is indeed substantially diminished in SETD2-deficient HeLa-shSETD2 cells relative to the SETD2-proficient HeLa-shScr cells (Figure 4.5a & Figure B9a). Thus, SETD2-mediated H3K36me3 promotes the localization of TIP60 to chromatin. To further investigate whether H3K36me3 facilitates the recruitment of TIP60 to chromatin through the chromo

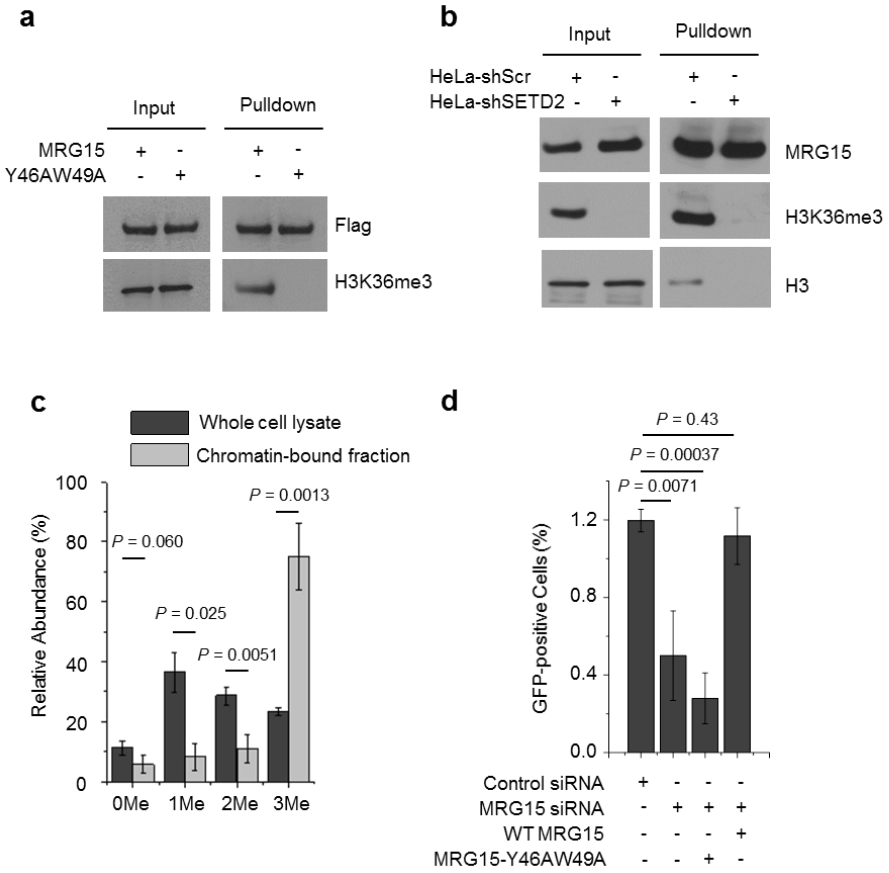

Figure 4. 4. The chromo domain of MRG15 promotes homologous recombination repair and confers cellular resistance toward ionizing radiation and MMC. (a) Western blot revealed diminished interaction of the chromo domain mutant of MRG15 (MRG15-Y46AW49A) with H3K36me3. Whole cell lysate of HEK293T cells expressing FLAG-tagged wild-type MRG15 and MRG15-Y46AW49A were titrated (input) to equal amounts and incubated with excess amount of core histones extracted from HEK293T cells. The FLAG-tagged proteins were immunoprecipitated using anti-FLAG M2 beads and detected using antibody specifically recognizing H3K36me3. (b) The loss of SETD2 in Hela-shSETD2 abolished the interaction between MRG15 and H3 as demonstrated by Western blot. Similar amounts of Hela-shScr and shSETD2 lysate (input) were incubated with Dynabeads protein A prebound with MRG15 antibody to pulldown MRG15, H3 and H3K36me3. (c) LC-MS-based relative quantification showed that the chromatin-bound MRG15, but not that isolated from the whole cell lysate, is primarily trimethylated. (d) MRG15 knockdown in U2OS-DR-GFP cells led to diminished homologous recombination repair, which can be fully restored by complementing the cells with wild-type MRG15, but not MRG15-Y46AW49A. The results for (c)-(d) represent the mean and standard deviation of data obtained from three biological replicates. The *P* values were calculated by using unpaired two-tailed Student's t-test.

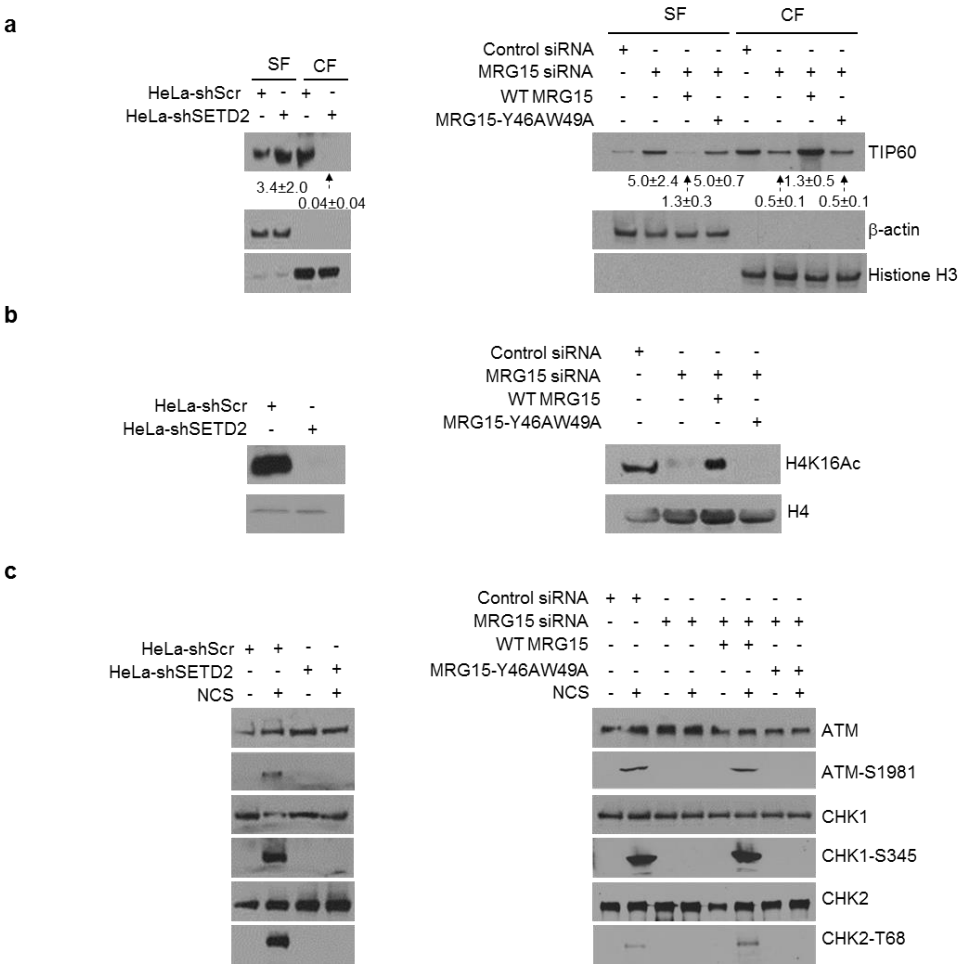

Figure 4. 5. Interaction between H3K36me3 and the chromo domain of MRG15 facilitates TIP60's recruitment to chromatin, H4K16 acetylation and ATM activation. (a) TIP60 is present at a higher level in chromatin fraction from SETD2-proficient HeLa-shScr cells than the corresponding SETD2-deficient HeLa-shSETD2 cells, and depletion of endogenous MRG15 in HEK293T cells led to a reduced chromatin localization of TIP60, which could be restored by ectopic expression of wild-type MRG15, but not MRG15-Y46AW49A. β-actin and histone H3 were employed as loading controls for the soluble (SF) and chromatin (CF) fractions, respectively. The relative level of TIP60 in SF and CF as compared to the one in HeLa-shScr or the one in HEK293T with control siRNA knockdown were labeled underneath the Tip60 band. The data represent mean and standard deviation of results obtained from two biological replicates. (b) Defective SETD2 or MRG15 chromo domain resulted in loss of H4K16 acetylation. Core histone extracts were used for the Western blot. (c) Dysfunctional SETD2 or MRG15 chromo domain led to compromised ATM activation in response to NCS treatment. Cells were treated with 100 ng/mL NCS for 1 hr. During cell lysis, 5 mM sodium orthovanadate was added to prevent dephosphorylation by phosphatase.

domain of MRG15, we compared the chromatin occupancy of TIP60 in HEK293T cells treated with non-targeting control siRNA, MRG15 siRNA, as well as in the MRG15 siRNA-treated cells complemented with wild-type MRG15 or its chromo domain mutant (i.e., MRG15-Y46AW49A). Our results showed that complementation with wild-type MRG15, but not MRG15-Y46AW49A, restored the chromatin localization of TIP60 in HEK293T cells depleted of endogenous MRG15 (Figure 4.5a & Figure B9a). In this vein, Western analysis showed similar levels of expression of the wild-type and mutant MRG15 proteins (Figure B7b). These results supported that the binding between H3K36me3 and the chromo domain of MRG15 stimulated the recruitment of TIP60 to chromatin.

We next examined whether the level of H4K16Ac is modulated by the interaction between the chromo domain of MRG15 and H3K36me3. In accordance with the compromised recruitment of TIP60 to chromatin, H4K16Ac was largely abolished in the SETD2-deficient HeLa-shSETD2 cells and UOK143 cells as compared with the SETD2-proficient HeLa-shScr and UOK121 cells, respectively (Figure 4.5b & Figure B9b). In addition, the loss of H4K16Ac emanating from the depletion of endogenous MRG15 could be rescued by ectopic expression of wild-type MRG15, but not MRG15-Y46AW49A (Figure 4.5b & Figure B9b). Thus, the interaction between the chromo domain of MRG15 and H3K36me3 is essential for H4K16 acetylation.

In line with our observations of the H4K16Ac, the NCS-induced ATM activation was abolished in HeLa-shSETD2 and UOK143 cells (Figure 4.5c). Moreover, wild-type MRG15, but not MRG15-Y46AW49A, could fully restore the NCS-induced ATM

activation that was lost upon the siRNA-mediated knockdown of endogenous MRG15 (Figure 4.5c & Figure B9c). Hence, our results support that the MRG15-mediated recruitment of TIP60 to chromatin is enabled, in part, by the binding between the chromo domain of MRG15 and H3K36me3, and this latter binding is essential for H4K16 acetylation and DNA damage-triggered ATM activation.

The interaction between the chromo domain of MRG15 and H3K36me3 promotes HR repair and elicits cellular resistance toward genotoxic agents

We next assessed the importance of this interaction in HR repair and the cellular resistance toward genotoxic agents. The aforementioned GFP reporter assay revealed that the marked reduction in HR efficiency arising from the siRNA-induced depletion of endogenous MRG15 could be restored by complementing the cells with wild-type MRG15, but not its chromo domain mutant (Figure4d&B10a,b). Consistently, clonogenic survival assay results showed that the MRG15 siRNA-mediated decline in survival of HeLa cells after treatment with NCS, ionizing radiation, or mitomycin C could be rescued by reconstituting the cells with wild-type MRG15, but not by its chromo domain mutant (Figures B11&B12). Moreover, we observed that deficiency in SETD2 led to reduced HR repair and elevated sensitivity toward genotoxic agents in multiple lines of human cells (Figure B11-14), which is agreement with the important role of the interaction between the chromo domain of MRG15 and H3K36me3 in HR repair and is in line with recent findings (41,42).

Discussion

DNA DSBs, when left unrepaired, can elicit catastrophic consequences to cells. HR and nonhomologous end-joining (NHEJ) represent two major pathways for repairing DNA DSBs; while the NHEJ pathway is error-prone, the HR pathway is error-free because of its utilization of homologous regions as templates for repair (43). The results from the present study led to several important and novel findings about the roles of protein methylation in regulating ATM activation and HR repair.

First, we discovered the α-N-methylation of MRG15 and previously unrecognized functions of α-N-methylation in protein-protein interaction (Figure 4.6). Protein α-N-methylation is an evolutionarily conserved type of post-translational modification (18); however, its biological functions remain poorly investigated. On the grounds that trimethylation introduces a quaternary ammonium ion, a permanent cation, to the N-termini of proteins, α-N-trimethylation was thought to enhance the binding of proteins to DNA through electrostatic interaction between the trimethylated protein N-terminus and phosphate groups in DNA (19,44). Here we found that the NTM1A-mediated α-N-methylation of MRG15 enables the direct interaction between MRG15 and TIP60 via the chromo domain of the latter protein (Figure 6). Thus, similar as methylation of the side chains of lysine and arginine, α-N-methylation also provides a molecular hook for holding the chromo domain of another protein. From this finding, we conclude that the ligands of chromo domain perhaps can be expanded to the α-N-methylated N-termini of proteins. Considering the similar recognition mechanisms of methylation marks by chromo, Tudor and PWWP domains, it can be envisaged that this

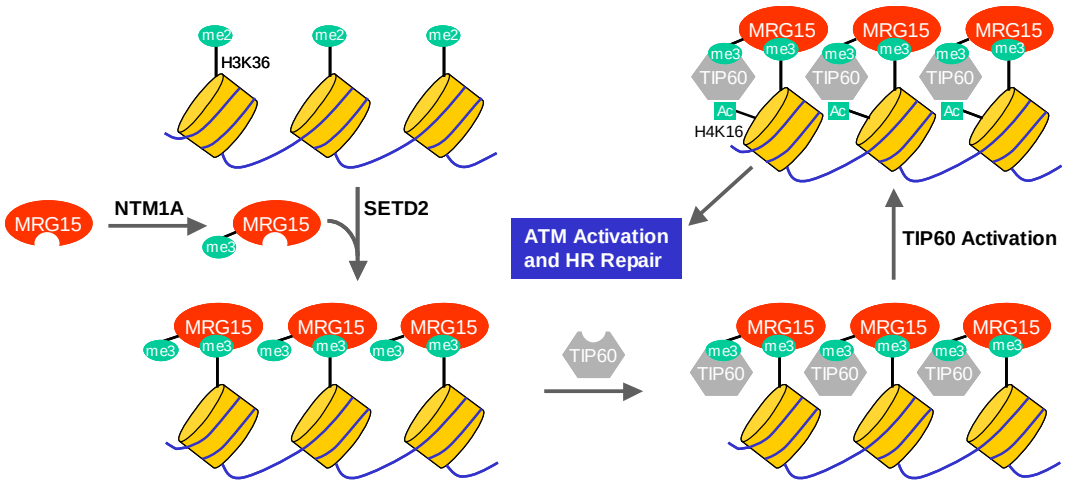

Figure 4. 6. MRG15 as a molecular determinant in trans-histone crosstalk between H3K36me3 and H4K16ac.

recognition of protein α-N-methylation can be expanded to other members of the 'Royal family' proteins (45). Furthermore, we found that, similar to H3K9me3 (26), α-N-methylation of MRG15 allosterically stimulates the enzymatic activity of TIP60 (Figure 6). Future studies are needed for determining whether the allosteric stimulations of TIP60's enzymatic activity by α-N-methylation of MRG15 and by H3K9me3 are cooperative or mutually exclusive.

Second, our study led to the discovery of a novel histone crosstalk in mammalian cells, where H3K36me3 drives H4K16Ac, and we defined the molecular link between these two types of histone epigenetic marks (Figure 6). In particular, we found that the SETD2-mediated H3K36me3 is recognized by the chromo domain of MRG15, which further enables the recruitment of TIP60 histone acetyltransferase to chromatin thereby inducing H4K16Ac. The latter recruitment involves the interaction between the α-N-methylation of the N-terminal tail of MRG15 and the chromo domain of TIP60. This histone crosstalk was also discovered recently in Arabidopsis, suggesting that this may constitute a conserved mechanism of epigenetic regulation (46). In addition, this trans-histone modification parallels a previous observation made by Wu et al. (47), who demonstrated that the MRG domain of MRG15 can interact with ubiquitinated histone H2B and stimulate the chromatin recruitment of TIP60 and H4K16 acetylation. Thus, MRG15 is a versatile molecule that can recognize both H2B ubiquitination and H3K36me3, both of which are important for the recruitment of TIP60 to chromatin.

Third, we uncovered a novel regulatory mechanism of ATM activation and HR repair. ATM activation constitutes a crucial element of DNA damage response pathway

and is important in triggering HR repair (48). Several recent studies showed the importance of SETD2-mediated H3K36me3 in HR repair in human cells (41,42,49). Here we found that MRG15 can bind directly to the H3K36me3 mark via its chromo domain, and this binding, together with the α-N-methylation of MRG15, facilitates the recruitment of TIP60 to chromatin and stimulates its acetyltransferase activity, thereby promoting H4K16Ac and DNA damage-induced ATM activation (Figure 6). Thus, our study provided an important mechanistic link between SETD2-mediated H3K36me3 and ATM activation. PARP1 inhibitor has been found to be particularly effective for treating certain breast cancer patients with deficiency in other elements of HR repair (BRCA1 and BRCA2) pathway (50,51). It can be envisaged that this previously unrecognized mechanism of ATM activation may also be harnessed for cancer therapy in the future.

Taken together, we discovered a novel crosstalk between two common histone epigenetic marks (i.e., H3K36me3 and H4K16Ac) in mammalian cells, defined MRG15 as the molecular determinant for this crosstalk, established its importance in HR repair, and unveiled novel functions of protein α-N-methylation.

References

1. Papamichos-Chronakis, M. and Peterson, C.L. (2013) Chromatin and the genome integrity network. *Nat. Rev. Genet.*, **14**, 62-75.

2. Greenberg, R.A. (2011) Histone tails: Directing the chromatin response to DNA damage. *FEBS Lett.*, **585**, 2883-2890.

3. Fierz, B., Chatterjee, C., McGinty, R.K., Bar-Dagan, M., Raleigh, D.P. and Muir, T.W. (2011) Histone H2B ubiquitylation disrupts local and higher-order chromatin compaction. *Nat Chem Biol*, **7**, 113-119.

4. Moyal, L., Lerenthal, Y., Gana-Weisz, M., Mass, G., So, S., Wang, S.Y., Eppink, B., Chung, Y.M., Shalev, G., Shema, E. *et al.* (2011) Requirement of ATM-dependent monoubiquitylation of histone H2B for timely repair of DNA double-strand breaks. *Mol Cell*, **41**, 529-542.

5. Nakamura, K., Kato, A., Kobayashi, J., Yanagihara, H., Sakamoto, S., Oliveira, D.V., Shimada, M., Tauchi, H., Suzuki, H., Tashiro, S. *et al.* (2011) Regulation of homologous recombination by RNF20-dependent H2B ubiquitination. *Mol Cell*, **41**, 515-528.

6. Krishnan, V., Chow, M.Z., Wang, Z., Zhang, L., Liu, B., Liu, X. and Zhou, Z. (2011) Histone H4 lysine 16 hypoacetylation is associated with defective DNA repair and premature senescence in Zmpste24-deficient mice. *Proc Natl Acad Sci U S A*, **108**, 12325-12330.

7. Taipale, M., Rea, S., Richter, K., Vilar, A., Lichter, P., Imhof, A. and Akhtar, A. (2005) hMOF histone acetyltransferase is required for histone H4 lysine 16 acetylation in mammalian cells. *Mol Cell Biol*, **25**, 6798-6810.

8. Bertram, M.J. and Pereira-Smith, O.M. (2001) Conservation of the MORF4 related gene family: identification of a new chromo domain subfamily and novel protein motif. *Gene*, **266**, 111-121.

9. Tominaga, K., Kirtane, B., Jackson, J.G., Ikeno, Y., Ikeda, T., Hawks, C., Smith, J.R., Matzuk, M.M. and Pereira-Smith, O.M. (2005) MRG15 regulates embryonic development and cell proliferation. *Mol Cell Biol*, **25**, 2924-2937.

10. Hayakawa, T., Zhang, F., Hayakawa, N., Ohtani, Y., Shinmyozu, K., Nakayama, J. and Andreassen, P.R. (2010) MRG15 binds directly to PALB2 and stimulates homology-directed repair of chromosomal breaks. *J Cell Sci*, **123**, 1124-1130.

11. Sy, S.M., Huen, M.S. and Chen, J. (2009) MRG15 is a novel PALB2-interacting factor involved in homologous recombination. *J Biol Chem*, **284**, 21127-21131.

12. Zhang, F., Fan, Q., Ren, K. and Andreassen, P.R. (2009) PALB2 functionally connects the breast cancer susceptibility proteins BRCA1 and BRCA2. *Mol Cancer Res*, **7**, 1110-1118.

13. Pardo, P.S., Leung, J.K., Lucchesi, J.C. and Pereira-Smith, O.M. (2002) MRG15, a novel chromodomain protein, is present in two distinct multiprotein complexes involved in transcriptional activation. *J Biol Chem*, **277**, 50860-50866.

14. Chen, M., Takano-Maruyama, M., Pereira-Smith, O.M., Gaufo, G.O. and Tominaga, K. (2009) MRG15, a component of HAT and HDAC complexes, is essential for proliferation and differentiation of neural precursor cells. *J Neurosci Res*, **87**, 1522-1531.

15. Yochum, G.S. and Ayer, D.E. (2002) Role for the mortality factors MORF4, MRGX, and MRG15 in transcriptional repression via associations with Pf1, mSin3A, and Transducin-Like Enhancer of Split. *Mol Cell Biol*, **22**, 7868-7876.

16. Cai, Y., Jin, J., Tomomori-Sato, C., Sato, S., Sorokina, I., Parmely, T.J., Conaway, R.C. and Conaway, J.W. (2003) Identification of new subunits of the multiprotein mammalian TRRAP/TIP60-containing histone acetyltransferase complex. *J Biol Chem*, **278**, 42733-42736.

17. Doyon, Y., Selleck, W., Lane, W.S., Tan, S. and Cote, J. (2004) Structural and functional conservation of the NuA4 histone acetyltransferase complex from yeast to humans. *Mol Cell Biol*, **24**, 1884-1896.

18. Stock, A., Clarke, S., Clarke, C. and Stock, J. (1987) N-terminal methylation of proteins: structure, function and specificity. *FEBS Lett.*, **220**, 8-14.

19. Chen, T., Muratore, T.L., Schaner-Tooley, C.E., Shabanowitz, J., Hunt, D.F. and Macara, I.G. (2007) N-terminal α-methylation of RCC1 is necessary for stable chromatin association and normal mitosis. *Nat. Cell Biol.*, **9**, 596-603.

20. Tooley, C.E., Petkowski, J.J., Muratore-Schroeder, T.L., Balsbaugh, J.L., Shabanowitz, J., Sabat, M., Minor, W., Hunt, D.F. and Macara, I.G. (2010) NRMT is an α-N-methyltransferase that methylates RCC1 and retinoblastoma protein. *Nature*, **466**, 1125-1128.

21. Cai, Q., Fu, L., Wang, Z., Gan, N., Dai, X. and Wang, Y. (2014) α-N-methylation of damaged DNA-binding protein 2 (DDB2) and its function in nucleotide excision repair. *J. Biol. Chem.*, **289**, 16046-16056.

22. Bailey, A.O., Panchenko, T., Sathyan, K.M., Petkowski, J.J., Pai, P.J., Bai, D.L., Russell, D.H., Macara, I.G., Shabanowitz, J., Hunt, D.F. *et al.* (2013) Posttranslational modification of CENP-A influences the conformation of centromeric chromatin. *Proc Natl Acad Sci U S A*, **110**, 11827-11832.

23. Petkowski, J.J., Schaner Tooley, C.E., Anderson, L.C., Shumilin, I.A., Balsbaugh, J.L., Shabanowitz, J., Hunt, D.F., Minor, W. and Macara, I.G. (2012) Substrate specificity of mammalian N-terminal α-amino methyltransferase NRMT. *Biochemistry*, **51**, 5942-5950.

24. Gunn, A. and Stark, J.M. (2012) I-SceI-based assays to examine distinct repair outcomes of mammalian chromosomal double strand breaks. *Methods Mol Biol*, **920**, 379-391.

25. Li, F., Mao, G., Tong, D., Huang, J., Gu, L., Yang, W. and Li, G.M. (2013) The histone mark H3K36me3 regulates human DNA mismatch repair through its interaction with MutSalpha. *Cell*, **153**, 590-600.

26. Sun, Y., Jiang, X., Xu, Y., Ayrapetov, M.K., Moreau, L.A., Whetstine, J.R. and Price, B.D. (2009) Histone H3 methylation links DNA damage detection to activation of the tumour suppressor Tip60. *Nat. Cell Biol.*, **11**, 1376-1382.

27. Zhang, F., Dai, X. and Wang, Y. (2012) 5-Aza-2'-deoxycytidine induced growth inhibition of leukemia cells through modulating endogenous cholesterol biosynthesis. *Mol. Cell. Proteomics*, **11**, M111 016915.

28. Ziv, Y., Bielopolski, D., Galanty, Y., Lukas, C., Taya, Y., Schultz, D.C., Lukas, J., Bekker-Jensen, S., Bartek, J. and Shiloh, Y. (2006) Chromatin relaxation in response to DNA double-strand breaks is modulated by a novel ATM- and KAP-1 dependent pathway. *Nat. Cell Biol.*, **8**, 870-876.

29. Aygun, O., Svejstrup, J. and Liu, Y. (2008) A RECQ5-RNA polymerase II association identified by targeted proteomic analysis of human chromatin. *Proc Natl Acad Sci U S A*, **105**, 8580-8584.

30. Xiong, L., Ping, L., Yuan, B. and Wang, Y. (2009) Methyl group migration during the fragmentation of singly charged ions of trimethyllysine-containing peptides: precaution of using MS/MS of singly charged ions for interrogating peptide methylation. *J Am Soc Mass Spectrom*, **20**, 1172-1181.

31. Garcia, S.N., Kirtane, B.M., Podlutsky, A.J., Pereira-Smith, O.M. and Tominaga, K. (2007) Mrg15 null and heterozygous mouse embryonic fibroblasts exhibit

DNA-repair defects post exposure to gamma ionizing radiation. *FEBS Lett*, **581**, 5275-5281.

32. Kusch, T., Florens, L., Macdonald, W.H., Swanson, S.K., Glaser, R.L., Yates, J.R., 3rd, Abmayr, S.M., Washburn, M.P. and Workman, J.L. (2004) Acetylation by Tip60 is required for selective histone variant exchange at DNA lesions. *Science*, **306**, 2084-2087.

33. Kaidi, A. and Jackson, S.P. (2013) KAT5 tyrosine phosphorylation couples chromatin sensing to ATM signalling. *Nature*, **498**, 70-74.

34. Shogren-Knaak, M., Ishii, H., Sun, J.M., Pazin, M.J., Davie, J.R. and Peterson, C.L. (2006) Histone H4-K16 acetylation controls chromatin structure and protein interactions. *Science*, **311**, 844-847.

35. Rea, S., Xouri, G. and Akhtar, A. (2007) Males absent on the first (MOF): from flies to humans. *Oncogene*, **26**, 5385-5394.

36. Bakkenist, C.J. and Kastan, M.B. (2003) DNA damage activates ATM through intermolecular autophosphorylation and dimer dissociation. *Nature*, **421**, 499-506.

37. Caparelli, M.L. and O'Connell, M.J. (2013) Regulatory motifs in Chk1. *Cell Cycle*, **12**, 916-922.

38. Matsuoka, S., Huang, M. and Elledge, S.J. (1998) Linkage of ATM to cell cycle regulation by the Chk2 protein kinase. *Science*, **282**, 1893-1897.

39. Weinstock, D.M., Nakanishi, K., Helgadottir, H.R. and Jasin, M. (2006) Assaying double-strand break repair pathway choice in mammalian cells using a targeted endonuclease or the RAG recombinase. *Methods Enzymol*, **409**, 524-540.

40. Zhang, P., Du, J., Sun, B., Dong, X., Xu, G., Zhou, J., Huang, Q., Liu, Q., Hao, Q. and Ding, J. (2006) Structure of human MRG15 chromo domain and its binding to Lys36-methylated histone H3. *Nucleic Acids Res.*, **34**, 6621-6628.

41. Pfister, S.X., Ahrabi, S., Zalmas, L.P., Sarkar, S., Aymard, F., Bachrati, C.Z., Helleday, T., Legube, G., La Thangue, N.B., Porter, A.C. *et al.* (2014) SETD2-dependent histone H3K36 trimethylation is required for homologous recombination repair and genome stability. *Cell Rep.*, **7**, 2006-2018.

42. Carvalho, S., Vitor, A.C., Sridhara, S.C., Martins, F.B., Raposo, A.C., Desterro, J.M., Ferreira, J. and de Almeida, S.F. (2014) SETD2 is required for DNA double-strand break repair and activation of the p53-mediated checkpoint. *eLife*, **3**, e02482.

43. Chapman, J.R., Taylor, M.R. and Boulton, S.J. (2012) Playing the end game: DNA double-strand break repair pathway choice. *Mol Cell*, **47**, 497-510.

44. Dai, X., Otake, K., You, C., Cai, Q., Wang, Z., Masumoto, H. and Wang, Y. (2013) Identification of novel alpha-n-methylation of CENP-B that regulates its binding to the centromeric DNA. *J Proteome Res*, **12**, 4167-4175.

45. Maurer-Stroh, S., Dickens, N.J., Hughes-Davies, L., Kouzarides, T., Eisenhaber, F. and Ponting, C.P. (2003) The Tudor domain 'Royal Family': Tudor, plant Agenet, Chromo, PWWP and MBT domains. *Trends Biochem. Sci.*, **28**, 69-74.

46. Xu, Y., Gan, E.S., Zhou, J., Wee, W.Y., Zhang, X. and Ito, T. (2014) Arabidopsis MRG domain proteins bridge two histone modifications to elevate expression of flowering genes. *Nucleic Acids Res.*, **42**, 10960-10974.

47. Wu, J., Chen, Y., Lu, L.Y., Wu, Y., Paulsen, M.T., Ljungman, M., Ferguson, D.O. and Yu, X. (2011) Chfr and RNF8 synergistically regulate ATM activation. *Nat Struct Mol Biol*, **18**, 761-768.

48. Jazayeri, A., Falck, J., Lukas, C., Bartek, J., Smith, G.C., Lukas, J. and Jackson, S.P. (2006) ATM- and cell cycle-dependent regulation of ATR in response to DNA double-strand breaks. *Nat. Cell Biol.*, **8**, 37-45.

49. Aymard, F., Bugler, B., Schmidt, C.K., Guillou, E., Caron, P., Briois, S., Iacovoni, J.S., Daburon, V., Miller, K.M., Jackson, S.P. *et al.* (2014) Transcriptionally active chromatin recruits homologous recombination at DNA double-strand breaks. *Nat. Struct. Mol. Biol.*, **21**, 366-374.

50. Bryant, H.E., Schultz, N., Thomas, H.D., Parker, K.M., Flower, D., Lopez, E., Kyle, S., Meuth, M., Curtin, N.J. and Helleday, T. (2005) Specific killing of BRCA2-deficient tumours with inhibitors of poly(ADP-ribose) polymerase. *Nature*, **434**, 913-917.

51. Farmer, H., McCabe, N., Lord, C.J., Tutt, A.N., Johnson, D.A., Richardson, T.B., Santarosa, M., Dillon, K.J., Hickson, I., Knights, C. *et al.* (2005) Targeting the DNA repair defect in BRCA mutant cells as a therapeutic strategy. *Nature*, **434**, 917-921.

Chapter 5. Conclusions and future research

The research in this dissertation concentrates on the identification and characterizations of the functional roles of novel PTMs of DDB2 and MRG15 which are important in nucleotide excision repair (NER) and homologous recombination (HR), respectively. Specifically, in HEK293T cells, DDB2 was found to be α-N-methylated and phosphorylated at Serine 26, and MRG15 was found to be α-N-methylated. The functional characterizations of these novel modifications provide a better understanding for the regulation of DNA repair pathway by protein PTMs.

In Chapter two, by using LC-MS/MS, I discovered, for the first time, that DDB2 was α-N-methylated in human cells. I also found that NTMT1 was able to catalyze the α-N-methylation of DDB2 *in vitro* and in human cells. In addition, this methylation promoted DDB2's nuclear localization and recruitment to CPD foci. Moreover, the α-N-methylation of DDB2 promoted the repair of the CPD lesion, enabled ATM activation and conferred the resistance of human cells toward UV damage. Together, my study extended the biological functions of protein α-N-methylation to DNA repair.

In Chapter three, I reported that the ectopically expressed DDB2 was phosphorylated at Serine 26 in HEK293T cells. The phosphorylation is mediated by Cdks, as supported by the observations that the phosphorylation level is decreased dramatically upon treatment with flavopiridol, a Cdk inhibitor. I also observed that a DDB2 mutant deficient in Ser26 phosphorylation failed to be recruited to UV light-induced CPD foci. In addition, loss of the Ser26 phosphorylation abolished ATM activation and CPD repair, and resulted in hypersensitivity to UV damage. The functions

of this phosphorylation may reside in its role on the ubiquitination and proteasomal degradation of DDB2. Together, my investigation characterized the functional importance of this phosphorylation in NER. Further studies are in need for uncovering the identities of Cdk(s) involved in the phosphorylation.

In Chapter four, by employing a similar LC-MS/MS-based approach, I identified that MRG15 is α-N-methylated in HEK293T cells. I also demonstrated that the α-N-methylated N-terminus of MRG15 promoted the recruitment of TIP60 to chromatin through its interaction with chromo domain of TIP60, and it serves as an allosteric regulator to stimulate the enzymatic activity of the latter. Furthermore, I found that the TIP60's chromo domain recognition of α-N-methylation of MRG15 is pivotal for H4K16Ac, DNA damage-induced ATM activation, HR repair and cellular resistance toward genotoxic agents that induce DNA DSBs and interstrand cross-links. In addition, I identified H3K36me3 as a docking site for MRG15's binding to chromatin through the chromo domain of MRG15, which drives H4K16Ac in human cells. Collectively, I uncovered a novel crosstalk between H3K36me3 and H4K16Ac in mammalian cells, defined MRG15 as the molecular determinant for this crosstalk via its α-N-methylated N-terminal tail and chromo domain, and established its importance in HR repair and ATM activation.

Besides the above-characterized PTMs of DDB2 and MRG15 in human cells, I also identified several additional PTMs, including putative ubiquitination sites of lysine 151 and lysine 309 in DDB2, as well as the phosphorylation of serine 127 in MRG15. Characterizations of these novel PTMs may provide a better understanding about how

DDB2 and MRG15 are regulated. Moreover, it is intriguing to explore the possible crosstalk between these novel PTMs in DDB2 and MRG15.

On the ground that *in vitro* assay largely expanded the potential α-N-methylated proteins (1), it is of great importance to design experiments to investigate the presence and importance of α-N-methylation in other proteins. For instance, LATS2, which carries an N-terminal RPK motif, was recently identified to be critical in maintenance of genome stability through regulating cytokinesis (2). Specifically, the LATS2 kinase is activated in tetraploid cells, which suppresses YAP-dependent transcription and induces cell cycle arrest (2). Viewing that LATS2 is predicted to be α-N-methylated, studies are in need to confirm this α-N-methylation and elucidate its function.

In our study, we uncovered, for the first time, the role of α-N-methylation in protein-protein interaction. In particular, NTMT1-mediated α-N-methylation of MRG15 is recognized by the chromo domain of TIP60. Since "Royal family" modules, including the chromo, Tudor and PWWP domains, can bind to methylated lysine and arginine marks through a similar mechanism (3), it is foreseeable that other 'Royal family' proteins can recognize the α-N-methylation proteins. Additional readers of α-N-methylation can be explored by stable isotope labeling by amino acids in cell culture (SILAC). In this vein, the FLAG-tagged wild-type α-N-methylated protein and the corresponding mutant abrogating α-N-methylation could be expressed in HEK293T cells cultured in ^{13}C, ^{15}N-enriched amino acid-carrying (heavy) medium or unlabeled amino acid-containing (light) medium. The wild-type and mutant proteins will serve as baits to pull down their interaction proteins. The amount of total proteins in cell lysate can be

quantified by using Bradford assay and an equal amounts of cell lysates can be passed through anti-FLAG M2 affinity gel. The beads will then be combined and digested with trypsin followed by LC-MS/MS analysis. In forward experiment, FLAG-tagged wild-type α-N-methylated protein will be cultured in the heavy medium and the corresponding α-N-methylation-deficient mutant will be cultured in the light medium. The basis of this method lies in that proteins bearing no specific binding toward wild-type and mutant proteins will occur equally in the two eluents. However, proteins displaying specific binding toward the α-N-methylated protein bait will have a heavy/light ratio substantially greater than 1 for their constituent peptides. Proteins exhibiting specific binding toward the α-N-methylation-deficient mutant bait will have a heavy/light ratio less than 1 for their constituent peptides. To ensure that the preferential binding of proteins to wild-type over mutant protein target is not due to experimental error, we will also perform reverse SILAC labeling experiment, where the wild-type and mutant proteins are cultured in light and heavy medium, respectively.

Last but not least, viewing the fact that α-N-methylation seems to be dynamic, it is interesting to elucidate how this modification is regulated. In this respect, protein expression level of NTMT1 showed no difference upon MMC and NCS treatment. Further investigations can be conducted to examine whether the chromatin localization of NTMT1 is altered upon these treatments. To dissect the mechanisms about the regulation of the enzymatic activity of NTMT1, another approach could be identification and characterization of novel PTMs in NTMT1 by employing a similar affinity-purification coupled with mass spectrometry-based method described before.

References

1. Petkowski, J. J., Schaner Tooley, C. E., Anderson, L. C., Shumilin, I. A., Balsbaugh, J. L., Shabanowitz, J., Hunt, D. F., Minor, W., and Macara, I. G. (2012) *Biochemistry* **51**, 5942-5950.

2. Ganem, N. J., Cornils, H., Chiu, S. Y., O'Rourke, K. P., Arnaud, J., Yimlamai, D., Thery, M., Camargo, F. D., and Pellman, D. (2014) *Cell* **158**, 833-848.

3. Patel, D. J., and Wang, Z. (2013) *Annu Rev Biochem* **82**, 81-118.

Appendix A. Supporting Information for Chapter 2

"α-N-Methylation of Damaged DNA-Binding Protein 2 (DDB2) and Its Function in Nucleotide Excision Repair"

Figure A. 1. MS/MS/MS of y_6 ion observed in the MS/MS of the di-methylated form of the peptide $_1$APKKRPE$_7$.

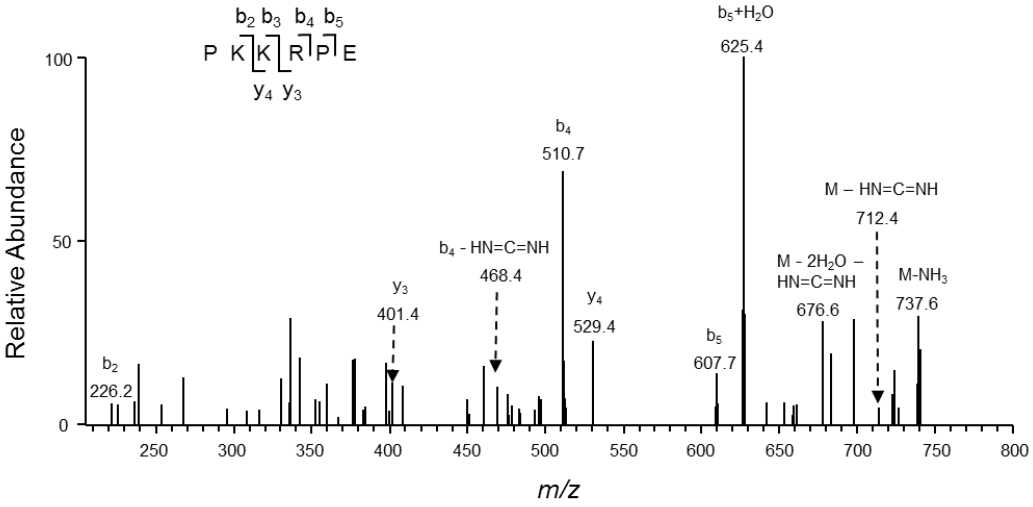

Figure A. 2. ESI-MS/MS of unmodified, mono-, di-, tri-α-N-methylated forms of the peptide $_1$APKKRPE$_7$ from X-factor-cleaved recombinant DDB2: (a) without the addition of NRMT, (b) with the addition of NRMT. (c) ESI-MS/MS of unmodified, mono-, di-, tri-α-N-methylated forms of the peptide $_1$AAKKRPE$_7$ arising from Glu-C digestion of X-factor-cleaved recombinant DDB2 with incubation with NRMT. Certain regions of the spectra were amplified to visualize better the peaks for some fragment ions.

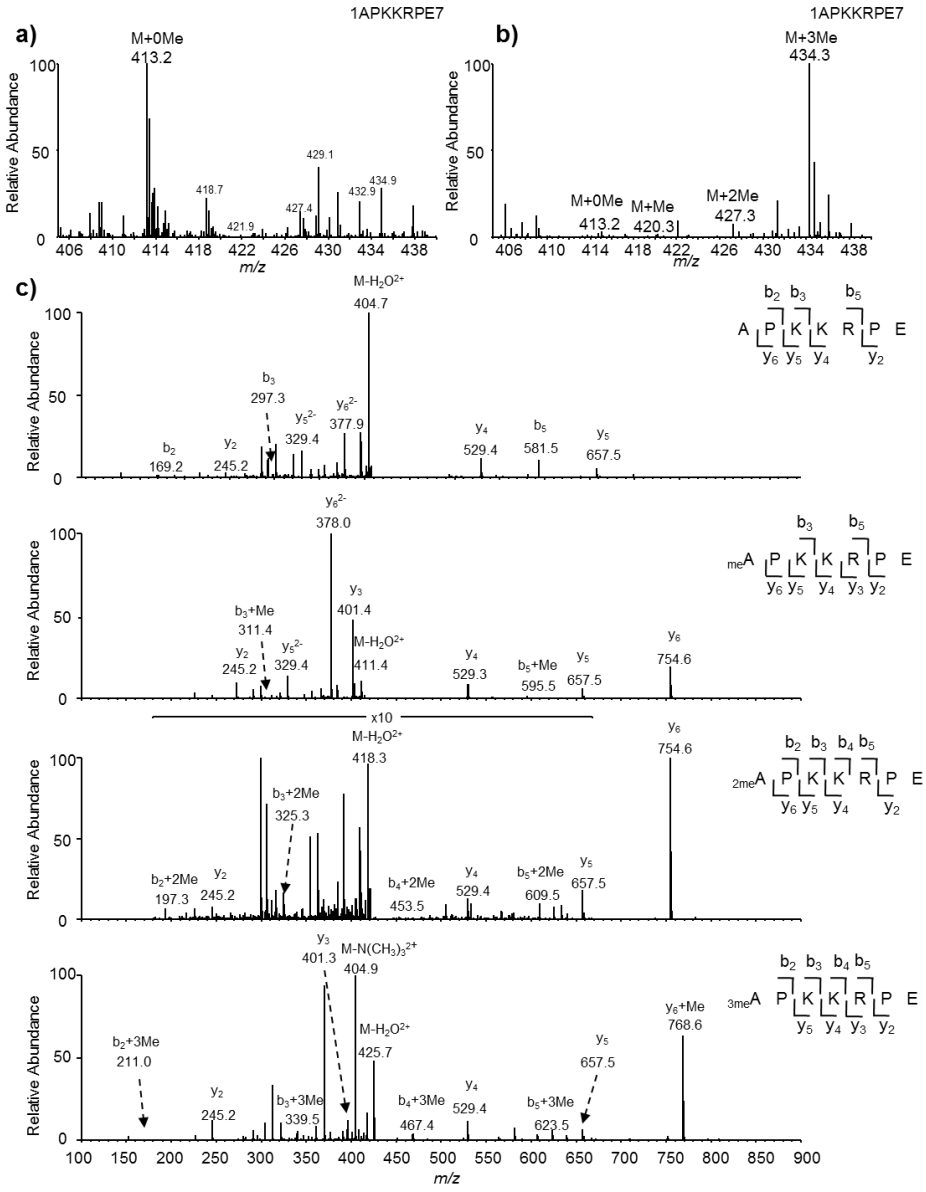

Figure A. 3. ESI-MS/MS of unmodified as well as mono-, di-, tri-α-N-methylated forms of the peptide $_{1}$APKKRPETQKTS$_{12}$. Certain regions of the spectra were amplified to visualize better the peaks for some fragment ions.

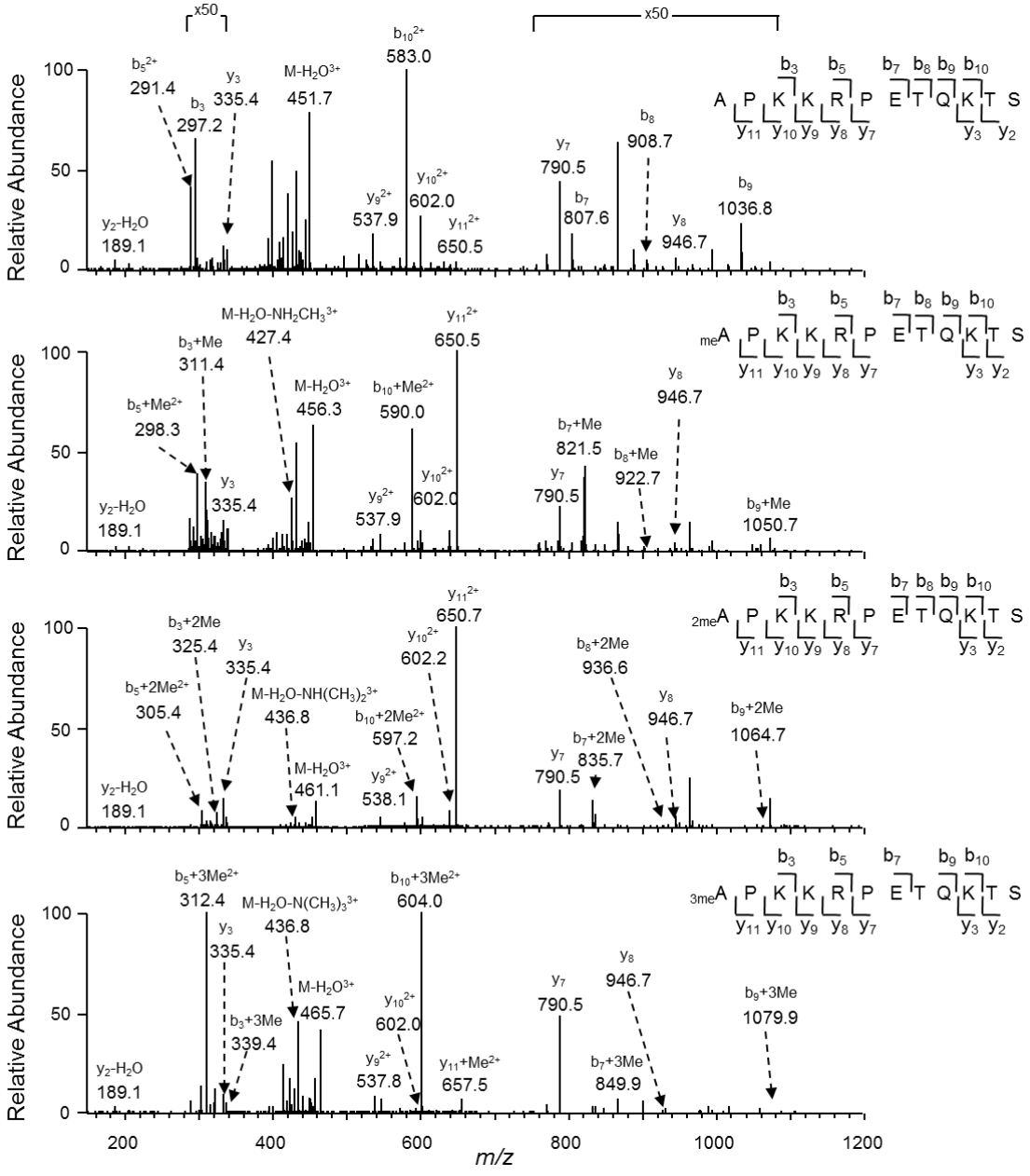

Figure A. 4. ESI-MS/MS of unmodified as well as mono-, di-, tri-α-N-methylated forms of the peptide $_{1}$AAKKRPETQKTS$_{12}$. Certain regions of the spectra were amplified to visualize better the peaks for some fragment ions.

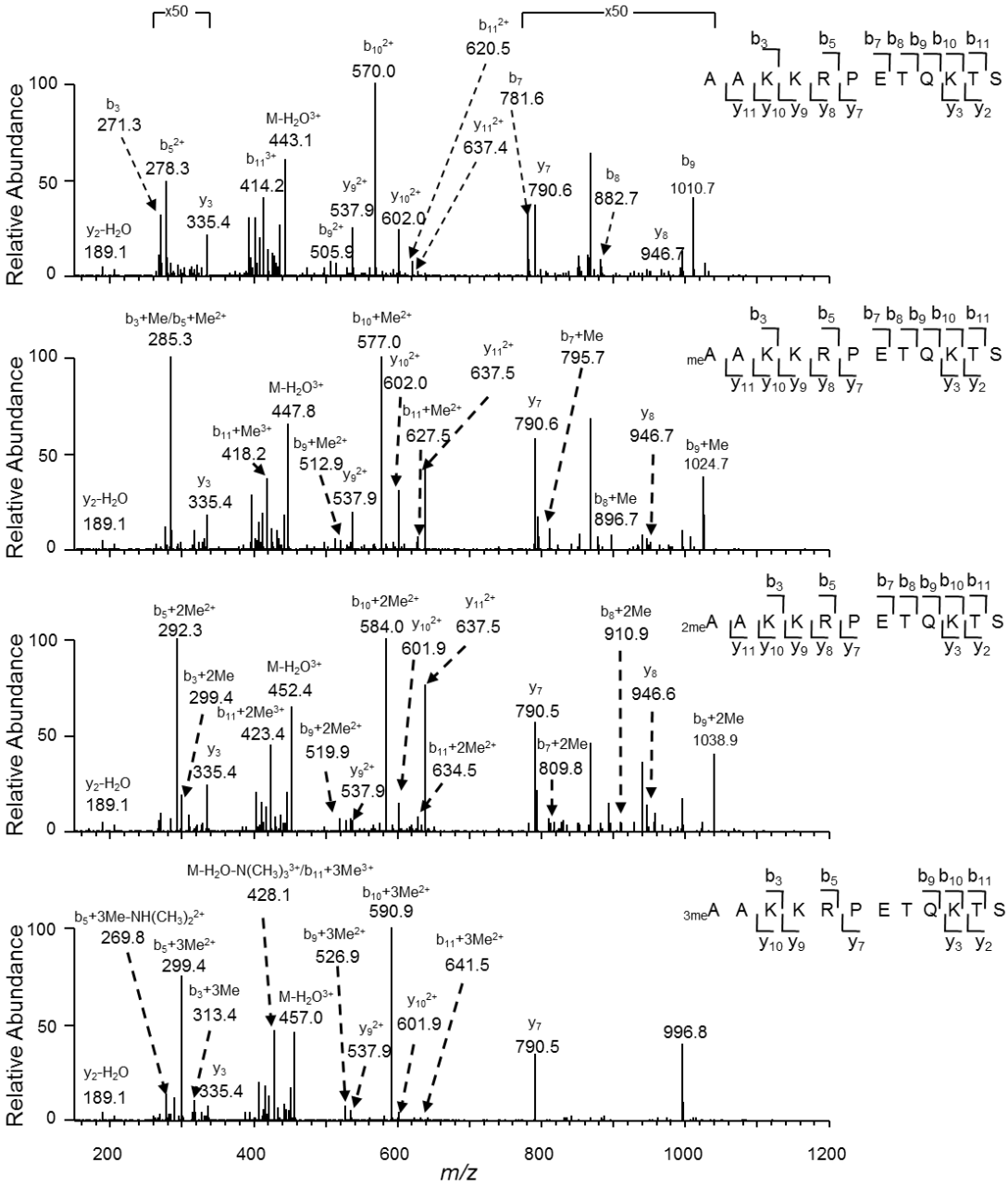

Figure A. 5. ESI-MS/MS of unmodified and monomethylated forms of the peptide $_{1}$APQKRPETQKTS$_{12}$. Certain regions of the spectrum were amplified to visualize better the peaks for some fragment ions.

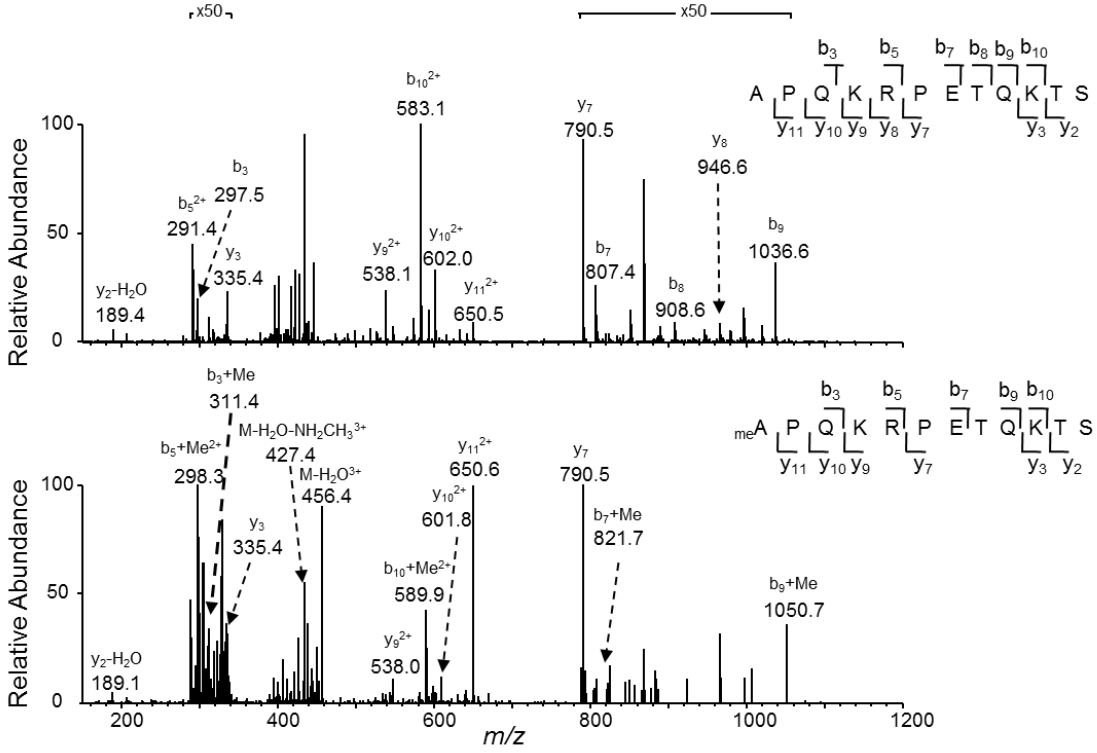

Figure A. 6. ESI-MS of unmodified forms of the peptide $_1$APQKRPE$_7$.

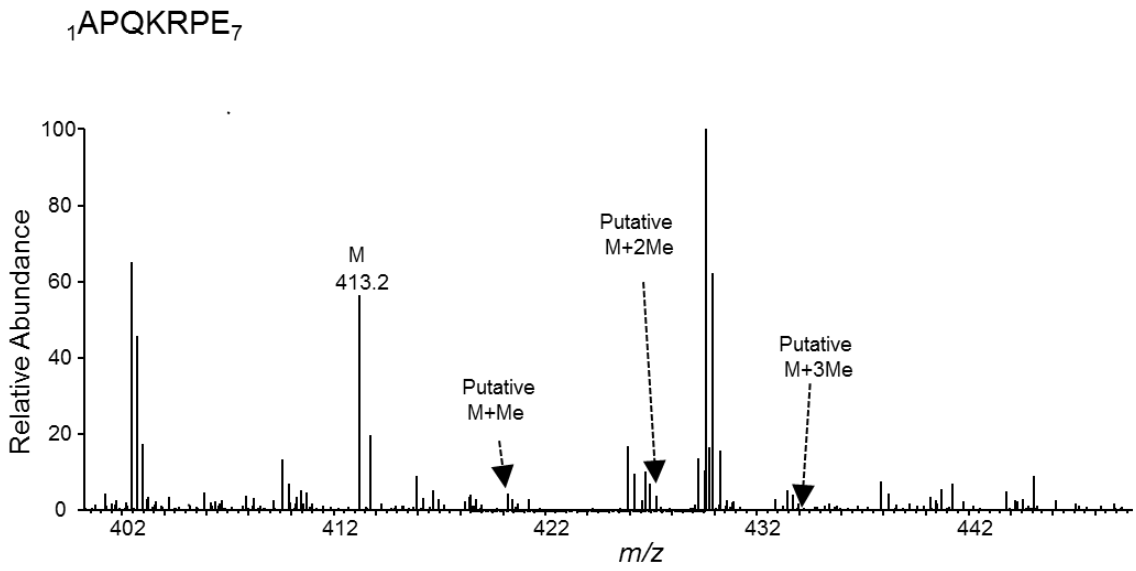

Appendix B. Supporting Information for Chapter 4

"α-N-Methylation of MRG15 Facilitates H3K36me3-H4K16Ac Crosstalk and ATM Activation through Chromatin Recruitment and Allosteric Regulation of TIP60"

Supplementary Materials and methods

Preparation of Recombinant proteins

NRMT-His_6 and MRG15-His_6 were expressed and purified following similar procedures as previously described (1). Briefly, after growth to an optical density at 600 nm of approximately 0.8, Rosetta (DE3) pLysS *E. coli* strain was induced by supplementing with 0.5 mM isopropyl 1-thio-β-D-galactopyranoside at room temperature overnight for NRMT-His_6, and at 37°C for 4 hr for MRG15-His_6. The proteins were then purified by using Talon affinity resin (Clontech) following the manufacturer's recommended procedures.

In vitro methylation assay

Purified NRMT-His_6 (0.3 μg) was incubated with 1 μg X-factor-cleaved MRG15-His_6 or synthetic N-terminal peptide of MRG15 (Genemed Synthesis, Inc.) with 100 μM *S*-adenosyl-L-methionine (*S*-AdoMet) as the methyl donor and brought to 50 μL with methyltransferase buffer (50 mM Tris, 50 mM potassium acetate, pH 8.0). Reactions were continued at 30°C for 2 hr.

Reference

1. Cai, Q., Fu, L., Wang, Z., Gan, N., Dai, X. and Wang, Y. (2014) alpha-N-Methylation of Damaged DNA-binding Protein 2 (DDB2) and Its Function in Nucleotide Excision Repair. *J Biol Chem*, 289, 16046-16056.

Figure B. 1. ESI-MS/MS of unmodified (a) as well as mono- (b), di- (c) and tri-methylated (d) forms of the peptide $_{1}$APKQDPKPKFQE$_{12}$ of C-terminally FLAG-tagged MRG15 isolated from HEK293T cells.

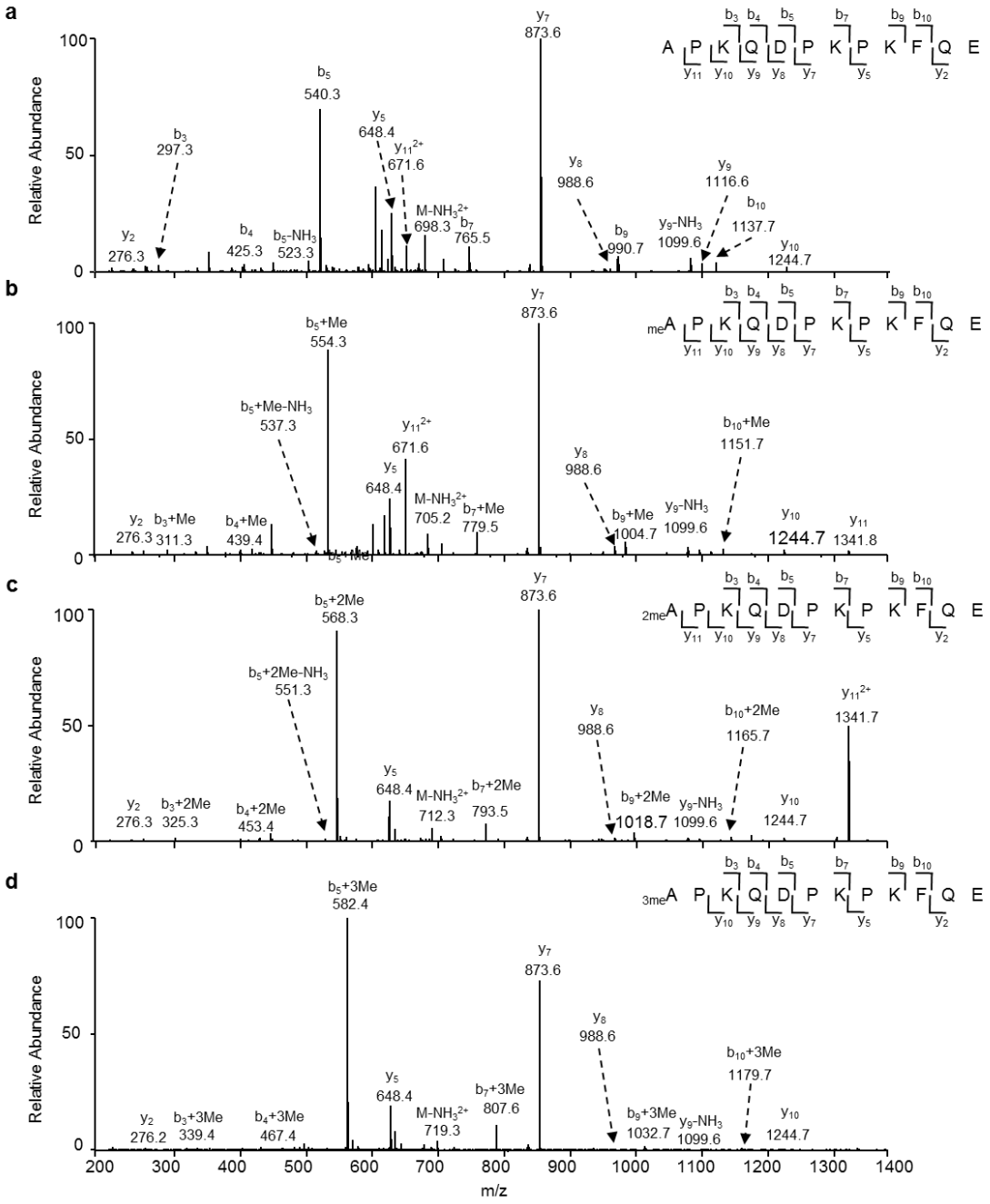

Figure B. 2. MS/MS/MS of b_5+3Me ion found in the MS/MS of the tri-methylated form of the peptide 1APKQDPKPKFQE12.

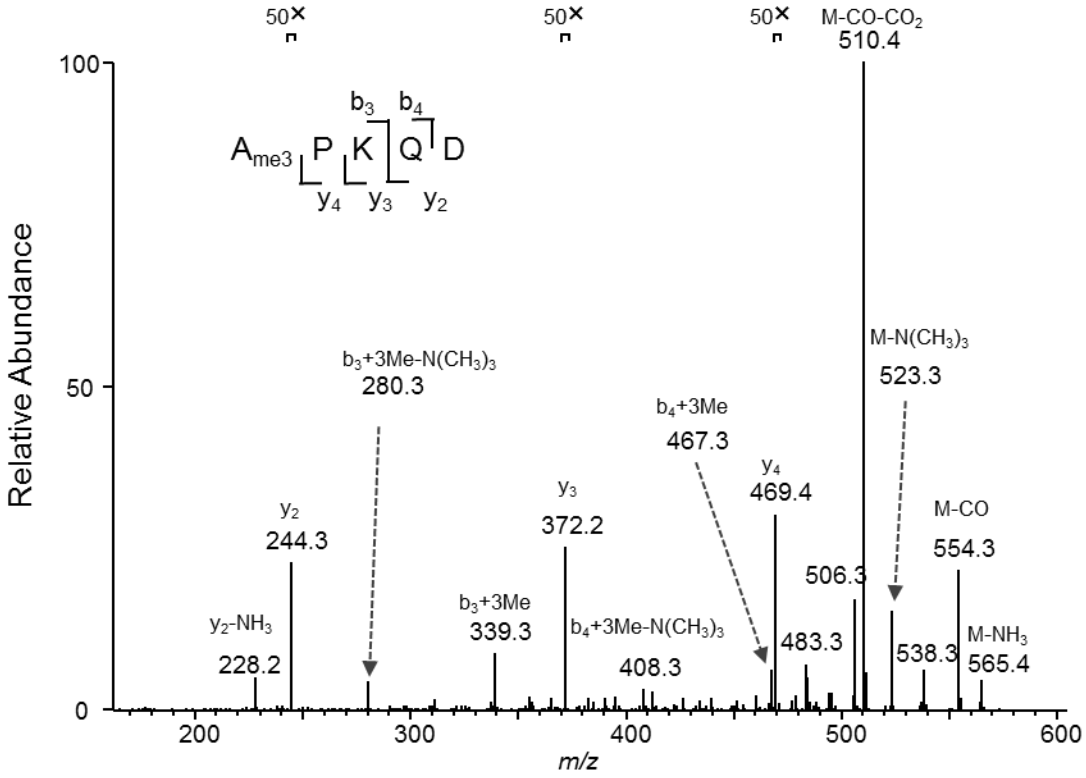

Figure B. 3. NTMT1 was efficiently knockdown by the NTMT1 siRNA in HEK293T cells. (a) Relative mRNA level of NTMT1 gene measured by real-time PCR with the use of GAPDH gene as control; (b) Expression level of NTMT1 protein measured by Western blot with the use of β-actin as a loading control. The results for (a) represent the mean and standard deviation of data obtained from three biological replicates. The *P* values were calculated by using unpaired two-tailed Student's t-test.

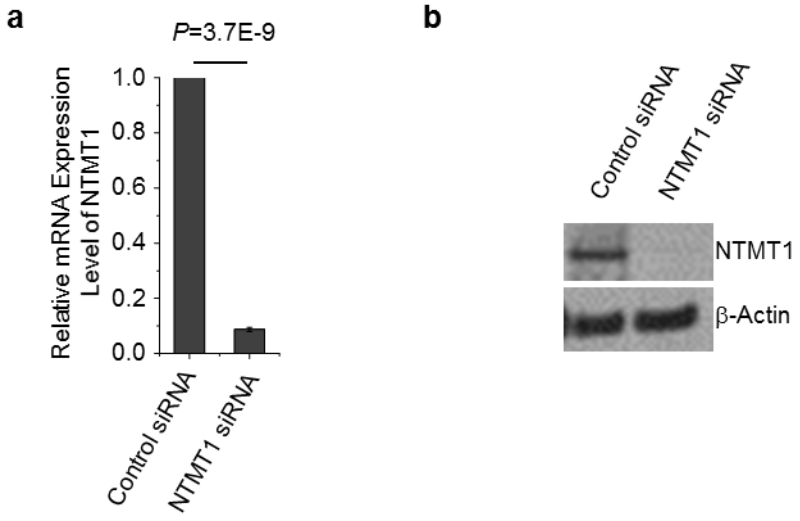

Figure B. 4. ESI-MS of unmodified, mono-, di-, tri-α-N-methylated forms of the peptide $_{1}$APKQDPKPKFQE$_{12}$ from X-factor-cleaved recombinant MRG15 with the addition of NTMT1.

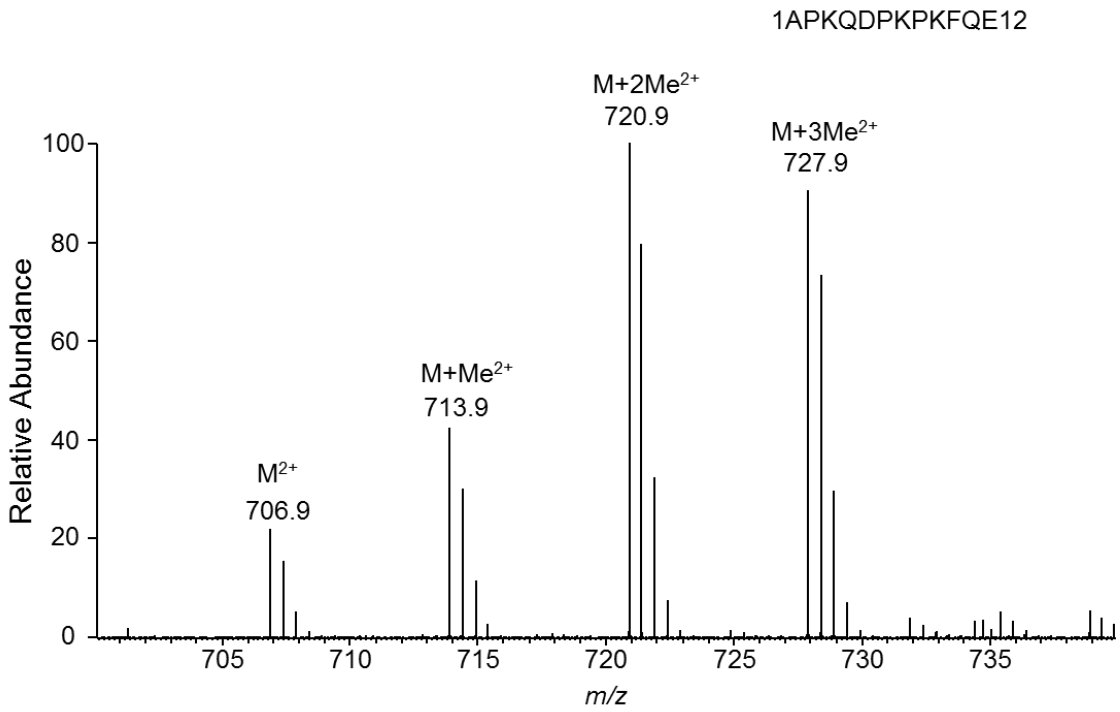

Figure B. 5. NTMT1 can catalyze the α-N-methylation of synthetic N-terminal peptide from MRG15. (a) ESI-MS of unmodified forms of the peptide 1APKQDPKPKFQE12 without addition of NRMT; (b) ESI-MS of unmodified, mono-, di-, tri-α-N-methylated forms of the peptide MRG15-K4Q, i.e., $_1$APQQDPKPKFQE$_{12}$ without addition of NRMT; (c) ESI-MS of unmodified forms of the peptide 1APKQDPKPKFQE12 with addition of NRMT; (b) ESI-MS of unmodified, mono-, di-, tri-α-N-methylated forms of the peptide MRG15-K4Q, i.e., $_1$APQQDPKPKFQE$_{12}$ with addition of NTMT1; (e) Relative abundances of different methylation forms of N-terminal 12 amino acids of MRG15, MRG15-K4Q as determined by semi-quantitative MS analysis. The results represent the mean and standard deviation of results obtained from three independent experiments.

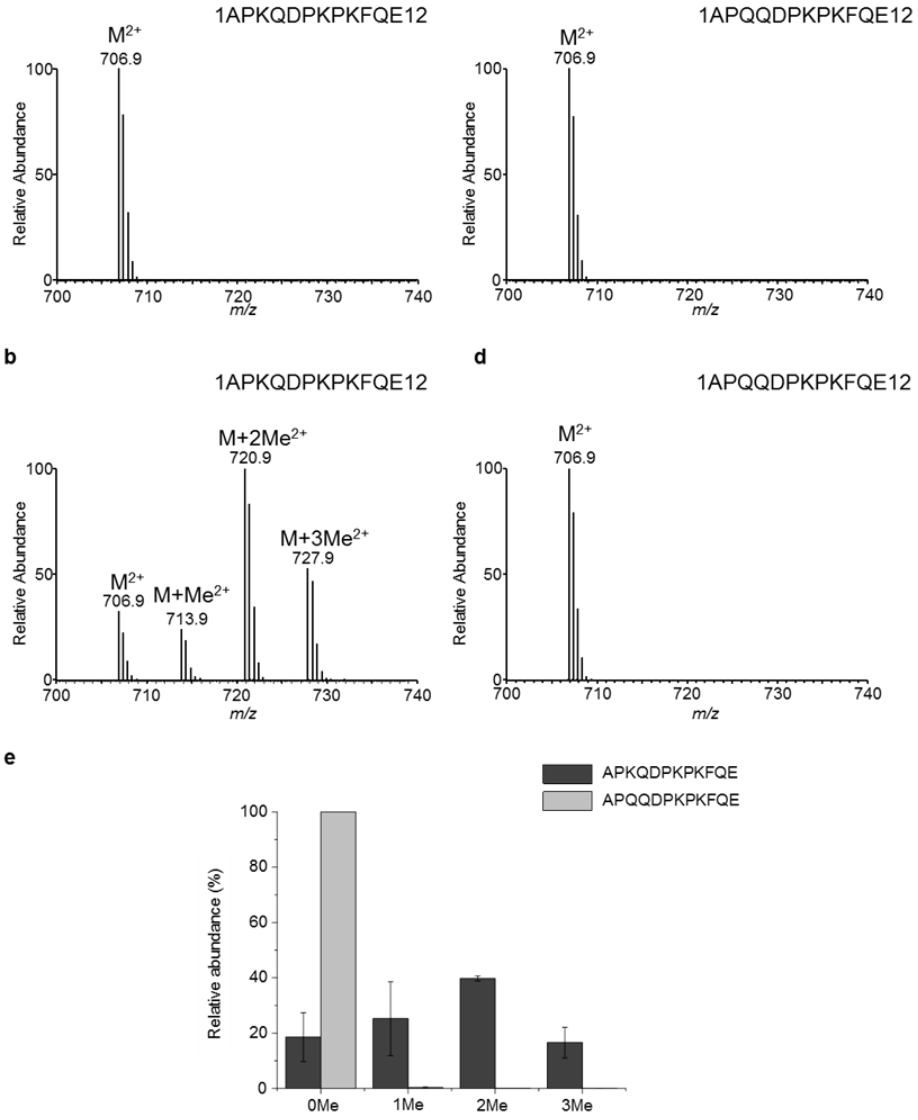

Figure B. 6. MRG15-K4Q cannot be α-N-methylated in human HEK293T cells. (a) ESI-MS and (b) MS/MS of unmodified forms of the peptide $_{1}$APQQDPKPKFQE$_{12}$ of C-terminally FLAG-tagged MRG15-K4Q isolated from HEK293T cells.

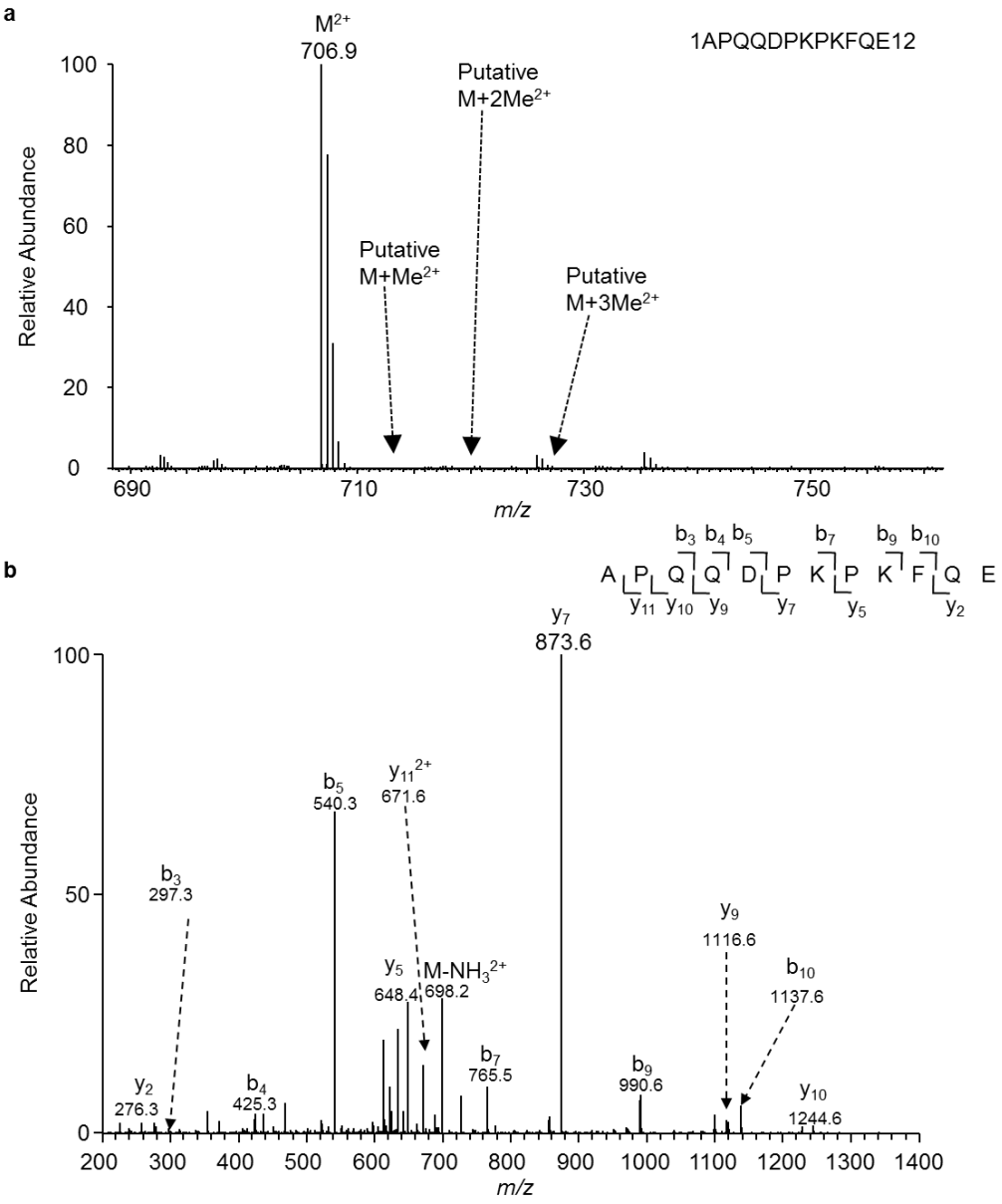

Figure B. 7. Western blot showing that the expression level of (a) MRG15 and MRG15-K4Q, (b) MRG15 and MRG15-Y46W49A are similar in HEK293T cells. β-actin was used as a loading control.

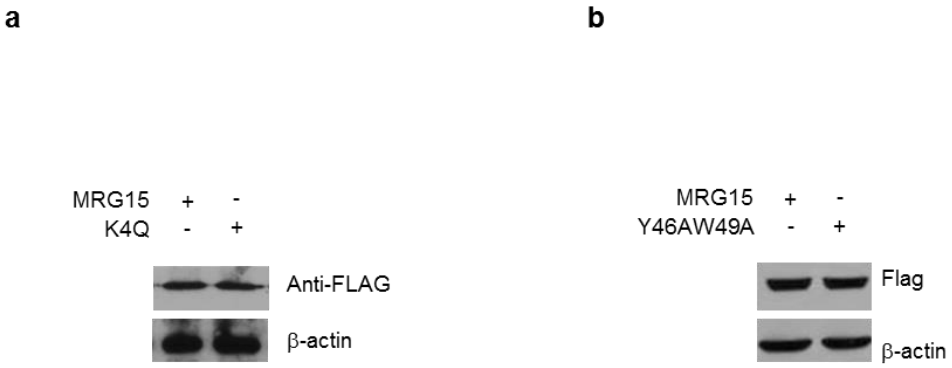

Figure B. 8. Replicate of Figure 4.2f.

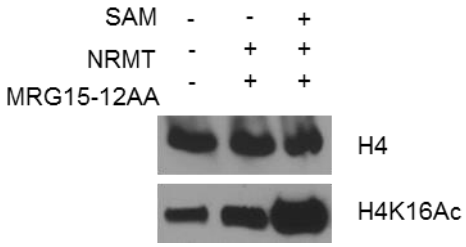

Figure B. 9. Replicate of Figure 4.4 to demonstrate the reproducibility of the experiment.

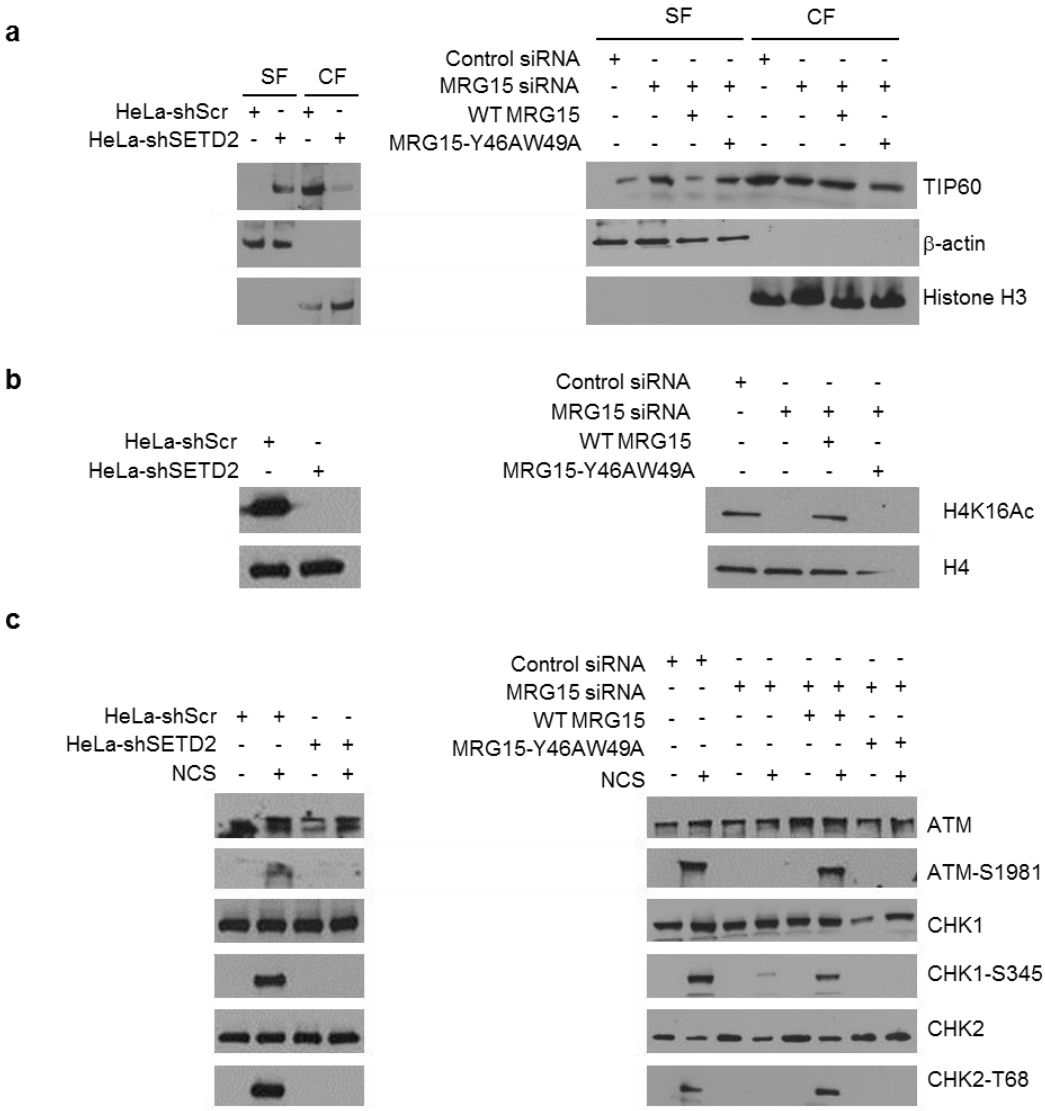

Figure B. 10. Endogenous MRG15 is efficiently knockdown by the 3'-UTR MRG15 siRNA in U2OS-DRGFP, HEK293T, and HeLa cells. (a) Relative mRNA level of MRG15 measured by real-time PCR with the use of GAPDH gene as a control; (b) Protein expression level of MRG15 monitored by Western blot with the use of β-actin as a loading control. The results for (a) represent the mean and standard deviation of data obtained from three biological replicates. The *P* values were calculated by using unpaired two-tailed Student's t-test.

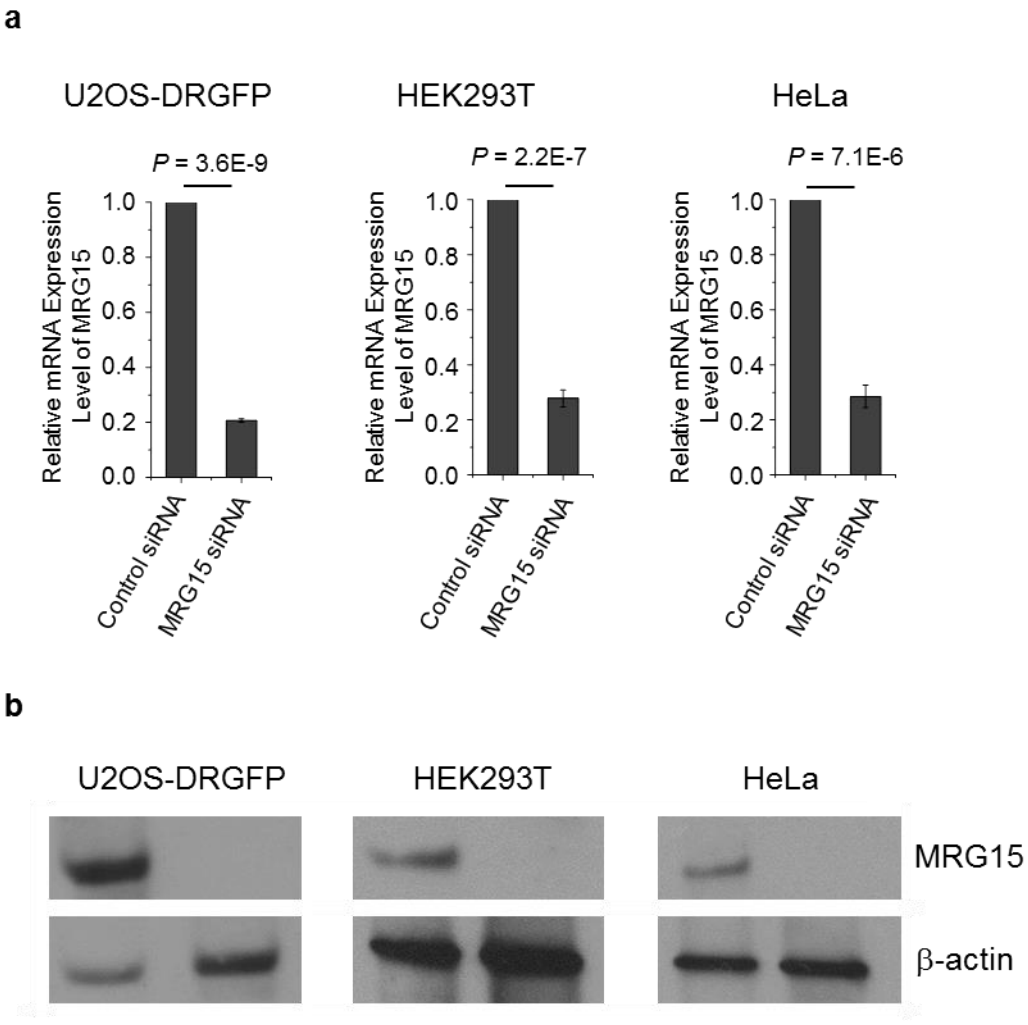

Figure B. 11. The hypersensitivity to MMC, NCS, and γ-rays in HeLa cells arising from MRG15 knockdown could be restored by transfecting cells with the plasmid for expressing wild-type MRG15, but not MRG15-Y46W49A. The results represent the mean and standard deviation of data obtained from three independent experiments. "*", $P < 0.05$; "**", $P < 0.01$; "***", $P < 0.001$. The P values were calculated by using unpaired two-tailed Student's t-test.

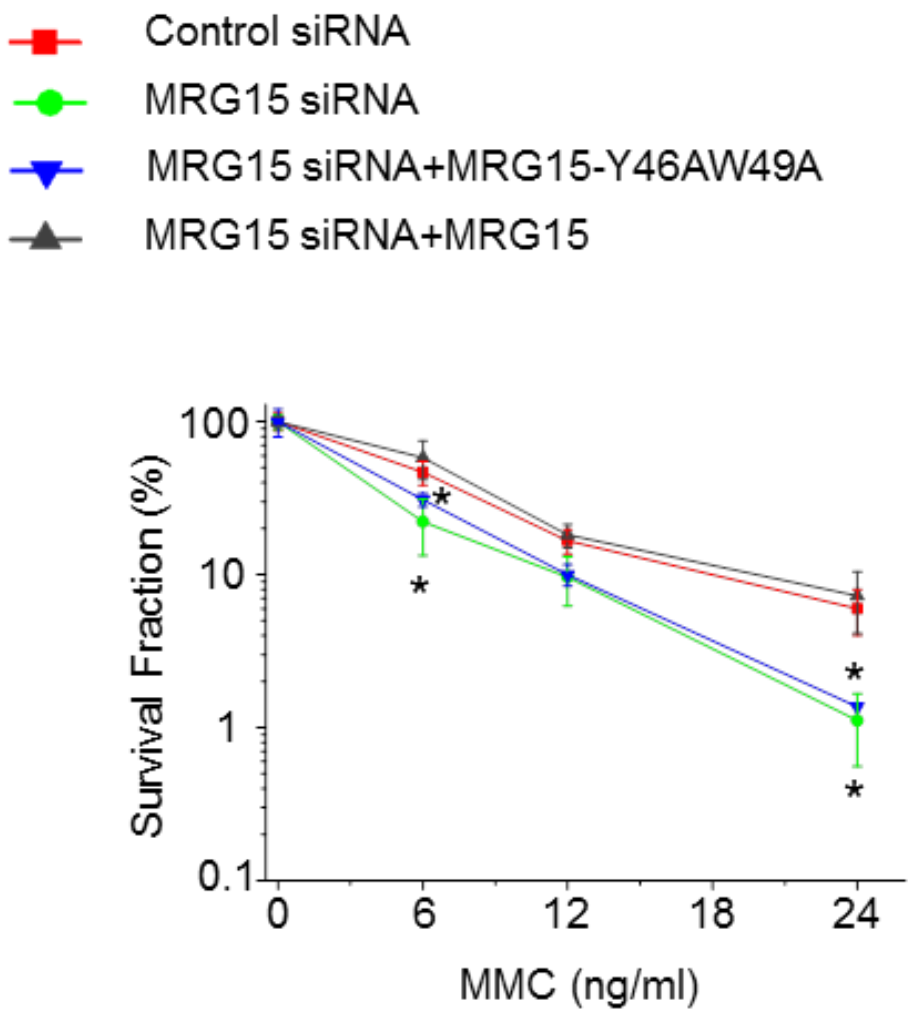

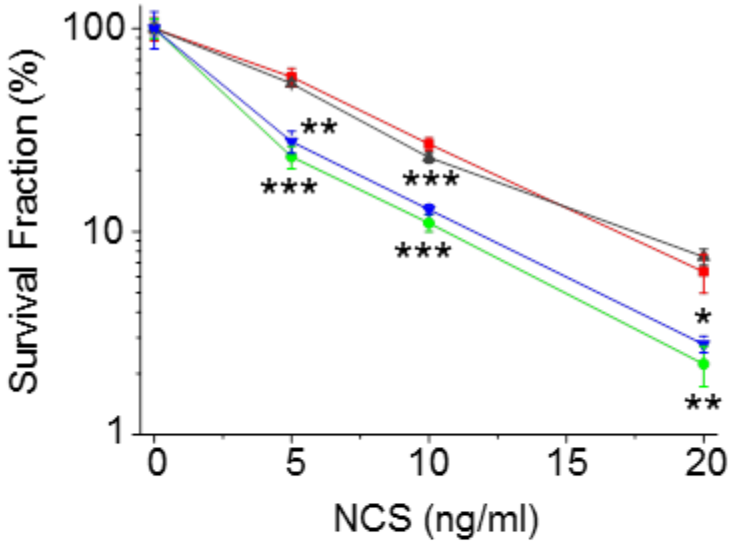
100
10
1
Survival Fraction (%)
0
5
10
15
20
NCS (ng/ml)
**
***
***
***
*
**

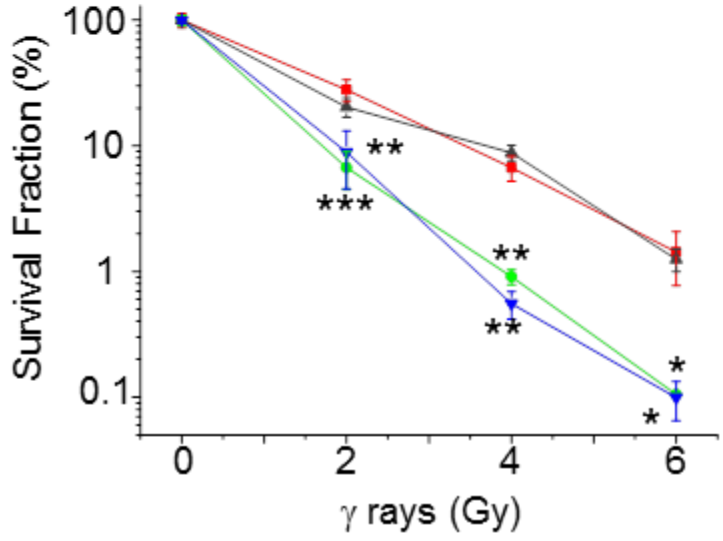
100
10
1
0.1
Survival Fraction (%)
0
2
4
6
γ rays (Gy)
**
***
**
**
*
*

Figure B. 12. H3K36me3 plays a very important role in homologous recombination. (a) HeLa cells stably expressing SETD2 shRNA, but not scrambled control shRNA, led to a reduced efficiency in HR. (b) SETD2-deficient UOK143 cells displayed diminished HR efficiency than the SETD2-proficient UOK121 cells. (c) Flow cytometry analysis showing that the transfection efficiencies were similar for UOK121 and UOK143 cells at the same density. (d) Western blot revealed loss of H3K36me3 in HeLa-shScr and UOK143 cells due to the deficient SETD2 as compared with HeLa-shSETD2 and UOK121 cells, respectively. The results represent the mean and standard deviation of data obtained from three biological replicates. The *P* values were calculated by using unpaired two-tailed Student's t-test.

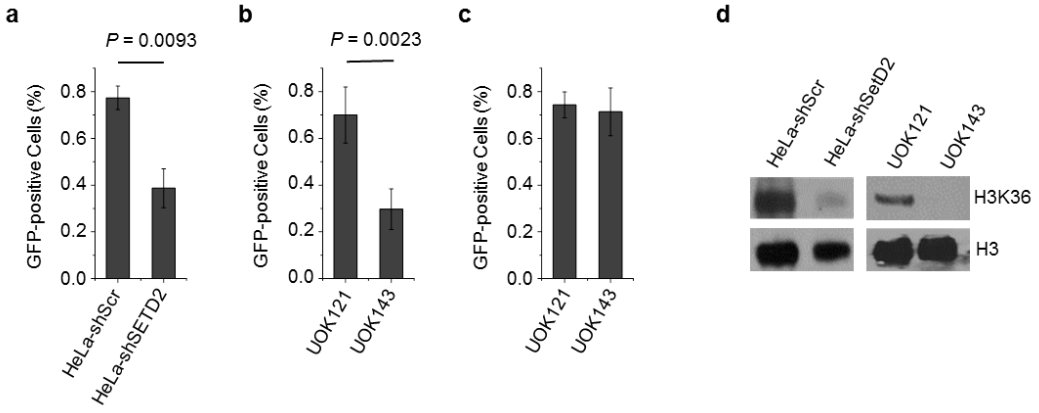

Figure B. 13. HeLa-shSETD2 and UOK143 cells exhibited elevated sensitivity toward (a) MMC, (b) NCS, and (c) γ-rays, and the elevated sensitivity in HeLa-shSETD2 could be rescued by complementing cells with yeast SETD2. The results represent the mean and standard deviation of data obtained from three biological replicates. "*", $P < 0.05$; "**", $P < 0.01$; "***", $P < 0.001$ (n = 3). The P values were calculated by using unpaired two-tailed Student's t-test.

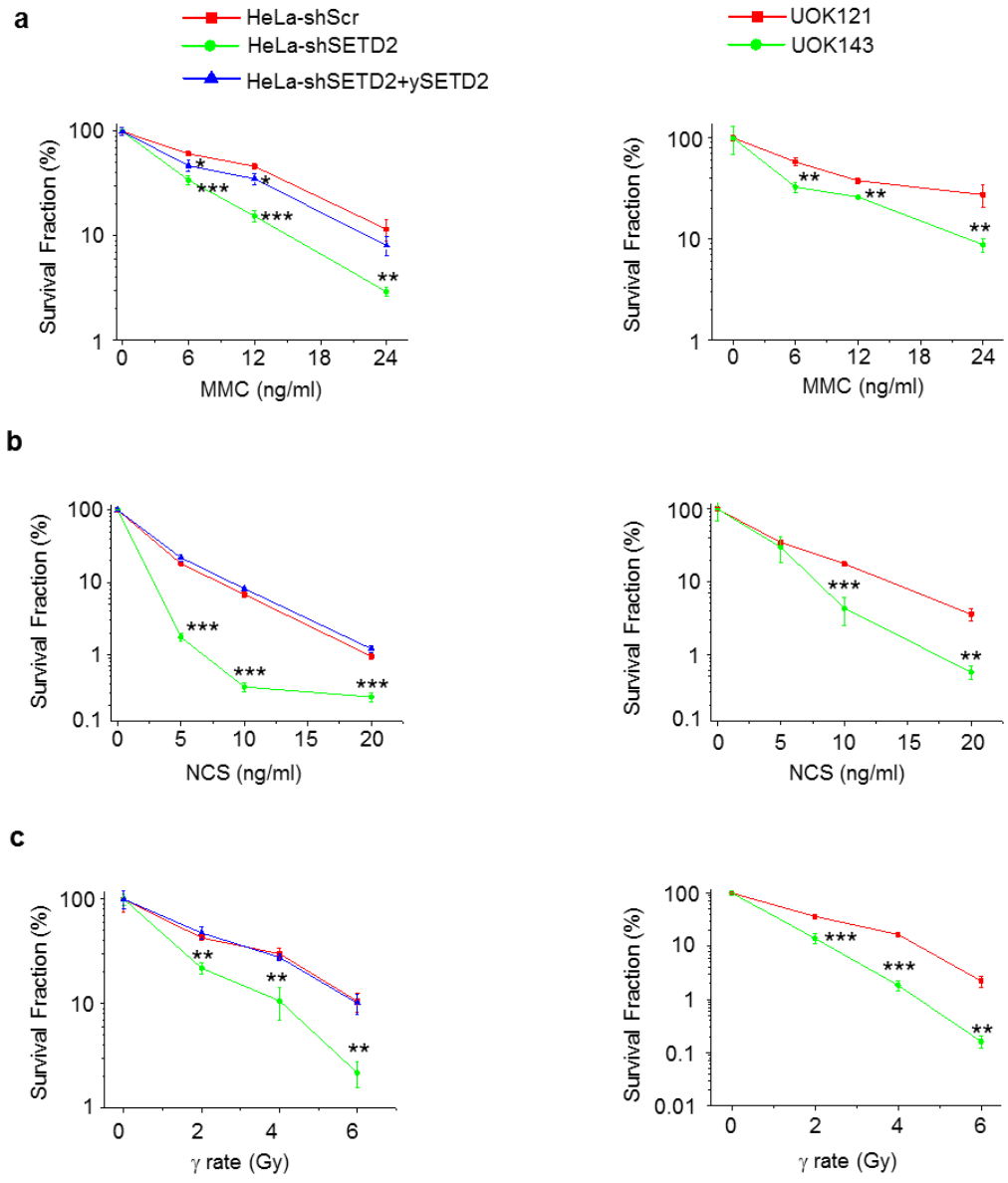

Figure B. 14. (a) TIP60 is present at a higher level in chromatin fraction from SETD2-proficient UOK121 cells than the corresponding SETD2-deficient UOK143 cells. β-actin and histone H3 were employed as loading controls for the soluble (SF) and chromatin (CF) fractions, respectively. (b) Defective resulted in loss of H4K16 acetylation. Core histone extracts were used for the Western blot.